(cf., e.g., [1,5]). We will later focus our attention on delay equations of the form (1.1) in which the nonlinearity f satisfies:

- $\bullet f: \mathbb{R}_+ = [0, \infty) \to \mathbb{R}_+$  is continuous.
- There is a unique equilibrium  $\hat{r} > 0$ , so  $\mu \bar{r} = f(\bar{r}) > 0$ .

$$\bullet \begin{cases} f(r) > \mu r & \text{for } 0 < r < \hat{r}, \\ f(r) < \mu r & \text{for all } r > \bar{r}. \end{cases}$$
(1.8)

#### 2. Comparison theorem and consequences

An easy argument then provides the following basic comparison theorem.

**Theorem 2.** Let  $f, \xi$  and correspondingly  $g, \eta$  be as above with g nondecreasing. Set  $x := x_{f,\xi}$  and  $y := x_{g,\eta}$ .

- (1) Suppose  $f \leq g$  where relevant (i.e.,  $f(r) \leq g(r)$  for each r in the range of f(x)) and suppose  $\xi \leq \eta$  on  $[-\tau, 0]$ . Then  $x(t) \leq y(t)$  for all t.
- (2) Suppose  $f \ge g$  where relevant and  $\xi \ge \eta$  on  $[-\tau, 0]$ . Then  $x(t) \ge y(t)$  for all t.

**Proof.** Both cases go in essentially the same fashion, so we only consider the first case (with  $f \leq g$ , etc.). Now suppose the result were false. We could then find a largest  $t_*$  such that  $x(s) \leq y(s)$  on  $[-\tau, t_*)$ . For any  $t < t_* + \tau$  we would have  $r = t - s - \tau < t_*$  for  $0 \leq s < t$  whence  $x(r) \leq y(r)$  for such r so  $f(x(r)) \leq g(x(r)) \leq g(y(r))$ . It follows from (1.2) and the corresponding integrated formulation involving g that  $x(t) \leq y(t)$  for such  $t \in [t_*, t_* + \tau)$  as well, contradicting the definition of  $t_*$ .  $\square$ 

We remark that this comparison theorem generalizes to equations in partially ordered Banach spaces, etc., but we do not pursue this here.

**Corollary 3.** Let  $f, \xi, x$  be as above in (1.1).

- (1) Suppose there is some M > 0 such that  $f(r) \le \mu \max\{r, M\}$  and suppose  $x \le M$  on  $[t_* \tau, t_*]$ . Then, also  $x(t) \le M$  for all  $t \ge t_*$ .
- (2) Suppose there is some m > 0 such that  $f(r) \ge \mu \min\{r, m\}$  and suppose  $x \ge m$  on  $[t_* \tau, t_*]$ . Then, also  $x(t) \ge m$  for all  $t \ge t_*$ .

**Proof.** Again, both cases go in essentially the same fashion so we need only consider the first. Further, since we can restart at any  $t_*$  it is sufficient to consider  $t_* = 0$  so we may assume  $\xi \leq M$  on  $[-\tau, 0]$ .

Take  $\eta \equiv M$  and  $g(r) := \mu \max\{r, M\}$ . Clearly, g is nondecreasing and the hypotheses yield  $\xi \leqslant \eta$  and  $f \leqslant g$ . We immediately verify that  $y \equiv M$  satisfies the delay differential equation to have  $y = x_{g,\eta}$  so that the result follows from Theorem 2.  $\square$ 

We will be seeking asymptotic upper and lower bounds for solutions x(t) of (1.1) and to this end it is convenient to introduce

$$\tilde{m} = \tilde{m}(x) = \liminf_{t \to \infty} x(t), \qquad \tilde{M} = \tilde{M}(x) = \limsup_{t \to \infty} x(t).$$
 (2.1)

**Lemma 4.** Let f be bounded with  $0 < f(r) \le B$ . Then  $\overline{M} \le B/\mu$ .

**Proof.** From (1.2) we have

$$x(t) \le e^{-\mu t} x(0) + \int_{-\tau}^{t} B e^{-\mu(t-s)} ds,$$

which gives the desired result as  $t \to \infty$ .  $\square$ 

We also note some information about the  $\omega$ -limit set of a nontrivial solution x, e.g., as used in [10].

**Lemma 5.** For any bounded solution  $x = x_{f,\xi}$  of (1.1), there are functions u, v defined on  $\mathbb{R}$  such that

- (i) u, v satisfy (1.1) on  $\mathbb{R}$ .
- (ii)  $\bar{m} \leq u(t), v(t) \leq \bar{M}$ .

(iii) 
$$u(0) = \bar{M}, \quad \dot{u}(0) = 0; \quad v(0) = \hat{m}, \quad \dot{v}(0) = 0,$$
 (2.2)

with  $\bar{m} = \bar{m}(x)$ ,  $\bar{M} = \bar{M}(x)$  as in (2.1).

For completeness, we sketch a proof here.

**Proof.** By the definition of  $\bar{M}$  there is a sequence  $t_k \to \infty$  such that  $x(t_k) \to \bar{M}$  and we set  $u_k(t) = x(t_k + t)$ —e.g., for  $t \ge -t_k$ . The set  $\{u_k(\cdot)\}$  is uniformly bounded with uniformly bounded derivatives, so there is a function u such that  $u_k \to u$  uniformly on compact sets in  $\mathbb{R}$ . Since the derivatives also converge uniformly on compact subsets and each  $u_k$  satisfies (1.1), so does u. Since, for compact set  $\mathcal{I}$  and any  $\varepsilon > 0$ , the definition of  $\bar{M}$  gives  $\bar{m} - \varepsilon < u_k < \bar{M} + \varepsilon$  for large enough k, we have (ii) in the limit. Since  $u_k(0) = x(t_k) \to \bar{M}$ , we have  $u(0) = \bar{M}$  and, as that is necessarily a maximum, we also have  $\dot{u}(0) = 0$ . The construction of  $v(\cdot)$  is similar.  $\square$ 

#### 3. Asymptotic bounds and attraction

**Theorem 6.** Let f,  $\xi$ , and x be as above in (1.1).

(1) Suppose there is some  $\bar{r} \geqslant 0$  such that

$$f(r) \leq \mu \bar{r}$$
 for  $0 < r \leq \bar{r}$ ,  
 $f(r) < \mu r$  for all  $r > \bar{r}$ . (3.1)

Then,  $\bar{M} \leqslant \bar{r} < \infty$  and there is a nonincreasing positive function  $z_+$  such that

$$x(t) := x_{f,\xi}(t) \leqslant z_{+}(t) \quad \text{with } z_{+}(t) \to \bar{r} \text{ as } t \to \infty.$$
 (3.2)

(2) Suppose there is some  $\bar{r} \geqslant 0$  such that

$$f(r) \geqslant \mu \bar{r}$$
 for  $r \geqslant \bar{r}$ ,  
 $f(r) > \mu r$  for all  $0 < r < \bar{r}$ . (3.3)

Then,  $\tilde{m} \geqslant \tilde{r}$  and there is a nondecreasing nonnegative function  $z_{-}$  such that

$$x(t) := x_{f,\xi}(t) \geqslant z_{-}(t) \quad \text{with } z_{-}(t) \to \tilde{r} \text{ as } t \to \infty.$$

$$(3.4)$$

**Proof.** Yet again, both cases go in essentially the same fashion. For the first case we begin by fixing  $M > \bar{r}$ ,  $M \ge \xi$ , and any  $\varepsilon = \varepsilon_0 > 0$  with  $\bar{r} + \varepsilon < M$ . We then let

$$\gamma_{\varepsilon} := \max\{f(r)/r \colon \bar{r} + \varepsilon \leqslant r \leqslant M\} < \mu \tag{3.5}$$

and, choosing  $\gamma$  so  $\gamma_{\varepsilon} \leqslant \gamma < \mu$ , set

$$g(r) = g_{\varepsilon}(r) := \max \{ \mu(\bar{r} + \varepsilon), \gamma r \}. \tag{3.6}$$

Now, let  $\lambda_{\varepsilon} > 0$  satisfy the characteristic equation

$$\lambda_{\varepsilon} + \gamma e^{\lambda_{\varepsilon} \tau} = \mu \tag{3.7}$$

and set

$$y^*(t) := y_{\varepsilon}^*(t) := Me^{-\lambda_{\varepsilon}t}. \tag{3.8}$$

If we did not have  $\xi$  bounded on  $[-\tau, 0]$ , we note that x is continuous for  $t \ge 0$  so we could restart at  $\tau$  with bounded initial data. Note also that, since f was assumed continuous and  $[\bar{r} + \varepsilon, M]$  is compact and nonempty, the 'max' in (3.5) is achieved and  $\gamma_{\varepsilon} < \mu$ .

Moreover, one easily sees that (3.7) has a unique positive solution since  $\gamma < \mu$ .

The construction yields  $y^*$  which satisfies the delay differential equation

$$\dot{y}(t) = -\mu y(t) + \gamma y(t - \tau) \tag{3.9}$$

so, taking  $\eta = \eta_{\varepsilon}$  to be  $y^*$  on  $[-\tau, 0]$ , this  $y^*$  must coincide with  $y = x_{g,\eta}$  so long as  $y^*(t-\tau) \geqslant \bar{r} + \delta$ , where  $\gamma(\bar{r} + \delta) = \mu(\bar{r} + \varepsilon)$ . Note that we can—and do—choose  $\gamma$  close enough to  $\mu$  to ensure that  $\delta \leqslant 2\varepsilon$ .

To apply Theorem 2, we note that g, as given by (3.6), is clearly nondecreasing and observe that our hypotheses ensure directly that  $f(r) \leq g(r)$  for  $r \leq \bar{r}$  and for  $\bar{r} \leq r \leq \bar{r} + \varepsilon$ , while choosing  $\gamma \geqslant \gamma_{\varepsilon}$  ensures that  $f(r) \leq g(r)$  for  $\bar{r} + \varepsilon \leq r \leq M$ . Since Corollary 3 ensures  $x(t) \leq M$ , it follows that  $f \leq g$  where relevant and that  $\xi \leq M \leq \eta$ . Thus, Theorem 2 applies and we have  $x \leq y := x_{g,\eta}$ —whence  $x \leq y^*$  as long as  $y^*$  coincides with y. Noting that this includes an interval of length  $\tau$  on which  $y \leq \bar{r} + \delta \leq \bar{r} + 2\varepsilon$ , we can apply Corollary 3 again (now restarting at the end of this interval) to see that x thereafter remains below  $\bar{r} + 2\varepsilon$ —i.e., we have shown that

$$x(t) \leqslant z_{\varepsilon}(t) := \max\{Me^{-\lambda_{\varepsilon}t}, \bar{r} + 2\varepsilon\}$$

for all t. Since this holds for arbitrarily small  $\varepsilon > 0$ , we have (3.2), as desired, with  $z_+(t) := \inf\{z_{\varepsilon}(t): \varepsilon > 0\}$ . This completes the proof for the first case.

Using the second case in Theorem 2, we will get a corresponding lower bound. First, however, we note that (1.2) gives

$$x(\tau) = e^{-\mu \tau} x(0) + \int_{-\tau}^{0} e^{-\mu(\tau+s)} f(\xi(s)) ds,$$

which will be strictly positive for nonnegative, nontrivial  $\xi$ —and then x(t) will be strictly positive for all  $t \ge \tau$ . We can therefore assume, restarting if necessary, that  $\xi \ge m$  for some m > 0. The rest of the proof is then almost exactly like that for the first case.  $\square$ 

**Theorem 7.** Let  $f, \xi, x$  be as above in (1.1) and suppose there is some  $\bar{r} \ge 0$  such that

$$f(r) > \mu r \quad for \ 0 < r < \bar{r},$$
  
$$f(r) < \mu r \quad for \ all \ r > \bar{r}.$$
 (3.10)

Suppose, also, that

either 
$$f(r) \leq \mu \bar{r}$$
 for  $0 < r < \bar{r}$   
or  $f(r) \geq \mu \bar{r}$  for all  $r \geq \bar{r}$ . (3.11)

Then,  $x_{f,\xi}(t) \to \hat{r}$  as  $t \to \infty$  for every nontrivial initial data  $\xi \geqslant 0$ —i.e.,  $\bar{m} = \bar{r} = \bar{M}$ .

**Proof.** We consider explicitly only the first alternative in (3.11). Since this with (3.10) include (3.1), the first case of Theorem 6 applies to give  $\bar{M} \leq \bar{r}$ . If  $\bar{r} = 0$ , we are now done so we need only show  $\bar{m} \geqslant \bar{r}$  when  $\bar{r} > 0$ . For any  $\varepsilon > 0$  we can choose  $\delta > 0$  so  $f(r) \geqslant f(\bar{r}) - \mu \varepsilon$  on  $[\bar{r}, \bar{r} + \delta]$  and there is some  $t_{\delta}$  such that  $x(t) \leqslant \bar{r} + \delta$  for all  $t \geqslant t_{\delta} - \tau$ . Setting  $\bar{r} = \bar{r} - \varepsilon$ , this gives  $f(r) \geqslant \mu \bar{r}$  for  $\bar{r} \leqslant r \leqslant \bar{r} + \delta$ . Restarting at  $t_{\delta}$ , and noting that only values of r below  $\bar{r} + \delta$  are relevant, we thus have the hypotheses for the second case of Theorem 6 for the restarted problem with  $\bar{r}$  replaced by  $\bar{r}$ . Thus,  $\bar{m} \geqslant \bar{r} = \bar{r} - \varepsilon$  for arbitrary  $\varepsilon > 0$  so  $\bar{m} \geqslant \bar{r}$ . Combining these upper and lower asymptotic bounds is just the desired result.  $\square$ 

We henceforth will consider equations of the form (1.1) subject to the hypotheses (1.8). If  $\max\{f(r): r > 0\} = B \le \mu \bar{r}$ , giving the first case of (3.11), then we already know from Theorem 7 that all solutions converge to the equilibrium  $\bar{r}$ , so we will also assume henceforth that  $B > \mu \bar{r}$  with  $y_0 < \bar{r}$ : (1.8) then gives (3.10) but we have neither case of (3.11).

#### 4. Attraction dependent on the delay

As noted, we henceforth assume (1.8):

•  $f: \mathbb{R}_+ = [0, \infty) \to \mathbb{R}_+$  is continuous.

• There is a unique equilibrium 
$$\bar{r} > 0$$
, so  $\mu \bar{r} = f(\bar{r}) > 0$ .

$$\bullet \begin{cases}
f(r) > \mu r & \text{for } 0 < r < \bar{r}, \\
f(r) < \mu r & \text{for all } r > \bar{r}.
\end{cases}$$
(4.1)

Lemma 8. Assume (4.1). Then, for every nontrivial solution x of (1.1) we have

$$e^{-\mu\tau}\bar{r} \leqslant \bar{m} \leqslant \bar{r} \leqslant \bar{M} \leqslant \max_{e^{-\mu\tau}\bar{r} \leqslant r \leqslant \bar{r}} f(r)/\mu$$
 (4.2)

with  $\bar{m} = \bar{m}(x)$ ,  $\bar{M} = \bar{M}(x)$  as in (2.1).

**Proof.** From Corollary 3 we know x is bounded and let u, v be as in Lemma 5. Then, as  $\dot{u}(0) = 0 = \dot{v}(0)$ ,

$$f(u(-\tau)) = \mu u(0) = \mu \tilde{M} \geqslant \mu u(-\tau)$$

and, similarly,  $f(v(-\tau)) = \mu v(0) \leqslant \mu v(-\tau)$ . But  $f(r) > \mu r$  if and only if  $x < \bar{r}$ , so  $u(-\tau) \leqslant \bar{r} \leqslant v(-\tau)$ . Thus,

$$v(0) = \bar{m} \leqslant u(-\tau) \leqslant \bar{r} \leqslant v(-\tau) \leqslant \bar{M}. \tag{4.3}$$

Since u, v satisfy (1.1) on all of  $\mathbb{R}$ , we may apply (1.2) with t = 0,  $a = -\tau$  to get, as  $f(\cdot) \ge 0$ ,

$$\tilde{m} = v(0) = e^{-\mu\tau} v(-\tau) + \int_{-\tau}^{0} e^{\mu s} f(x(s-\tau)) ds \geqslant e^{-\mu\tau} v(-\tau) \geqslant e^{-\mu\tau} \bar{r}$$

and consequently,  $u(-\tau) \geqslant v(0) \geqslant e^{-\mu \tau} \bar{r}$ . Therefore,

$$u(0) = f(u(-\tau))/\mu \leqslant \max_{e^{-\mu\tau}\bar{r} \leqslant r \leqslant \bar{r}} f(r)/\mu.$$

The proof is complete.  $\Box$ 

Our next objective is to show global attraction to the equilibrium when the delay  $\tau$  is not too large.

**Theorem 9.** Assume (4.1) and the following pair of one-sided Lipschitz conditions:

$$0 \leq f(r) - \mu \bar{r} \leq L_1(\bar{r} - r) \quad \text{for } e^{-\mu \tau} \bar{r} \leq r < \bar{r},$$

$$0 \leq \mu \bar{r} - f(r) \leq L_2(r - \bar{r}) \quad \text{for } \bar{r} < r \leq B.$$

$$(4.4)$$

Suppose t is such that

$$(1 - e^{-\mu \tau}) < \frac{\mu}{\sqrt{L_1 L_2}}. (4.5)$$

Then, every nontrivial solution of (1.1) converges to the equilibrium  $\bar{r}$ .

**Proof.** Let u, v be as in Lemmas 5 and 8. It then follows from (4.3) that there is some  $a \in [-\tau, 0]$  such that  $u(a) = \bar{r}$  and we set

$$\mathcal{A} = \left\{ s \in [a, 0] \subset [-\tau, 0] \colon u(s - \tau) \leqslant \tilde{r} \right\}.$$

Note that for  $s \in [-\tau, 0] \setminus A$  we have  $u = u(s - \tau) > \bar{r}$  so  $f(u) - \mu \bar{r} \le 0$  by (4.1), while for  $t \in A$  we have  $u \le \bar{r}$  and  $e^{-\mu \tau} \bar{r} \le \bar{m} \le u$  from (4.2) in Lemma 8 so (4.4) gives

$$f(u) - \mu \bar{r} \leqslant L_1(\bar{r} - u) \leqslant L_1(\bar{r} - \bar{m}).$$

638

Thus.

$$\int_{A} e^{\mu s} [f(u) - \mu \bar{r}] ds \leqslant L_{1}(\bar{r} - \bar{m}) \int_{-\tau}^{0} e^{\mu t} ds = L_{1}(\bar{r} - \bar{m})(1 - e^{-\mu \tau}).$$

Applying (1.2) with t = 0 and this a, we then have

$$\bar{M} - \bar{r} = \left[ u(0) - e^{\mu a} u(a) \right] + \mu \int_{a}^{0} e^{\mu s} ds = \int_{a}^{0} e^{\mu s} \left[ f(u(s - \tau)) - \mu \bar{r} \right] ds$$

$$\leq \int_{A} e^{\mu s} \left[ f(u) - \mu \bar{r} \right] ds \leq L_{1} (\bar{r} - \bar{m}) (1 - e^{-\mu \tau}) / \mu.$$

Somewhat similarly, we have some  $a \in [-\tau, 0]$  such that  $v(a) = \bar{r}$  and now set  $A = \{s \in [a, 0]: v(s - \tau) \ge \bar{r}\}$ , noting that (4.4) ensures that  $f(r) \ge \mu \bar{r}$  for  $r \in [e^{-\mu \tau} \bar{r}, \bar{r}]$ . Much as before we then get

$$\bar{r} - \bar{m} \leqslant L_2(\bar{M} - \bar{r})(1 - e^{-\mu\tau})/\mu$$

and combining gives  $(\bar{r} - \bar{m}) \le [L_1 L_2 (1 - e^{-\mu \tau})^2 / \mu^2] (\bar{r} - \bar{m})$ . Thus, using the assumption (4.5), we have  $\bar{m} = \bar{r}$  and then  $\bar{M} = \bar{r}$  as well.  $\Box$ 

Essentially the same argument gives a localized version when, instead of (4.4) and (4.5), we have |f'| suitably small near  $\bar{r}$ .

#### 5. Another stability result

We now return to the integral formula (1.4), noting that if x is a solution of (1.1), then  $y = x - \bar{r}$  is a solution of (1.3) and an appropriate choice of g:

$$g(t) = f_1(y(t-\tau)) \text{ with } f_1(r) := [f(\bar{r}+r) - f(\bar{r})] + \nu r,$$
 (5.1)

where, of course, we anticipate taking  $v = -f'(\bar{r})$  for differentiable functions f, although this is not required.

It is worth noting that with this choice of  $\nu$  we necessarily have  $L_1, L_2 \ge |f'(\bar{r})| = \nu$  in Theorem 9 so that Lemma 1 suggests that we could not expect asymptotically stable convergence to equilibrium when  $\nu > \mu$  if we do not have (1.7); indeed, as we will note in more detail in the following section, (1.1) will then have a nontrivial periodic solution. Even ignoring the constraint on  $\tau$  in requiring that  $f(r) \ge \mu \bar{r}$  for  $r \in [e^{-\mu \tau} \bar{r}, \bar{r}]$ , the assumption (4.5) taking  $L_1 = L_2 = -f'(\bar{r}) = \nu$  leads to  $(1 - e^{-\mu \tau}) < \mu/\nu$  or

$$\tau < \frac{1}{\mu} \ln \left[ \frac{1}{1 - \mu/\nu} \right]. \tag{5.2}$$

Since we anticipate having f(0) = 0, this part of (4.4) must be treated as a significant constraint on  $\tau$ .

Clearly this, as a sufficient condition for convergence to equilibrium, is the best one can obtain using Theorem 9 and it is interesting to compare with the (necessarily weaker) condition (1.7). There is obviously a gap between these, and we now seek to handle intermediate delays under appropriate conditions.

**Theorem 10.** Suppose f is a unimodal function and  $\tau > 0$  satisfies (1.7) with  $\nu = -f'(\bar{r})$ . Further, suppose

$$\left| f(\bar{r} + r) - f(\bar{r}) + \nu r \right| \le L|r| \quad \text{for } e^{-\mu \tau} \bar{r} - \bar{r} \le r \le B - \bar{r}. \tag{5.3}$$

If f is 'flat enough near equilibrium' such that (5.3) holds with

$$L < 1/\|X\|_1,\tag{5.4}$$

where X is as in (1.4), then every nontrivial nonnegative solution of (1.1) converges to the equilibrium  $\bar{r}$  as  $t \to \infty$ .

**Proof.** Set  $\hat{M} = \max\{\bar{M} - \bar{r}, \bar{r} - \bar{m}\}$  and, again, let u, v be as in Lemmas 5 and 8. First suppose  $\hat{M} = \bar{M} - \bar{r}$ . We then let  $y(t) = u(t - T) - \bar{r}$  so  $\hat{M} = u(0) - \bar{r} = y(T)$  with T > 0 arbitrary. We note that  $\bar{m} \leq y \leq \hat{M}$  gives  $|y| \leq \hat{M}$ . Therefore, (5.3) gives  $|f_1(y)| \leq L\hat{M}$  uniformly. Thus, using (1.3) with (5.1), we have

$$\hat{M} = y_0(T) + \int_0^T X(T - s) f_1(y(s - \tau)) ds \le \bar{y}_0(T) + \int_0^T |X(T - s)| L \hat{M} ds$$

$$\le \bar{y}_0(T) + L ||X||_1 \hat{M}$$
(5.5)

using (1.6) and letting  $\bar{y}_0 = y_0(\cdot; \hat{M})$ . For the alternative case  $\hat{M} = \bar{r} - \bar{m}$ , we let  $y(t) = v(t-T) - \bar{r}$  and, similarly, again obtain (5.5) for arbitrary T. Since  $\bar{y}_0(T) \to 0$  as  $T \to \infty$ , (5.4) ensures that  $\hat{M} = 0$  so  $x(t) \to \bar{r}$  as  $t \to \infty$ .  $\square$ 

#### 6. Nonconstant periodic solution for large delay

In this section we will use Hopf bifurcation and fixed point theory to prove the existence of a nonconstant periodic solution when the delay  $\tau$  is large enough. To see more clearly the effect of delay we let  $\mu=1$ . The usual linearized analysis lets  $x=\bar{r}+\varepsilon y$  and notes that, to first order in  $\varepsilon$ , the perturbation satisfies

$$\dot{y} + y = f'(\bar{r})y(\cdot - \tau).$$

Seeking a solution of the form  $y(t) = \exp(\lambda t)$ , we obtain the characteristic equation for  $\lambda$ :

$$\lambda + 1 = f'(r) \exp(-\tau \lambda).$$

We will have linearized stability if all complex roots of this characteristic equation have negative real parts. If |f'(r)| < 1 we have the local convergence to the positive equilibrium for all delays. If |f'(r)| > 1, the effect of delay will occur. More exactly, in this case with

$$\tau > \tau_* = \frac{1}{\sqrt{|f'(\bar{r})|^2 - 1}} \arccos \frac{1}{f'(\bar{r})}$$

there is a nonconstant periodic solution of Eq. (1.1).

Atay [1] used the Schauder fixed point theory to prove that there is a nonconstant periodic solution of the equation

$$\dot{y} = \tau h(y, y(\cdot - 1)),$$

provided

$$\tau > \tau_* = \frac{1}{\sqrt{D^2 - C^2}} \arccos\left(-\frac{C}{D}\right),$$

where h(u, v) is differentiable at the origin, h(0, 0) = 0 and

$$0 < C := -\frac{\partial h}{\partial u}(0,0) < D := -\frac{\partial h}{\partial v}(0,0).$$

We let  $y(t) = x(\tau t) - \bar{r}$  and

$$h(u, v) = \bar{r} - u + f(v + \bar{r}).$$

Then,

$$C=1,$$
  $D=-f'(\bar{r})$ 

and we reproduce

$$\tau_* = \frac{1}{\sqrt{|f'(\bar{r})|^2 - 1}} \arccos \frac{1}{f'(\bar{r})}.$$

Here, we assume that  $f'(\bar{r}) < -1$  and the function arc cosine takes its value in  $[0, \pi]$ .

**Lemma 11.** If a positive solution x of (1.1) does not oscillate around the positive equilibrium  $\bar{r}$  then x(t) tends to  $\bar{r}$  as  $t \to \infty$ . Consequently, every nonconstant positive periodic solution should oscillate around the positive equilibrium.

**Proof.** If x does not oscillate around  $\bar{r}$ , then either

$$\limsup_{t\to\infty} x(t) \leqslant \bar{r} \quad \text{or} \quad \liminf_{t\to\infty} x(t) \geqslant \bar{r}.$$

From Lemma 8, in the first case, we have  $\limsup x(t) = \bar{r}$ . For the second case, we have  $\liminf x(t) = \bar{r}$ . So it is enough to consider the second case. Using the proof of Lemma 8, we get  $\bar{r} \ge u(-\tau) \ge v(0) = \bar{r}$ . Hence,  $u(-\tau) = \bar{r}$  and  $u(0) = f(u(-\tau)) = \bar{r}$ . The proof is now complete.  $\Box$ 

Y. Cao [2] proved that for  $\tau \le \tau_*$  there is no periodic solution which is larger than  $y_0$  and oscillates slowly around the only positive equilibrium  $\bar{r}$ . For  $\tau > \tau_*$ , there is at most one periodic solution which is larger than  $y_0$  and oscillates slowly around  $\bar{r}$ . Recall that a T-periodic solution is called *slowly oscillated around the positive equilibrium*, if  $T > \tau$ ,  $x(0) = x(T) = \bar{r}$ , and there is  $t_0 \in (0, T - \tau)$  such that

$$x(t_0) = \overline{r},$$
  $x(t) > \overline{r}$  for  $t \in (0, t_0)$  and  $x(t) < \overline{r}$  for  $t \in (t_0, T)$ .

Cao assumes that f is decreasing from  $y_0 < \bar{r}$  until  $f(y_0)$ . He also requires that the function h(x) = xf'(x)/f(x) is monotonically increasing in  $[y_0, \bar{r}]$  and decreasing in

 $[\bar{r}, f(y_0)]$ . Recall that  $f(y_0)$  is the maximal value of f(y), when y > 0. Without these assumptions on h one can construct several slowly oscillated periodic solutions for (1.1). Also, it is known that, if a periodic solution is not oscillated slowly, it should be unstable. Of course, Cao did not prove these results directly, but from his works one can deduce this.

#### 7. Some applications

Equation (1.1) with unimodal f has been proposed as a model for a variety of physiological processes, where in most cases, one of the model functions

$$f(x) = kx^{c} \exp(-x) \tag{7.1}$$

or

$$f(x) = \frac{kx}{1 + x^c},\tag{7.2}$$

with parameters k > 0 and c > 0, is considered [3,4,9,11–13].

The population dynamics of Nicholson's blowflies have been studied [9,12] using a function f of the form (7.1) with c = 1. In such a case, f is differentiable and one has

$$\bar{r} = \ln \frac{k}{\mu},\tag{7.3}$$

and

$$\nu = -f'(\bar{r}) = \mu \left( \ln \frac{k}{\mu} - 1 \right).$$

Thus, Theorem 9 yields, using (5.2),

$$\tau < \frac{1}{\mu} \ln \left[ \frac{\ln(k/\mu) - 1}{\ln(k/\mu) - 2} \right]$$

as a sufficient condition for convergence to equilibrium  $\bar{r}$  given in (7.3), provided  $k > \mu e^2$ . Moreover, there is a nonconstant periodic solution to the model equation if

$$\tau > \tau^* = \frac{1}{\mu \sqrt{(\ln(k/\mu) - 2) \ln(k/\mu)}} \arccos\left[\frac{1}{1 - \ln(k/\mu)}\right],$$

using (1.7)

In respiratory studies, (1.1) has been employed in which the response function takes the form (7.2). In such a case, one has the positive equilibrium

$$\bar{r} = \left(\frac{k}{\mu} - 1\right)^{1/c},\tag{7.4}$$

provided  $k/\mu > 1$ . Then,

$$v = -f'(\bar{r}) = \frac{\mu}{k} [(c-1)k - c\mu].$$

Thus, Theorem 9 yields, using (5.2),

$$\tau < \frac{1}{\mu} \ln \left[ \frac{c(1-\mu/k) - 1}{c(1-\mu/k) - 2} \right]$$

as a sufficient condition for convergence to equilibrium  $\bar{r}$  given in (7.4), provided

$$c\left(1-\frac{\mu}{k}\right) > 2.$$

Moreover, there is a nonconstant periodic solution to the model equation (1.1) with f as in (7.2) if

$$\tau > \tau^* = \frac{1}{\mu \sqrt{c(c(1-\mu/k)-2)(1-\mu/k)}} \arccos \left[ \frac{1}{1-c(1-\mu/k)} \right],$$

using (1.7).

#### 8. Conclusion

We have given a basic comparison theorem and discussed some of their consequences. The effect of delay on the asymptotic behavior has then been studied and the periodicity of positive solutions investigated for large delays. Our discussions allow the nonlinearity f to be nonmonotonic and nondifferentiable which are then more general than those of [8]. Thus, our results should be applicable to a wider range of population models; for example, models arising from the study of an optically bistable device [3,4], blood cells production, respiration dynamics, or cardiac arrhythmias [11,13]. We can also find application with a system in which the growth function is not smooth, such as a population where growth occurs in birth pulses (during the breeding season) and not continuously throughout the year.

Open problem. Investigate the stability of periodic solutions of (1.1) and the structure of  $\omega$ -limit sets when the delay is large enough!

#### Acknowledgment

Deepest appreciation is extended towards the National Research Council of Thailand and the Thailand Research Fund for the financial support.

#### References

- [1] F.M. Atay, Periodic solutions of a delay-differential equation with a restorative condition, Nonlinear Anal. 45 (2001) 555-576.
- [2] Y. Cao, Uniqueness of periodic solution for differential delay equations, J. Differential Equations 128 (1996)
- [3] M.W. Derstine, H.M. Gibbs, F.A. Hopf, D.L. Kaplan, Bifurcation gap in a hybrid optically bistable system, Phys. Rev. A 26 (1982) 3720-3722.
- [4] M.W. Derstine, H.M. Gibbs, F.A. Hopf, D.L. Kaplan, Alternate paths to chaos in optical bistability, Phys. Rev. A 27 (1983) 3200-3208.
- [5] K.P. Hadeler, J. Tomiuk, Periodic solutions of difference differential equations, Arch. Rational Mech. Anal. 65 (1977) 87-95.

- [6] J. Hale, Introduction to Functional Differential Equations, Springer-Verlag, 1993.
- [7] M. Kot, Elements of Mathematical Ecology, Cambridge Univ. Press, 2001.
- [8] Y. Kuang, Delay Differential Equations with Applications in Population Dynamics, Academic Press, 1993.
- [9] M. Kulenovic, G. Ladas, Y. Sficas, Global attractivity in Nicholson's blowflies, Appl. Anal. 43 (1992) 109– 124.
- [10] Y. Lenbury, D.V. Giang, Nonlinear delay differential equations involving population growth, Math. Comput. Modelling, in press.
  - [11] M.C. Mackey, U. an der Heiden, Dynamical diseases and bifurcations: understanding functional disorders in physiological systems, Funkt. Biol. Med. 256 (1982) 156-164.
  - [12] S.H. Saker, S. Agarwal, Oscillation and global attractivity in a periodic Nicholson's blowflies model, Math. Comput. Modelling 35 (2002) 719-731.
  - [13] M. Wazewska-Czyewska, A. Lasota, Mathematical models of the red cell system, Mat. Stos. 6 (1976) 25-40 (in Polish).



## Available online at www.sciencedirect.com

MATHEMATICAL AND COMPUTER MODELLING

Mathematical and Computer Modelling 40 (2004) 583-590

www.elsevier.com/locate/mcm

### Nonlinear Delay Differential Equations Involving Population Growth

Y. LENBURY\*

Department of Mathematics, Mahidol University Rama 6, Bangkok, 10400 Thailand scylb@mahidol.ac.th

D. V. GIANG

Hanoi Institute of Mathematics
18 Hoang Quoc Viet, 10307 Hanoi, Vietnam dangvugiang@yahoo.com

(Received June 2003; revised and accepted September 2003)

Abstract—Conditions are given on the function f, such that population x(t) given by

$$\dot{x}(t) = -\mu x(t) + f(x(t-\tau)),$$

becomes extinct or remains globally stable. Our theorems are shown to be applicable to the Nicholson's model of blowfiles and the population dynamics of baleen whales. In some of these cases, the function f is unimodal rather than monotone. © 2004 Elsevier Ltd. All rights reserved.

Keywords—Constant variation formula, Positivity of population models,  $\omega$ -limit set of a persistent solution, One parameter semigroup.

#### 1. INTRODUCTION

Consider the following delay differential equation,

$$\dot{x}(t) = -\mu x(t) + f(x(t-\tau)), \tag{1.1}$$

for t > 0, where  $f : [0, \infty) \to [0, \infty)$  is a continuous function, f(0) = 0, while  $\mu$  and  $\tau$  are positive parameters. The initial condition  $x|_{[-\tau,0]} = \phi$  is given by a positive continuous function in  $[-\tau,0]$ . The corresponding constant variation formula is given as

$$x(t) = e^{-\mu t}x(0) + \int_0^t e^{-\mu(t-\xi)} f(x(\xi-\tau)) d\xi, \quad \text{for } t > 0.$$
 (1.2)

This can be proved by differentiating both sides. This formula also shows that x(t) > 0, for all t > 0, hence, (1.1) really is a model for population growth. The following theorem gives a sufficient and necessary condition for the population to become extinct.

0895-7177/04/\$ - see front matter © 2004 Elsevier Ltd. All rights reserved. doi:10.1016/j.mcm.2003.09.038

Typeset by AMS-TEX

<sup>\*</sup>Author to whom all correspondence should be addressed. The authors would like to extend their deepest appreciation to the Thailand Research Fund for the financial support of this research project, which is also partially funded by a grant from the Ministry of University Affairs.

THEOREM 1. If  $f(u) < \mu u$ , for all u > 0, then, every solution x(t) of (1.1) converges to 0 as  $t \to \infty$ . Conversely, if every solution of (1.1) converges to 0, then,  $f(u) < \mu u$ , for all u > 0.

PROOF. First, assume that  $f(u) < \mu u$ , for all u > 0. Let x(t) be a positive solution of (1.1) and  $M = \max_{-\tau \le \xi \le 0} x(\xi) + 1$ . We prove that x(t) < M, for all t > 0. Indeed, assume, for the sake of contradiction, that  $t_0$  is the *first positive point*, such that  $x(t_0) = M$ . The "first positive point" only means that  $x(\xi - \tau) < M$ , for all  $\xi < t_0$ . Then, by the constant variation formula

$$\begin{split} M &= x(t_0) = e^{-\mu t_0} x(0) + \int_0^{t_0} e^{-\mu(t_0 - \xi)} f(x(\xi - \tau)) \, d\xi, \\ &< e^{-\mu t_0} M \left( 1 + \int_0^{t_0} e^{\mu \xi} \mu \, d\xi \right) = M, \end{split}$$

which is a contradiction. Therefore, x(t) < M, for all t. Let

$$\ell_1 = \limsup_{t \to \infty} x(t),$$
  
$$\ell_2 = \limsup_{t \to \infty} f(x(t - \tau)).$$

Let  $\epsilon > 0$  be a small number, and let  $T = T(\epsilon)$  be, such that  $f(x(t - \tau)) < \ell_2 + \epsilon$ , for all t > T. Now, if t > T, then, we have

$$\begin{split} x(t) &= e^{-\mu t} x(0) + \int_0^T e^{-\mu(t-\xi)} f(x(\xi-\tau)) \, d\xi + \int_T^t e^{-\mu(t-\xi)} f(x(\xi-\tau)) \, d\xi \\ &\leq e^{-\mu t} x(0) + e^{-\mu t} \int_0^T e^{\mu \xi} f(x(\xi-\tau)) \, d\xi + (\ell_2 + \epsilon) e^{-\mu t} \int_T^t e^{\mu \xi} \, d\xi \\ &\leq e^{-\mu t} x(0) + e^{-\mu t} \int_0^T e^{\mu \xi} f(x(\xi-\tau)) \, d\xi + \frac{(\ell_2 + \epsilon)}{\mu} \left(1 - e^{-\mu(t-T)}\right). \end{split}$$

Taking lim sup on both sides, we have

$$\ell_1 \leq \frac{\ell_2 + \epsilon}{\mu}.$$

Since  $\epsilon$  is as small as we wish, this gives

$$\mu \ell_1 \le \ell_2. \tag{1.3}$$

On the other hand, from the definition of  $\limsup$ , we can choose a sequence  $\{t_k\}$  tending to infinity for which

$$\ell_{2} = \lim_{k \to \infty} f\left(x\left(t_{k} - \tau\right)\right).$$

The sequence  $\{x(t_k - \tau)\}$  is bounded because the function x(t) is bounded. Hence, this sequence should contain some convergent subsequence. Without loss of generality, we assume that the sequence  $\{x(t_k - \tau)\}$  converges to a limit  $\ell_3$ , say. Since the function f is continuous, we have

$$\ell_{2} = \lim_{k \to \infty} f(x(t_{k} - \tau)) = f(\ell_{3}).$$

If  $\ell_3 > 0$ , then,

$$\ell_2 = f(\ell_3) < \mu \ell_3.$$

Clearly,  $\ell_3 \leq \ell_1$ . Therefore,  $\ell_2 < \mu \ell_1$ . Considering (1.3), we have a contradiction. Consequently,  $\ell_3 = 0$ . However,  $\ell_2 = f(\ell_3)$ , and so,  $\ell_2$  is zero also. Combining this with (1.3), we have  $\ell_1 = 0$ , and hence, the solution x(t) tends to 0 as  $t \to \infty$ .

Conversely, suppose that  $f(u) < \mu u$  is not satisfied, for all u > 0. Two cases are possible.

- (i)  $f(a) = \mu a$ , for some a > 0.
- (ii)  $f(u) > \mu u$ , for all u > 0.

In the first case,  $x(t) \equiv a$  is a positive solution which does not tend to 0. For the second case, let x(t) = 2 for  $t \in [-\tau, 0]$ . We shall prove that x(t) > 1, for all t. Suppose, for the sake of contradiction, that  $t_0 > 0$  is the the first point, such that  $x(t_0) = 1$ , and x(t) > 1, for all  $0 \le t < t_0$ . Then,

$$1 = x(t_0) = 2e^{-\mu t_0} + e^{-\mu t_0} \int_0^{t_0} e^{\mu \xi} f(x(\xi - \tau)) d\xi$$
$$> e^{-\mu t_0} \left( 2 + \int_0^{t_0} e^{\mu \xi} \mu d\xi \right) = e^{-\mu t_0} \left( 1 + e^{\mu t_0} \right) > 1,$$

which is a contradiction. Therefore, x(t) > 1, for all t, which does not tend to 0. The proof is complete.

#### 2. THE PERSISTENCE

A positive solution x(t) is called persistent if

$$0 < \liminf_{t \to \infty} x(t) \le \limsup_{t \to \infty} x(t) < \infty.$$

The following theorem gives a sufficient condition for the population to be persistent.

THEOREM 2. Assume that f(x) > 0, for all x > 0 and

$$\limsup_{x \to \infty} \frac{f(x)}{x} < \mu,\tag{2.1}$$

$$\liminf_{x \to 0+} \frac{f(x)}{x} > \mu.$$
(2.2)

Then, every solution x(t) of (1.1) is persistent.

PROOF. First, we prove that  $\{x(t)\}$  is bounded from above. Assume, for the sake of contradiction, that  $\limsup x(t) = \infty$ . For each  $t \ge -\tau$ , we define

$$\alpha(t) := \max \left\{ \rho \le t : x(\rho) = \max_{-\tau \le \xi \le t} x(\xi) \right\}.$$

Observe that  $\alpha(t) \to \infty$  and that

$$\lim_{t\to\infty}x(\alpha(t))=\infty.$$

But  $x(\alpha(t)) = \max_{\xi \le t} x(\xi)$  and so,  $\dot{x}(\alpha(t)) \ge 0$ . Therefore,

$$0 \le \dot{x}(\alpha(t)) = -\mu x(\alpha(t)) + f(x(\alpha(t) - \tau)),$$

and consequently,

$$\mu x(\alpha(t)) \leq f(x(\alpha(t) - \tau)).$$

Since f is a continuous function, combining this inequality with the fact that

$$\lim_{t\to\infty}x(\alpha(t))=\infty,$$

we obtain

$$\lim_{t\to\infty}x(\alpha(t)-\tau)=\infty.$$

Therefore.

$$\limsup_{x\to\infty}\frac{f(x)}{x}\geq \limsup_{t\to\infty}\frac{f(x(\alpha(t)-\tau))}{x(\alpha(t)-\tau)}\geq \mu,$$

which contradicts (2.1). Thus, x(t) is bounded from above.

Next, we prove that  $\liminf_{t\to\infty} x(t) > 0$ . Suppose, for the sake of contradiction, that  $\liminf x(t) = 0$ . For each  $t \ge -\tau$ , we define

$$\beta(t) := \max \left\{ \rho \le t : x(\rho) = \min_{-\tau \le \xi \le t} x(\xi) \right\}.$$

Observe that  $\beta(t) \to \infty$  and that

$$\lim_{t\to\infty}x(\beta(t))=0.$$

However,  $x(\beta(t)) = \min_{\xi \le t} x(\xi)$ , and so  $\dot{x}(\beta(t)) \le 0$ . Therefore,

$$0 \ge \dot{x}(\beta(t)) = -\mu x(\beta(t)) + f(x(\beta(t) - \tau))$$

and consequently,

$$\mu x(\beta(t)) \ge f(x(\beta(t) - \tau)).$$

Since f is a continuous function, combining this inequality with the fact that

$$\lim_{t\to\infty}x(\beta(t))=0,$$

we obtain

$$\lim_{t\to\infty}x(\beta(t)-\tau)=0.$$

Therefore,

$$\liminf_{x\to 0+}\frac{f(x)}{x}\leq \liminf_{t\to \infty}\frac{f(x(\beta(t)-\tau))}{x(\beta(t)-\tau)}\leq \mu,$$

which contradicts (2.2). The proof is complete.

Inequalities (2.1) and (2.2) give the lower and upper bounds for the death rate  $\mu$  in order that the population may persist. As x becomes very large, to prevent the population from overflowing, the lim sup of the ratio of the growth function f(x) and the population density x should be smaller than the death rate  $\mu$ . On the other hand, as x becomes very small, the lim inf of that ratio should remain bigger that the death rate  $\mu$  to keep the population from extinction.

In what follows, we will assume that  $x(\cdot)$  is a persistent solution of (1.1) with  $x|_{[-\tau,0]} = \psi$ . We let s be a variable in the interval  $[-\tau,0]$  and denote by  $\mathcal{C}[-\tau,0]$ , the Banach space of continuous functions in the interval  $[-\tau, 0]$ . For each persistent solution  $x(\cdot)$  and  $t \ge 0$ , let  $x_t(s) = x(t+s)$ be a function with the variable  $s \in [-\tau, 0]$ . We consider the semigroup  $\{T(t)\}_{t>0}$  of operators from  $\mathcal{C}[-\tau,0]$  into itself defined by letting  $T(t)\psi=x_t$ , where x is a persistent solution beginning from  $\psi$ . Clearly, the operator T(t) is injective, for all  $t \geq 0$ . The  $\omega$ -limit set of  $\psi$  is defined to be the set of all limit points of the set  $\{x_t:t\geq 0\}$ . This  $\omega$ -limit set is often denoted by  $\omega(x)$  and is (nonempty) compact and invariant under T(t), for each  $t \geq 0$ . Moreover, T(t) is a bijective mapping from this  $\omega$ -limit set into itself, for each  $t \geq 0$  (see [1]). Therefore, we can define T(t) = T(-t), for all t < 0, to obtain a one-parameter group  $\{T(t)\}_{t \in R}$  of operators from  $\omega(x)$  into itself. Letting  $u_0$  and  $v_0$  be functions in  $\omega(x)$ , such that  $u_0(0) = \sup\{\phi(0) : \phi \in \omega(x)\}$ and  $v_0(0) = \inf\{\phi(0) : \phi \in \omega(x)\}$ , it is easy to see that  $u_0(0) = \limsup_{t\to\infty} x(t)$  and  $v_0(0) = \max_{t\to\infty} x(t)$  $\liminf_{t\to\infty} x(t)$ . We now let  $u(t)=T(t)u_0(0)$  and  $v(t)=T(t)v_0(0)$ . Then, both u and v are solutions of (1.1), which can be extended to the whole real line. Moreover,  $u(t), v(t) \in [v(0), u(0)]$ , for all  $t \in \mathbb{R}$ . The constant variation formulae for the two full time solutions u(t) and v(t) are as follows:

$$u(t) = \int_{-\infty}^{t} e^{-\mu(t-\xi)} f(u(\xi-\tau)) d\xi,$$
 (2.3)

$$v(t) = \int_{-\infty}^{t} e^{-\mu(t-\xi)} f(v(\xi - \tau)) d\xi.$$
 (2.4)

587

#### 3. THE STABILITY

In what follows, we shall assume that the algebraic equation,

$$\mu K = f(K),$$

has the unique solution  $K = \bar{x}$  in  $(0, \infty)$ .

THEOREM 3. Suppose that f(x) is monotonically increasing and

$$\limsup_{x \to \infty} \frac{f(x)}{x} < \mu,\tag{3.1}$$

$$\lim_{x \to 0} \inf \frac{f(x)}{\tau} > \mu.$$
(3.2)

Then, every solution x(t) of (1.1) converges to  $\bar{x}$ .

PROOF. By Theorem 2, every solution x(t) of (1.1) is persistent. We can, therefore, choose two (full time) solutions u(t) and v(t), such that

$$u(0) = \limsup_{t \to \infty} x(t), \qquad v(0) = \liminf_{t \to \infty} x(t). \tag{3.3}$$

Using the constant variation formula, we have

$$u(0) = \int_{-\infty}^{0} e^{\mu\xi} f(u(\xi - \tau)) d\xi \le \int_{-\infty}^{0} e^{\mu\xi} f(u(0)) d\xi = \frac{f(u(0))}{\mu}$$
(3.4)

and similarly,

$$v(0) = \int_{-\infty}^{0} e^{\mu\xi} f(v(\xi - \tau)) d\xi \ge \int_{-\infty}^{0} e^{\mu\xi} f(v(0)) d\xi = \frac{f(v(0))}{\mu}, \tag{3.5}$$

If we let

$$\varphi(x)=\frac{f(x)}{x}-\mu,$$

then, it follows from (3.4) that  $\varphi(u(0)) \geq 0$  and from (3.5) that  $\varphi(v(0)) \leq 0$ . On the other hand, it follows from (3.1) that  $\limsup_{x\to\infty} \varphi(x) < 0$ , and from (3.2) that  $\liminf_{x\to 0} \varphi(x) > 0$ . If v(0) < u(0), we have at least 2 distinct zeros of  $\varphi(x)$  in (0, v(0)), (v(0), u(0)) and in  $(u(0), \infty)$ . This contradicts our assumption that  $\bar{x}$  is the only zero of  $\varphi$ . Thus,  $v(0) = u(0) = \bar{x}$ . We conclude that

$$\lim_{t\to\infty}x(t)=\bar{x}.$$

The proof is complete.

Theorem 4. Suppose that f(x) is monotonically decreasing and the following system

$$a = \frac{f(b)}{\mu},$$
$$b = \frac{f(a)}{\mu},$$

has a unique solution  $a = b = \bar{x}$ . Then, every solution x(t) of (1.1) converges to  $\bar{x}$ .

PROOF. By Theorem 2, every solution x(t) of (1.1) is persistent. We can, therefore, choose two (full time) solutions u(t) and v(t), such that

$$u(0) = \limsup_{t \to \infty} x(t), \qquad v(0) = \liminf_{t \to \infty} x(t). \tag{3.3'}$$

588

Using the constant variation formula, we have

$$u(0) = \int_{-\infty}^{0} e^{\mu \xi} f(u(\xi - \tau)) d\xi \le \int_{-\infty}^{0} e^{\mu \xi} f(u(0)) d\xi \le \frac{f(u(0))}{\mu} := b_1$$
 (3.4')

and similarly,

$$v(0) = \int_{-\infty}^{0} e^{\mu \xi} f(v(\xi - \tau)) d\xi \ge \int_{-\infty}^{0} e^{\mu \xi} f(v(0)) d\xi \ge \frac{f(v(0))}{\mu} := a_1.$$
 (3.5')

We now let

$$a_{n+1} = \frac{f(b_n)}{\mu}, \quad b_{n+1} = \frac{f(a_n)}{\mu}, \quad \text{for } n = 1, 2, \dots$$

Similarly to (3.4') and (3.5'), u(0) and v(0) belong to the interval  $[a_n, b_n]$ , for all  $n = 1, 2, \ldots$  On the other hand, the sequence  $\{a_n\}$  is monotonically increasing and the sequence  $\{b_n\}$  is monotonically decreasing so that they converge. Let a and b be their respective limits. Then, a and b satisfy the above system in the statement of our theorem. Our assumptions assure that  $a = b = \bar{x}$ . Therefore,  $u(0) = v(0) = \bar{x}$ . The proof is complete.

From this point on, we shall assume that, for some  $y_0 > 0$ , we have

$$f(y_0) = \max_{x > 0} f(x)$$

and f(x) is increasing in  $[0, y_0]$  and decreasing in  $(y_0, \infty)$ . That is, f(x) is called a unimodal function as we have mentioned in the abstract. Suppose further that x(t) is a persistent solution of (1.1). Let u(t) and v(t) be two (full time) solutions of (1.1) with respect to a persistent solution x. Using the constant variation formula, we have

$$u(0) = \int_{-\infty}^{0} e^{\mu \xi} f(x(\xi - \tau)) d\xi \le \int_{-\infty}^{0} e^{\mu \xi} f(y_0) d\xi = \frac{f(y_0)}{\mu}.$$
 (3.6)

THEOREM 5. Suppose that  $f(y_0) \le \mu y_0$ . Also, (3.1) and (3.2) are assumed to be true. Let x(t) be a persistent solution of (1.1). Then,  $\lim_{t\to\infty} x(t) = \bar{x}$ .

PROOF. From (3.6), we have  $u(t) \le u(0) < f(y_0)/\mu \le y_0$ . Since the function f is increasing in  $[0, y_0]$ , it follows from the constant variation formula that

$$u(0) = \int_{-\infty}^{0} e^{\mu\xi} f(u(\xi - \tau)) d\xi \le \int_{-\infty}^{0} e^{\mu\xi} f(u(0)) d\xi = \frac{f(u(0))}{\mu}$$
(3.4")

and similarly,

$$v(0) = \int_{-\infty}^{0} e^{\mu \xi} f(v(\xi - \tau)) d\xi \ge \int_{-\infty}^{0} e^{\mu \xi} f(v(0)) d\xi = \frac{f(v(0))}{\mu}.$$
 (3.5")

Let

$$\varphi(x) = \frac{f(x)}{x} - \mu.$$

It follows from (3.4") that  $\varphi(u(0)) \geq 0$  and from (3.5") that  $\varphi(v(0)) \leq 0$ . On the other hand, it follows from (3.1) that  $\limsup_{x\to\infty} \varphi(x) < 0$ , and from (3.2) that  $\liminf_{x\to 0} \varphi(x) > 0$ . If v(0) < u(0), we have at least 2 distinct zeros of  $\varphi(x)$  in (0,v(0)), (v(0),u(0)) and in  $(u(0),\infty)$ . This contradicts our assumption that  $\bar{x}$  is the only zero of  $\varphi$ . Therefore,  $v(0) = u(0) = \bar{x}$ . We conclude that

$$\lim_{t\to\infty}x(t)=\bar x$$

The proof is complete.

We can now state the following result.

THEOREM 6. Suppose that (3.2) holds. Suppose, moreover, that the solution of the following system of difference equations

$$a_{n+1} = \inf_{x \in [a_n, b_n]} \frac{f(x)}{\mu},$$

$$b_{n+1} = \sup_{x \in [a_n, b_n]} \frac{f(x)}{\mu}, \qquad n = 1, 2, ...,$$

$$a_1 = \inf_{x > 0} \frac{f(x)}{\mu},$$

$$b_1 = \sup_{x > 0} \frac{f(x)}{\mu}$$

converges to  $\bar{x}$ . Then, every persistent solution of (1.1) converges to  $\bar{x}$ .

#### 4. APPLICATION

Consider the Nicholson's model of a population of blowflies [2],

$$\dot{N}(t) = -\mu N(t) + \alpha N(t-\tau) \exp\left(-\beta N(t-\tau)\right).$$

Here,  $\alpha$  and  $\beta$  are positive parameters and

$$f(x) = \alpha x \exp(-\beta x).$$

If  $\alpha \leq \mu$ , using Theorem 1, we have  $\lim N(t) = 0$ . This means that if the death rate  $\mu$  is higher than  $\alpha$ , then, the population becomes extinct. On the other hand, if we now let  $\alpha > \mu$ , then using Theorem 2, we have

$$0 < \liminf N(t) \le \limsup N(t) < \infty$$

and the population persists. Moreover,

$$f'(x) = \alpha(1 - \beta x) \exp(-\beta x),$$

and the (only) positive equilibrium is

$$\bar{x} = \frac{1}{\beta} \ln \left( \frac{\alpha}{\mu} \right).$$

We have  $f'(1/\beta) = 0$  and  $f(1/\beta) = \max f(x) = \alpha/(e\beta)$ . From (3.6), we have

$$\limsup_{t\to\infty}N(t)<\frac{\alpha}{e\mu\beta}.$$

If  $\alpha \leq e\mu$ , then, from Theorem 5, we conclude that

$$\lim_{t\to\infty}N(t)=\bar{x}.$$

Next, we consider the population dynamics of baleen whales [2]:

$$\dot{N}(t) = -\mu N(t) + \mu N(t-\tau) \left\{ 1 + q \left[ 1 - \left( \frac{N(t-\tau)}{K} \right)^z \right] \right\}.$$

Here, all parameters are positive and

$$f(x) = \mu x \left\{ 1 + q \left[ 1 - \left( \frac{x}{K} \right)^z \right] \right\}$$

satisfies conditions (2.1) and (2.2), and so this population is persistent. Moreover,

$$f'(x) = \mu \left\{ 1 + q \left[ 1 - \left( \frac{x}{K} \right)^z \right] \right\} + \mu x q \left[ \left( -\frac{z}{K} \right) \left( \frac{x}{K} \right)^{z-1} \right] = \mu \left[ 1 + q - \frac{q(1+z)}{K^z} \cdot x^z \right],$$

and hence,

$$\max f(x) = f(y_0) = \mu y_0(1+q) \cdot \frac{z}{1+z},$$

where

$$y_0 = K \sqrt[z]{\frac{1+q}{q(1+z)}}$$

and the only positive equilibrium is

$$\bar{x} \approx K$$
.

From (3.6), we have

$$\limsup_{t\to\infty} N(t) < y_0(1+q) \cdot \frac{z}{1+z}.$$

To use Theorem 5, we must assume that  $f(y_0) \le \mu y_0$  or, equivalently,  $qz \le 1$ . In this case, we have  $\lim N(t) = K$ .

#### 5. CONCLUSION

We have given conditions on the function f, such that the solution of the population model equation

$$\dot{x}(t) = -\mu x(t) + f(x(t-\tau))$$

will persist or remain globally stable. We then discussed the applications of our results to the population dynamics of Nicholson's model of blowflies and that of baleen whales.

Finally, we note that the results proven here have not been shown by earlier researchers, who have worked only with delay differential equations where the function f is monotone decreasing [3-6]. The assumptions imposed on f in our theorems are less stringent than in any previous work so that they should be applicable to a large variety of ecological models.

#### REFERENCES

- 1. J. Hale, Introduction to functional differential equations, Springer Verlag, (1993).
- 2. M. Kot, Elements of Mathematical Ecology, Cambridge University Press, (2001).
- 3. Y. Kuang, Delay Differential Equations, Academic Press, (1977).
- Kubiaczyk and S. Saker, Oscillation and stability in nonlinear delay differential equations of population dynamics, Mathl. Comput. Modelling 35 (3/4), 295-301, (2002).
- S.H. Saker and S. Agarwal, Oscillation and global attractivity in a periodic nicholson's blowfiles model, Mathl. Comput. Modelling 35 (7/8), 719-731, (2002).
- S. Saker, Oscillation and global attractivity in hematopoiesis model with delay time, Appl. Math. Comput. 136, 241-250, (2003).



ScienceAsia 28 (2002) : 205-215

## Chaos and Control Action in a Kolmogorov Type Model for Food Webs with Harvesting or Replenishment

#### Yongwimon Lenbury\*, Adoon Pansuwan, Nardfida Tumrasvin

Department of Mathematics Faculty of Science, Mahidol University, Rama 6 Rd, Bangkok 10400, Thailand.

\* Corresponding author, E-mail: scylb@mahidol.ac.th

Received 11 Sep 2001 Accepted 8 Feb 2002

**ABSTRACT** In this paper, we apply the feedback decoupling technique to a Kolmogorov type model for three species food webs with harvesting or replenishment. A feedback control law is derived to decouple the effect of predators from prey dynamics. It is found that the necessary and sufficient conditions for the existence of the decoupling control law rely on the persistence of the prey population and the fact that the specific growth rate of prey depends explicitly on the superpredator population density at any moment in time. It is shown that, without any control action of regulated replenishment or harvesting, irregular or chaotic behavior is possible in such a process for certain ranges of the system parameters. This is illustrated by the construction of a bifurcation diagram for a model of a three-species food web with response functions of the Holling type II. To make the system output or variables less sensitive to irregular disturbances, the feedback control technique is applied which produces the desirable effect of stabilizing the system. When such a model is applied to an activated sludge process, the objective of the control action can also be to regulate the inputs in order to obtain satisfactory water quality.

KEYWORDS: Kolmogorov model - control - chaos - stabilization.

#### INTRODUCTION

Ecological models may be classified as either strategic or tactical, as identified by Holling (1966). Tactical models are relatively more complex. They usually rely on a great amount of supporting data, and are used for making specific predictions. Strategic models, on the other hand, can provide broader insights into possible behaviors of the system based on simple assumptions (McLean and Kirkwood, 1990), such as the model considered by Hadeler and Freedman (1989) for predator-prey populations with parasitic infection, or the model of continuous bioreactor analyzed by Lenbury and Orankitjaroen (1995).

As Mosetti (1992) has observed, the control of ecological systems for management purposes is a difficult task due to the amount of supporting data needed as well as the conflicting management goals. In this respect, a simple reduced strategic model which requires fewer data for calibration can be quite a useful tool as a building block for the study of real problems in order to give a decision-maker some preliminary results.

The Kolmogorov model of population growth is, mathematically, probably the most general model of the types considered to date. It incorporates the principle that the growth rate of species is proportional to the number of interacting species present. The classical ecological models of interacting populations have typically focussed on two species. The first Kolmogorov model, developed in 1936, was expanded on by several researchers, including May (1972) and Albrecht et al (1974). Such models have been applied to plant and animal dynamics both in aquatic and terrestrial environments (Hastings and Powell, 1991). However, mathematical developments reveal that community models involving only two species as the building blocks may miss a great deal of important ecological behavior. In fact, it is now recognized that in community studies the essence of the behavior of a complex system may only be understood when attempts are made to incorporate the interactions among a larger number of species.

Researchers in the last decade or so have turned their attention to the theoretical study of food webs as the "building blocks" of ecological communities and have been faced with the problem of how to couple the large number of interacting species. Behavior of the entire community is then assumed to arise from the coupling of strongly interacting pairs. The approach is attractive by its virtue of being tractable to theoretical analysis (Hastings and Powell, 1991). Yet, many researchers have demonstrated that

very complex dynamics can arise in model systems with three species (Gilpin, 1979; Rai and Sreenivasan, 1993). For example, an investigation by Hastings and Powell (1991) showed that a continuous time model of a food chain incorporating nonlinear functional responses can exhibit chaotic dynamics in long-term behavior when reasonable parametric values are chosen. The key feature observed in this chaotic dynamics is the sensitive dependence on initial conditions.

In this paper, we first study the possibility of making the ecosystem output or variables less sensitive to irregular disturbances by applying the feedback control technique in order to stabilize the system. A feedback control law is derived to decouple the effect of the predators from the prey dynamics in a three-species food web of the Kolmogorov type. It is found that the necessary and sufficient conditions for the existence of the decoupling control law rely on the persistence of the prey population and the fact that the specific growth rate of prey depends explicitly on the superpredator population density at any moment in time.

We demonstrate by the construction of a bifurcation diagram for a model with response functions of the Holling type II that, without any control action, chaotic behavior may result through period doubling bifurcations. Once, the feedback decoupling control action is in place, the system can be stabilized and, in this context, we obtain a process which is more easily controllable.

Moreover, when the Kolmogorov type model with input / removal terms is applied to an activated sludge process, the main objective is perhaps to regulate the inputs in order to obtain satisfactory water quality. By simply fine-tuning the point in time when the control action is set in motion, the control technique considered here can be adjusted to give the desirable outcome.

## THE KOLMOGOROV TYPE MODEL AND THE STATIC DECOUPLING PROBLEM

We consider a general Kolmogorov type model of n-species food webs, which may be written as follows

$$X_i = X_i F_i + u_i, i = 1, 2, ..., n$$
 (1)

where  $X_i$  is the *i-th* species population density,  $u_i$  is the input/removal (replenishment/harvesting) rate

of the species which depends on the population densities of all n-species in the food web, and

$$F_i = F_i(X_1, X_2, ...X_n), i = 1, 2, ..., n$$

Such a system (1) can be used to model population dynamics of plant or animal interactions in an aquatic or terrestorial environment such as in the work of Lenbury and Siengsanan (1993), where an activated sludge process was analyzed using a three-species Kolmogorov type model. Also, in the study by Lenbury and Likasiri (1994), the dynamic behavior of a model for a food web was investigated through the application of the singular perturbation technique.

To formulate the static feedback decoupling problem, we let

$$X = (X_1, X_2, ... X_n)^t$$
  

$$F = (F_1, F_2, ... F_n)^t$$
  

$$U = (u_1, u_2, ... u_{n-1})^t$$

and

$$G(X) = \begin{pmatrix} 1 & 0 & 0 & \cdots & 0 \\ 0 & 1 & 0 & \cdots & 0 \\ \vdots & \vdots & \ddots & \cdots & \vdots \\ 0 & 0 & 0 & \cdots & 1 \\ 0 & 0 & 0 & \cdots & 0 \end{pmatrix}$$

an  $n \times (n-1)$  matrix.

Then, the system of equations (1) with  $u_n = 0$  can be rewritten as

$$X_i = X_i F_i + [GU]_i, \quad i = 1, 2, ..., n$$
 (2)

If we now take  $X_1$  to be the state variable which is more easily regulated externally, the "outcome" or output of equation (2) is then assumed to be

$$H(X) \equiv (X_n, X_2, \dots X_{n-1})^t$$
 (3)

The static feedback decoupling problem, as stated in the work by Mosetti (1992) and explained in greater detail by Isidori (1985), can be defined as follows. "Given equations (2) and (3), we need to find a feedback law  $\alpha(X)$  and a state-dependent change of coordinates  $\beta(X)$  in the input space  $\mathfrak{R}^n$  such that the closed-loop system formed by the combination of (2) and (3) with the control law

$$U = \alpha(X) + \beta(X)V$$
,  $U \in \Re^{n-1}$ ,  $V \in \Re^{n-1}$ 

has the i-th output dependent only on the i-th component of the new input V".

In order to accomplish this, we introduce the following notation. Letting

$$\nabla^* = \left( X_1 \frac{\partial}{\partial X_1} \quad X_2 \frac{\partial}{\partial X_2} \quad \cdots \quad X_n \frac{\partial}{\partial X_n} \right)$$

then the operator  $\nabla_F$  is defined as

$$\nabla_F H_i = F \nabla^* H_i$$

where  $H_i$  is the *i-th* component of the vector H(x)defined in (3).

We then understand that

$$\nabla_F^k H_i = \nabla_F (\nabla_F^{k-1} H_i)$$

while  $\nabla_{F}^{0}H_{i}=H_{i}$ .

Further, the characteristic number  $\rho_i$  associated with the output  $H_i$  can be defined as the largest integer such that for all  $k < \rho_i$ 

$$grad(\nabla_F^k H_i)G_j = 0$$
 ,  $j = 1, 2, ..., n-1$ 

where  $G_i$  is the *j-th* column of the matrix G.

Accordingly, the decoupling matrix A(X)associated with equations (2) and (3) is the (n-1)x(n-1) matrix

$$A(X) = \left(a_{ij}\right)$$

where

$$a_{ij} = \operatorname{grad}(\nabla_F^{\rho_i} H_i) G_j$$

The static state-feedback decoupling theory (Mosetti, 1992) can be stated as follows.

Theorem 1A necessary and sufficient condition for the existence of  $(\alpha, \beta)$  which solves the decoupling problem is that the decoupling matrix A(x) is nonsingular. If this is the case then a possible decoupling control is given by

$$\alpha(X) = -A^{-1}(X)J$$
 and 
$$\beta(X) = A^{-1}(X)$$

where

$$J = (\nabla_F^{\rho_1+1} H_1, \nabla_F^{\rho_2+1} H_2, ..., \nabla_F^{\rho_n+1} H_n)'$$

provided that the decoupling matrix A(X) is nonsingular.

Proof We refer readers to Isidori's work (1985) for the proof of this theorem in the general case.

In order to establish the control law for the Kolmogorov type model, we need to first prove the following Lemma.

Lemma 1The characteristic number  $\rho_1 = 1$  and  $\rho_i$ = 0, i = 2, 3, ..., n - 1.

Proof In the case of  $\rho_1$  (i = 1), we first consider grad  $(\nabla_F^k H_1)G_j$ , j=1, 2, ..., n-1, when k=0. We find that

$$\operatorname{grad}\left(\nabla_{F}^{0}H_{1}\right)G_{j}=\operatorname{grad}\left(X_{n}\right)G_{j}$$

$$= \left(\frac{\partial X_n}{\partial X_1} \frac{\partial X_n}{\partial X_2} \dots \frac{\partial X_n}{\partial X_n}\right) \begin{bmatrix} 0 \\ 0 \\ \vdots \\ 0 \\ 1 \\ 0 \\ \vdots \\ 0 \end{bmatrix} \leftarrow j - th \text{ row}$$

$$= \begin{pmatrix} 0 & 0 & \dots & 0 & 1 \end{pmatrix} \begin{pmatrix} 0 \\ 0 \\ \vdots \\ 0 \\ 1 \\ 0 \\ \vdots \\ 0 \end{pmatrix} \leftarrow j - th \text{ row}$$

$$= 0$$

since j < n.

However, when k = 1, we find  $\operatorname{grad} \left( \nabla_F^1 H_1 \right) G_j = \operatorname{grad} \left( \nabla_F^1 X_n \right) G_j$ 

$$= \operatorname{grad} \left\{ \begin{pmatrix} F_1 & F_2 & \cdots & F_n \end{pmatrix} \middle| \begin{array}{c} X_1 \frac{\partial X_n}{\partial X_1} \\ X_2 \frac{\partial X_n}{\partial X_2} \\ \vdots \\ X_n \frac{\partial X_n}{\partial X_n} \end{array} \right\} G_j$$

= grad  $(F_n X_n) G_n$ 

$$= \left(\frac{\partial}{\partial X_{1}} \left(F_{n} X_{n}\right) \frac{\partial}{\partial X_{2}} \left(F_{n} X_{n}\right) \dots \frac{\partial}{\partial X_{n}} \left(F_{n} X_{n}\right)\right) \begin{vmatrix} 0\\0\\\vdots\\0\\1\\0\\\vdots\\0 \end{vmatrix}$$

$$\leftarrow j - th \text{ row}$$

$$= \frac{\partial}{\partial X_{j}} (X_{n} F_{n}) = X_{n} \frac{\partial F_{n}}{\partial X_{j}}$$

$$\neq 0$$

if we assume that  $F_n$  is an explicit function of  $X_i$  for all  $j=1,\,2,\,...,\,n-1$ . Therefore,  $\rho_1=1$ .

Now, for  $\rho_i$ , i = 2, 3, ..., n - 1, we consider grad  $(\nabla_F^k H_i)G_j$  for  $i \ge 2$  when k = 0, and obtain  $\operatorname{grad}\left(\nabla_{F}^{0}H_{i}\right)G_{i}=\operatorname{grad}\left(X_{i}\right)G_{i}$ 

$$= \left(\frac{\partial X_{i}}{\partial X_{1}} \frac{\partial X_{i}}{\partial X_{2}} \cdots \frac{\partial X_{i}}{\partial X_{j}} \cdots \frac{\partial X_{i}}{\partial X_{n}}\right) \begin{bmatrix} 0\\0\\\vdots\\0\\1\\0\\\vdots\\0 \end{bmatrix} \leftarrow j-th \text{ row}$$

$$A(x) = \begin{bmatrix} X_{n} \frac{\partial F_{n}}{\partial X_{1}} & X_{n} \frac{\partial F_{n}}{\partial X_{2}} & \cdots & \cdots & X_{n} \frac{\partial F_{n}}{\partial X_{n-1}}\\0 & 1 & 0 & 0 & \cdots & 0\\0 & 0 & 1 & 0 & \cdots & 0\\\vdots & \vdots & \vdots & \vdots & \vdots & \cdots & \vdots\\0 & 0 & 0 & 0 & \cdots & 1 \end{bmatrix}$$

$$= \begin{cases} 1 & \text{if } i = j \\ 0 & \text{if } i \neq j \end{cases}$$

Thus, grad  $(\nabla_F^0 H_i)G_j \neq 0$  for some j, which means that  $\rho_i = 0$  for i = 2, 3, ..., n - 1.

We can now derive the entries  $a_{ij}$  of the decoupling matrix A(x) as follows.

$$a_{ij} = \operatorname{grad} \left( \nabla^{1}_{F} H_{i} \right) G_{j}$$

$$= \operatorname{grad} \left\{ \left( F_{1} \quad F_{2} \quad \cdots \quad F_{n} \right) \left( \begin{array}{c} X_{1} \frac{\partial X_{n}}{\partial X_{1}} \\ X_{2} \frac{\partial X_{n}}{\partial X_{2}} \\ \vdots \\ X_{n} \frac{\partial X_{n}}{\partial X_{n}} \end{array} \right) \right\} G_{j}$$

= grad 
$$(F_n X_n) G_j$$
  
=  $X_n \frac{\partial F_n}{\partial X_j}$ 

for j = 1, 2, ..., n - 1.

On the other hand, for  $i \ge 2$ ,  $\rho_i = 0$ , we therefore obtain -

$$a_{ij} = \operatorname{grad} \left( \nabla_F^0 H_i \right) G_j$$
$$= \begin{cases} 1 & \text{if } i = j \\ 0 & \text{if } i \neq j \end{cases}$$

for j = 1, 2, ..., n - 1 and i = 2, 3, ..., n - 1. Thus, the decoupling matrix is

$$A(x) = \begin{bmatrix} X_{n} \frac{\partial F_{n}}{\partial X_{1}} & X_{n} \frac{\partial F_{n}}{\partial X_{2}} & \cdots & \cdots & X_{n} \frac{\partial F_{n}}{\partial X_{n-1}} \\ 0 & 1 & 0 & 0 & \cdots & 0 \\ 0 & 0 & 1 & 0 & \cdots & 0 \\ \vdots & \vdots & \vdots & \vdots & \cdots & \vdots \\ 0 & 0 & 0 & 0 & \cdots & 1 \end{bmatrix}$$

209

ScienceAsia 28 (2002)

#### APPLICATION TO THREE SPECIES FOOD WEBS

The control law

We now derive the control law for the Kolmogorov type model for a three species food web which can be written as

$$x = x f(x, y, z) + u_1$$
 (4)

$$y = y g(x, y, z) + u_2$$
 (5)

$$z = z h (x, y, z)$$
 (6)

where z is the prey population density, y and x are the predator and superpredator, respectively, while  $u_1$  and  $u_2$  are the corresponding input rates. Then,

$$X = \begin{pmatrix} x & y & z \end{pmatrix}'$$

$$F = (f & g & h)$$

$$U = \begin{pmatrix} u_1 & u_2 \end{pmatrix}'$$

$$G(X) = \begin{pmatrix} 1 & 0 \\ 0 & 1 \\ 0 & 0 \end{pmatrix}$$

and the output is

$$H(X) = \begin{pmatrix} z & \nu \end{pmatrix}' \tag{7}$$

The main result of the static state-feedback decoupling theory can be stated as follows.

Theorem 2A necessary and sufficient condition for the existence of  $(\alpha, \beta)$  which solves the decoupling problem for equations (4)-(6) is that the prey population persists and the specific growth rate of prey h depends explicitly on the superpredator population density. If this is the case, then a possible decoupling control is given by:

$$\alpha(X) = \left(-xf - \frac{h}{h_x}(zh_z + h) - yg\right)^{t}$$

$$\beta(X) = \left(\frac{1}{zh_x} - \frac{h_y}{h_x}\right)$$

and

$$u_1 = -xf - \frac{h}{h_x}(zh_z + h) + \frac{1}{zh_x}v_1 - \frac{h_y}{h_x}v_2$$
 (8)

$$u_2 = -yg + V_2 \tag{9}$$

**Proof** From Lemma 1, we found that  $\rho_1 = 1$  and  $\rho_2 = 0$ . We then obtain

$$\nabla^* H_1 = \begin{pmatrix} 0 & 0 & z \end{pmatrix}'$$

so that  $\nabla^1_F H_1 = zh$ , and  $\nabla^0_F H_2 = y$ . Therefore, we are led to the decoupling matrix

$$A(X) = \begin{pmatrix} zh_x & zh_y \\ 0 & 1 \end{pmatrix} \tag{10}$$

Thus, A(X) is nonsingular if and only if det  $A \neq 0$ , namely

$$zh_{\nu} \neq 0$$
 (11)

This leads to the requirement that prey persists, in which case z > 0, and that  $h_x \neq 0$  or, equivalently, h depends explicitly on x.

Moreover, we have

$$\nabla_F^{\rho_1+1} H_1 = \nabla_F^2(z) = \nabla_F \{\nabla F(z)\}$$

$$= \nabla_{F} \left\{ \left( f \quad g \quad h \right) \begin{pmatrix} x \frac{\partial z}{\partial x} \\ y \frac{\partial z}{\partial y} \\ z \frac{\partial z}{\partial z} \end{pmatrix} \right\}$$

$$=\nabla_{F}(hz)$$

$$= \begin{pmatrix} f & g & h \end{pmatrix} \begin{pmatrix} x \frac{\partial}{\partial x} (hz) \\ y \frac{\partial}{\partial y} (hz) \\ z \frac{\partial}{\partial z} (hz) \end{pmatrix}$$

$$= xzfh_x + yzgh_y + z^2hh_z + zh^2$$

Also,

.

$$\nabla_F^{\rho_2+1} H_2 = \nabla_F^1(y)$$

$$= \begin{pmatrix} f & g & h \end{pmatrix} \begin{pmatrix} x \frac{\partial y}{\partial x} \\ y \frac{\partial y}{\partial y} \\ z \frac{\partial y}{\partial z} \end{pmatrix}$$

$$= gy$$

Therefore,

$$J = (\nabla_E^{\rho_1+1} H_1 \quad \nabla_E^{\rho_2+1} H_2)$$

$$= \begin{pmatrix} xzfh_x + yzgh_y + z^2hh_z + zh^2 \\ gz \end{pmatrix}$$

which leads us to

$$\alpha(X) = -A^{-1}(X)J$$

$$= -\left(\frac{1}{zh_x} \frac{h_y}{h_x}\right) \left(xzfh_x + yzgh_y + z^2hh_z + zh^2\right)$$

$$gy$$

$$= \begin{pmatrix} -xf - zh\frac{h_z}{h_x} - \frac{h^2}{h_x} \\ -gv \end{pmatrix}$$

while

$$\beta(X) = A^{-1}(X)$$

$$= \begin{pmatrix} \frac{1}{zh_x} & \frac{h_y}{h_x} \\ 0 & 1 \end{pmatrix}$$

as claimed.

If we now let

$$\xi = \frac{dz}{dt} \tag{12}$$

then, since z = zh, we have

$$\frac{d\xi}{dt} = \frac{\partial(zh)}{\partial x}x + \frac{\partial(zh)}{\partial y}y + \frac{\partial(zh)}{\partial z}z$$

$$= zh_x(xf + u_1) + zh_y(yg + u_2) + (zh_z + h)zh = V_1$$

by applying the law in equations (8) and (9). Also, using (9), we find

$$\frac{dy}{dt} = yg + u_2 = v_2$$

Therefore, in the new coordinate system  $(\xi, y, z)$  we have

$$\frac{d\xi}{dt} = V_1 \tag{13}$$

$$\frac{dy}{dt} = v_2 \tag{14}$$

$$\frac{dz}{dt} = \xi \tag{15}$$

which clearly shows the decoupled structure, namely, each of the control variables acts only on one state variable. In fact, to keep the system decoupled, one approach is to set  $v_1=0$ . Then,  $\xi$  now remains constant, say at  $\xi(t_0)$ .

Integrating (15), we obtain

$$z(t) = \xi(t_0)t = z(t_0)$$

Thus, if  $\xi(t_0) = 0$  at a given initial time  $t = t_0$  when the control is activated, then

$$z(t) = z(t_0)$$

for any subsequent time t, whatever the fluctuation of  $v_2$ . This means that the prey population will not depend upon variations in the predator or superpredator. This is the essential feature of this technique, whereby the variations in the predator and superpredators are decoupled from the prey dynamics.

#### Persistence conditions

The question of persistence has been dealt with in various literature in all its versions: weak persistence; strong persistence; and uniform persistence

211

ScienceAsia 28 (2002)

(Huaping and Zhien, 1991). We shall give, in the following Lemma, the persistence conditions for the standard food web consisting of equations (4)-(6) with

$$f(x, y, z) = \frac{c_2 y}{b_2 + y} + \frac{c_3 z}{b_3 + z} - d$$
 (16)

$$g(x, y, z) \equiv \frac{c_1 z}{b_1 + z} + \frac{a_2 x}{b_2 + y} - d$$
 (17)

$$h(x, y, z) \equiv r(1 - \frac{z}{k}) - \frac{a_1 y}{b_1 + z} - \frac{a_3 x}{b_1 + z}$$
 (18)

where d is the specific removal rate, and the terms

$$\frac{c_i z}{b_i + z}, \quad i = 1, 3$$

and

$$\frac{c_2y}{b_2+y}$$

ţ

are the population response functions of the Holling type II in which  $c_i$  is the maximum growth rate and  $b_i$  is the so-called half-saturation constant. The construction and analysis of the model in the case that  $u_1 = u_2 = 0$  may be found in the work of Lenbury and Likasiri (1994).

A standard food web given by equations (4)-(6) with (16)-(18) generally possesses only one positive equilibrium  $\hat{E} = (0, \hat{y}, \hat{z})$  and possibly only one

positive limit cycle  $\hat{\Gamma} = (0, \hat{y}(t), \hat{z}(t))$  for its subsystem (5)-(6) with x set equal to zero. Under this assumption, we are led to the following Lemma.

Lemma 2The food web given by equations (4)-(6) with (16)-(18) is persistent if

$$\frac{c_2 \stackrel{\circ}{y}}{\underset{b_2 + y}{\wedge}} + \frac{c_3 \stackrel{\circ}{z}}{\underset{\circ}{\wedge}} > d \tag{19}$$

and (in the case that  $\hat{\Gamma}$  exists)

$$\frac{1}{T} \int_{0}^{T} \left( \frac{c_{2} \dot{y}(t)}{b_{1} + \dot{y}(t)} + \frac{c_{3} \dot{z}(t)}{b_{1} + \dot{z}(t)} \right) dt > d \quad (20)$$

where T is the period of the limit cycle  $\prod$ , provided that  $u_1$  and  $u_2$  are identically zero. Otherwise, the population persists if

$$u_1(0, y, z) > 0$$
 (21)

and (in the case that  $\stackrel{\hat{}}{\Gamma}$  exists)

$$\frac{1}{T} \int_0^T u_1(0, \hat{y}(t), \hat{z}(t)) dt > 0$$
 (22)

**Proof** This is a straight forward extension of the result given in one of our earlier papers (Lenbury and Likasiri, 1994) with the addition of the input/removal terms  $u_1$  and  $u_2$ .

Consequently, on substituting (16)-(18) into (8) and (9), one obtains the following decoupling feedback law.

$$u_{1} = -x \left( \frac{c_{2}y}{b_{2} + y} + \frac{c_{3}z}{b_{3} + z} - d \right)$$

$$+ \frac{z(b_{3} + z)}{a_{3}} \left( x(1 - \frac{z}{k}) - \frac{a_{1}y}{b_{1} + z} + \frac{a_{3}x}{b_{3} + z} \right) \left( x(1 - \frac{2z}{k}) - \frac{a_{1}b_{1}y}{(b_{1} + z)^{2}} + \frac{a_{3}b_{3}x}{(b_{2} + z)^{2}} \right)$$

$$-\frac{b_3+z}{a_3z}V_1 - \frac{a_1(b_3+z)}{a_2(b_1+z)}V_2$$
 (25)

$$u_2 = -y \left( \frac{c_1 z}{b_1 + z} - \frac{a_2 x}{b_2 + y} - d \right) + v_2$$
 (26)

Figure 1 shows the time courses of the three state variables and the discharge rates  $u_1$  and  $u_2$  under normal conditions. We then chose to start our control action at the time  $t = t_0$  shown in the Figure

where  $z = \xi(t_0) = 0$ . Thus, the effect of the control action is seen in Figure 2 when the new input  $v_1$  is set equal to zero and  $v_2$  is taken to be of the form

$$V_2 = Ae^{-\mu} \sin \omega t$$

which corresponds to a damped sinusoidal input. The prey population density z becomes constant after the time  $t_0$ , while the predator and superpredator vary in a sinusoidal fashion with damping amplitude. As time passes, the new input rate  $\mathbf{v}_2$  becomes negligibly small and the corresponding population densities of all three species are maintained at constant levels as a result.

#### CONTROL ACTION ON A CHAOTIC SYSTEM

In the work by Lenbury and Likasiri (1994), the model of a food web given by equations (4)-(6) with (16)-(18) and  $u_1 = u_2 = 0$  have been analyzed using the singular perturbation method. Explicit conditions were derived which separate the various dynamic structures and identify the limit cycles composed of alternately slow and fast transitions. In particular, it was found that the system will have a unique global attractor in the first octant which is a low-frequency limit cycle with a period of high-frequency oscillation if the following conditions hold on the system parameters.

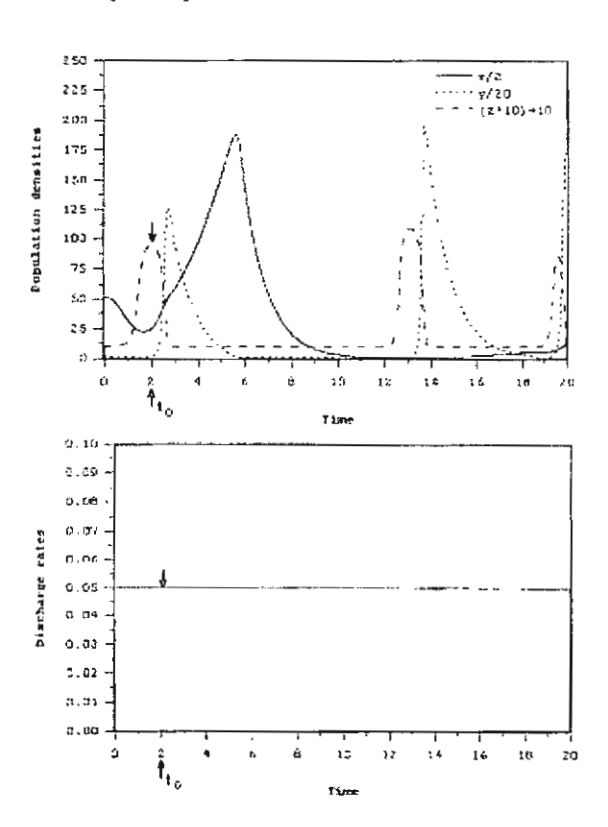


Fig 1. Time evolution of superpredator x (———), predator y (………), and prey z ( \_ \_ \_ \_ \_ \_ ), and constant discharge rates  $u_1$  and  $u_2$  with no control action. Here,  $a_1 = 0.05$ ,  $a_2 = 0.5$ ,  $a_3 = 0.5$ ,  $b_1 = 4.0$ ,  $b_2 = 8.0$ ,  $b_3 = 8.0$ ,  $c_1 = 15.0$ ,  $c_2 = 1.5$ ,  $c_3 = 1.5$ , d = 1.0, k = 10.0, r = 10.0,  $u_1 = 0.05$ , and  $u_2 = 0.05$ .

$$\frac{4a_1b_1b_2c_1k}{(b_1+k)^2} < \frac{r(b_3-b_1)[c_1(k-b_1)-d(b_1+k)]}{2b_3+k-b_1}$$
 (27)

$$k(c_1 - d) > b_1(c_1 + d)$$
 (28)

$$\frac{b2(c_1k-b_1d-dk)}{a_2(b_1+k)} < \frac{b_1b_3(a_1+r)[c_1(k-b_3)-d(2b_1+k-b_3)]}{(a_1b_3-a_3b_1d)(2b_1+k-b_3)+a_3b_1c_1(k-b_3)}$$
(29)

and 
$$\frac{c_i}{d}$$
 ( $i=1,2,3$ ) are sufficiently high.

We now carry out a numerical investigation to determine the ranges of parametric values where chaotic dynamics were likely. Our choice of parameters was guided by two factors. First, we follow the example of the work by Lenbury and Likasiri (1994) and assume that the ecological system under study may be characterized by highly diversified dynamics. Accordingly, we chose parametric values so that the time response of the

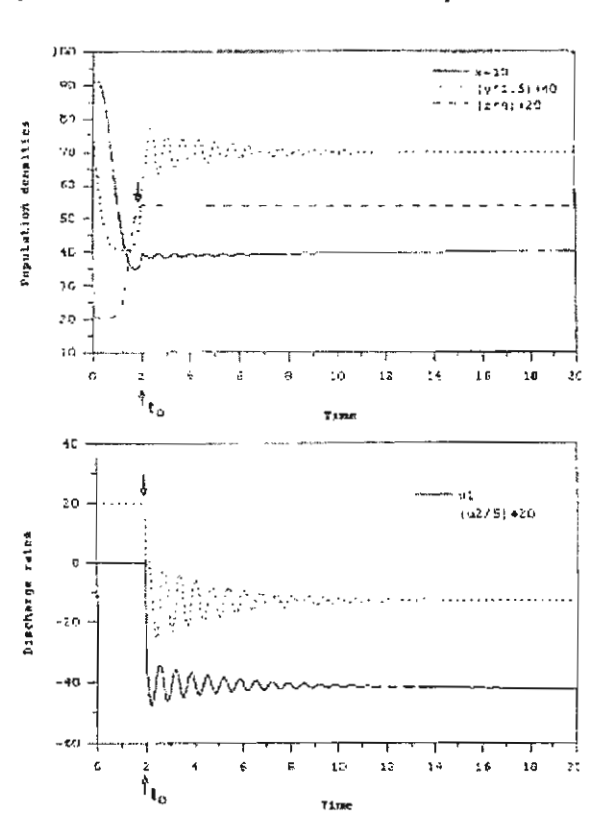


Fig 2. Time evolution of superpredator x, predator y, and prey z, and discharge rates  $u_1$  and  $u_2$  under control operations starting at  $t=t_0$  with  $v_1=0$  and  $v_2=100e^{\nu/3}\sin 3\pi t$ , and other system parameters as in Figure 1.

system equations (4)-(6) increases from top to bottom. The prey is assumed to have very fast dynamics, while the predator and superpredator have intermediate and slow dynamics, respectively. Phytoplankton - zooplankton - fish is a typical example of an ecosystem where the time response increases with the trophic levels. In fact, most food chains observed in nature have time responses increasing along the chain from top to bottom.

Second, as has been noted by many previous workers (Hastings and Powell, 1991; Rai and Sreenivasan, 1993), one may be able to generate chaos in a nonlinear system which already exhibits limit cycle behavior. We therefore chose parametric values to satisfy the conditions (27)-(29) found by Lenbury and Likasiri (1994) to lead to a solution trajectory on a low frequency limit cycle with bursts of high frequency oscillations.

Our investigation involves letting the system run for 100,000 time steps and examining only the last 80,000 time steps to eliminate transient behavior. We use values of  $b_1$  between 4.0 and 4.5, changing  $b_1$  in steps of 0.01. The relative maximum values  $\mathbf{x}_{\text{max}}^{1}$  of  $\mathbf{x}$ , collected during the last 80,000 time steps, are plotted as a function of  $b_1$  as shown in Figure 3.

We discover in this bifurcation diagram the appearance of a period doubling route to chaos, similar to those exhibited by one-dimensional difference equations such as the logistic population model. Apparently, the system of equations (4)-(6) with (16)-(18) exhibits chaotic dynamics for the values of  $b_1$  between 4.22 and 4.32. Windows in the bifurcation diagram are observed for  $b_1$  in the ranges of  $4.26 < b_1 < 4.32$  and  $4.34 < b_1 < 4.40$ , for example, where periodicity is re-established.

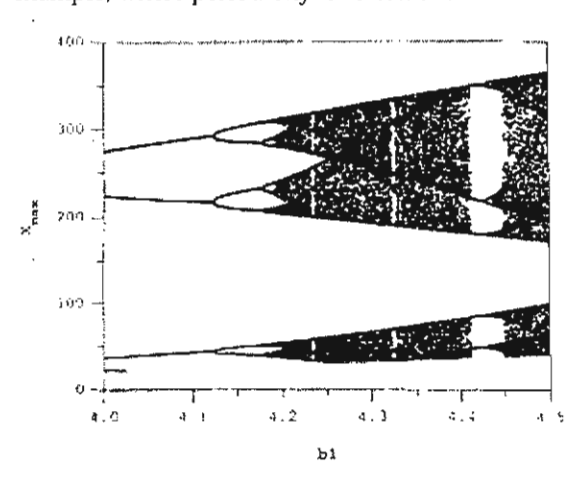


Fig 3. Bifurcation diagram for the model system (4)-(6) with (16)-(18), using the value of b<sub>1</sub> from 4.0 to 4.5, and other parametric values as in Figure 1. Plots are of the relative maximum values of x vs b<sub>1</sub>.

Figure 4 shows the solution trajectory of the model system (4)-(6) with (16)-(18) using  $b_1$  = 4.3 in the chaotic range identified in the bifurcation diagram. The strange attractor is projected onto the (y, z)-plane in Figure 4, and the corresponding chaotic time courses of x, y and z in uncontrolled conditions are shown in Figure 5 with the discharge rates  $u_1$  and  $u_2$ .

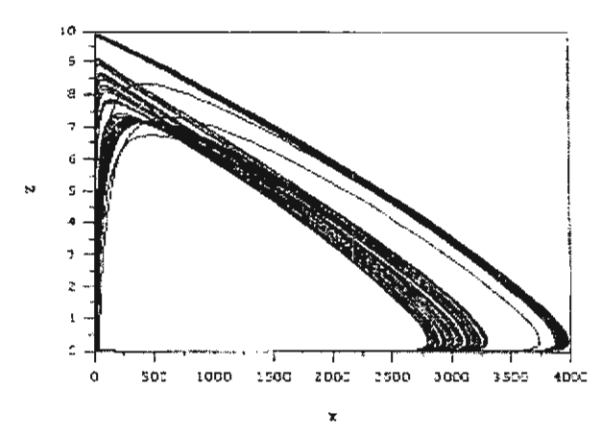


Fig 4. Projection onto the (y,z)-plane of the strange attractor obtained on simulating the model system (4)-(6) with (16)-(18) using  $b_1 = 4.3$  in the chaotic range identified in the bifurcation diagram, and other parametric values as in Figure 1.

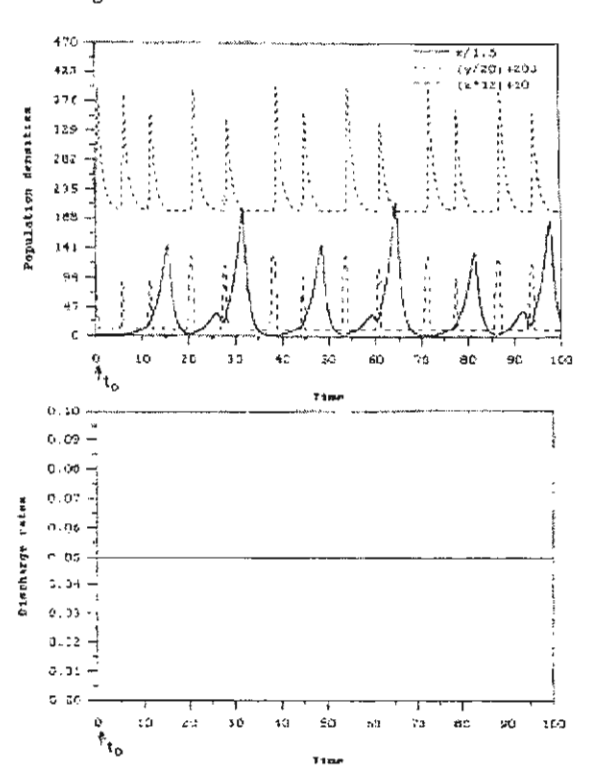


Fig 5. Time courses of the three state variables exhibiting chaotic behavior when there is no control action, and parametric values are as in Figure 4.

214 ScienceAsia 28 (2002)

Figure 6 shows the time courses of z starting from two different initial conditions. The difference in the two starting values of z is merely 0.01. We observe that, while the two plots follow indistinguishable paths during the initial short period, they begin to diverge and follow noticeably different paths eventually. This clearly demonstrates the sensitivity to initial conditions which is the essential characteristics of chaotic behavior.

Figure 7 then shows the effect of the control action on the chaotic system of Figure 4 with  $v_1$  set equal to zero and  $v_2$  irregular. Here, the control is ... initiated at the point where  $z(t_0) = 0$  and  $z(t_0) < 0$ . Once the control action is in place, prey is maintained at a constant high level, while the variations in predator, superpredator, and the discharge rates  $u_1$  and  $u_2$  are irregular.

On applying the model to an activated sludge process, the state variables can be nutrient-bacteria-protozoa, for example, and the objective of the control action is perhaps to regulate the inputs in order to obtain satisfactory water quality. In such a case, it is desirable to start the control action when the variable z falls to its first lowest point  $(z(t_0) = 0)$  and  $z(t_0) > 0$ . We will then be able to maintain z at a constant low level.

#### CONCLUSION

It has been demonstrated that while some inherent properties of a nonlinear model permit the emergence of chaotic dynamics, they also allow the existence of a feedback decoupling control mechanism. Since the behavior of the entire community is believed to arise from the coupling of these strongly interacting species, the detection and possibility of control of a chaotic system is of critical importance. If a generalization from a food web model depends crucially upon behavior after a long time, then the role of chaos may be extremely relevant.

On a cautious note, the question of whether or not deterministic chaos actually occurs in a real ecosystem is still open to discussion. As has been observed by Sabin and Summers (1993), "... there is still no generally accepted example of a chaotic ecosystem in nature. Moreover, some traditional ecologists believe that irregular oscillations in natural populations are attributed to random perturbations or noise in the environment rather than being the result of the intrinsic nonlinear dynamics of the system".

Perhaps the first concrete example of occurrence of chaos in nature is due to Sugihara and May (1990) who showed that there underlies a three-dimensional chaotic attractor in the dynamics of marine planktonic diatoms. Despite the fact that the corresponding time series is very noisy, they have been able to extract the information which allows them to describe some of the dynamics as deterministic chaos.

Such irregular behavior is not desirable when one is interested in managing a system, since chaos allows

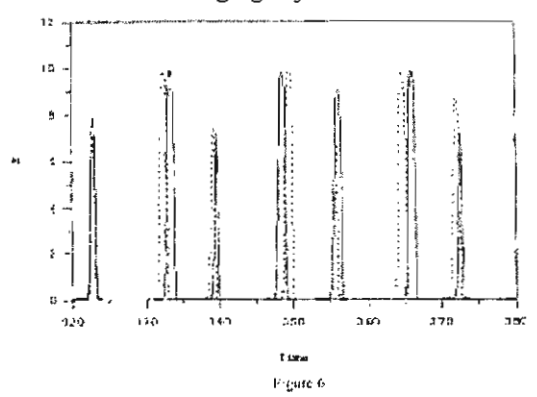


Fig 6. Divergence of solutions when the system exhibits chaotic dynamics. Prey densities are plotted for two different initial conditions ( \_\_\_\_\_ and \_\_\_\_), differing only by 0.01 in z.

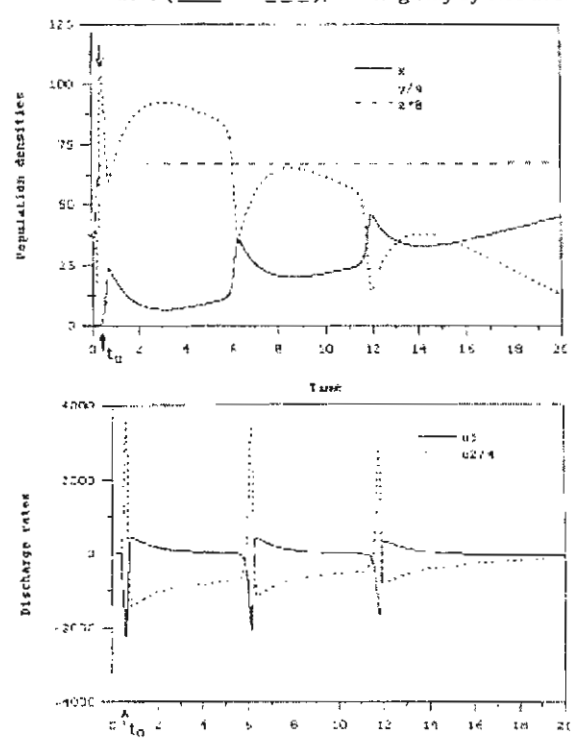


Fig 7. Time evolution of the three state variables, using parametric values of Figure 5. The chaotic system becomes stabilized when the control action is initiated at  $t = t_0$  with  $v_1 = 0$  and  $v_2$  irregular.

ScienceAsia 28 (2002) 215

only short-term predictions. Thus, a feedback control mechanism such as the one we have been discussing provides an attractive and useful tool to regulate the process since it can stabilize the system and make it less sensitive to the exogenous disturbances or noise input. The present study has potential to act as a spring board for a generalization to more complex models in the hope of obtaining a more manageable system.

#### **ACKNOWLEDGMENT**

Appreciation is expressed to the Thailand Research Fund and the National Research Council of Thailand for the financial support which has made this research project possible.

#### REFERENCES

- Albrecht F, A Gatzke, A Haddad and N Wax (1974) The dynamics of two interacting populations. J Math Anal Appl 46, 658-70. Gilpin ME (1979) Spiral chaos in a predator-prey model. American Naturalist 107, 306-8.
- Hadeler KP and HI Freedman (1989) Predator-prey populations with parasitic infection. J Math Biol 28, 609-31.
- Hastings A and T Powell (1991) Chaos in a three-species food chain. *Ecology* 72(3), 896-903.
- Holling CS (1966) In Systems Analysis in Ecology KEF Watt (ed) p 195. New York: Academic Press.
- Huaping L and M Zhien (1991) The threshold of survival for system of two species in a polluted environment. J Math Biol 30, 46-61.
- Isidori A. (1985) Non-linear Control Systems: An Introduction. Springer Lecture Notes in Control and Information Sciences. 297 pp Berlin: Springer-Verlag.
- Lenbury Y and S Orankitjareon (1995) Dynamic behavior of a membrane permeability sensitive model for a continuous bioreactor exhibiting culture rhythmicity. J Sci Soc Thailand 21, 97-116
- Lenbury Y and M Siengsanan (1993) Coexistence of competing microbial species in a chemostat where on population feeds on another. *Acta Biotechnol* 13, 1-18.
- Lenbury Y and C Likasiri (1994) Low- and high-frequency oscillations in a food chain where one of the competing species feeds on the other. Mathl Comput Modelling 20(7), 71-89.
- May RM (1972 Limit cycles in predator-prey communities. Science 177, 900-2.
- McLean AR and TBL Kirkwood (1990) A model of human immunodeficiency virus in T helper cell clones. J Theor Biol 147, 177-203.
- Mosetti R (1992) On the control of phytoplankton growth via a decoupling feedback law. Ecol Model 62, 71-81.
- Muratori S and S Rinaldi (1992) Low- and high-frequency oscillations in three dimensional food chain systems. SIAM J APPL MATH 52(6), 1688-1706.
- Rai V and R Sreenivasan (1993) Period-doubling bifurcations leading to chaos in a model food chain. Ecol Model 69, 63-77.
- Sabin GCW and D Summers (1993) Chaos in a periodically forced predator-prey ecosystem model. Math Biosci 113, 91-113.
- Sugihara G and RM May (1990) Nonlinear forecasting as a way of distinguishing chaos from measurement error in time series. Nature 344, 734-41.



BioSystems 70 (2003) 55-72



www.elsevier.com/locate/biosystems

# Modeling of bone formation and resorption mediated by parathyroid hormone: response to estrogen/PTH therapy

Chontita Rattanakul<sup>a</sup>, Yongwimon Lenbury<sup>a,\*</sup>, Nateetip Krishnamara<sup>b</sup>, David J. Wollkind<sup>c</sup>

Department of Mathematics, Faculty of Science, Mahidol University, Rama 6 Road, Bangkok 10400, Thailand
Department of Physiology, Faculty of Science, Mahidol University, Rama 6 Road, Bangkok 10400, Thailand
Department of Mathematics, Faculty of Science, Washington State University, Washington, WA 99164-3113, USA

Received 18 January 2002; received in revised form 11 September 2002; accepted 27 January 2003

#### Abstract #

Bone, a major reservoir of body calcium, is under the hormonal control of the parathyroid hormone (PTH). Several aspects of its growth, turnover, and mechanism, occur in the absence of gonadal hormones. Sex steroids such as estrogen, nonetheless, play an important role in bone physiology, and are extremely essential to maintain bone balance in adults. In order to provide a basis for understanding the underlying mechanisms of bone remodeling as it is mediated by PTH, we propose here a mathematical model of the process. The nonlinear system model is then utilized to study the temporal effect of PTH as well as the action of estrogen replacement therapy on bone turnover. Analysis of the model is done on the assumption, supported by reported clinical evidence, that the process is characterized by highly diversified dynamics, which warrants the use of singular perturbation arguments. The model is shown to exhibit limit cycle behavior, which can develop into chaotic dynamics for certain ranges of the system's parametric values. Effects of estrogen and PTH administrations are then investigated by extending on the core model. Analysis of the model seems to indicate that the paradoxical observation that intermittent PTH administration causes net bone deposition while continuous administration causes net bone loss, and certain other reported phenomena may be attributed to the highly diversified dynamics which characterizes this nonlinear remodeling process.

© 2003 Elsevier Science Ireland Ltd. All rights reserved.

Keywords: Bone remodeling; Parathyroid hormone control; Estrogen therapy

#### 1. Introduction

Bone is a highly organized tissue which differs from reproductive tissues in many aspects of its growth and turnover, are not dependent on gonadal hormones. It, however, provides support and protection as well as provides the environment for hemopoiesis. Moreover,

E-mail address: scylb@mahidol.ac.th (Y. Lenbury).

bone is the major calcium reservoir of the body since over 99% of total body calcium is stored in the skeleton (Heersche and Cherk, 1989).

In order to maintain its structural integrity, a great deal of new cells must be produced continuously (Heersche and Cherk, 1989). This involves two types of cells: the osteoblasts which are responsible for bone formation, and the osteoclasts which are responsible for bone resorption. The knowledge of how these cell types are regulated and how their proliferation and differentiation are stimulated is most important to our

<sup>\*</sup> Corresponding author. Tel.: +66-2-201-5341; fax: +66-2-201-5343.

3

understanding of factors regulating their number and activity in healthy or diseased human.

The skeleton undergoes continuous changes during growth and, until recently, was believed to reach its permanent shape after sexual maturation. However, it has now become clear that bone never attains permanent state (Albright and Sauders, 1990). After maximum skeletal mass has been reached, the final adult phase begins. A steady loss of bone mass, together with progressive architectural alterations continues throughout life, with the rate of change increasing with age. The severe loss of bone, especially cancellous (trabecular) bone, and the "spontaneous" fracturing of the remaining bone, characterizes the condition called osteoporosis (Whitfield et al., 1998).

Osteoporosis, a condition of generalized skeletal fragility caused by a reduction in bone mass as well as by a disruption of skeletal architecture, is a major cause of morbidity and mortality in postmenopausal women. It is estimated that women have lost 10% of their bone mass by the time they go through menopause and that 35% of cortical bone, and 50% of trabecular bone are lost over a lifetime (DeCherney, 1993).

Prevention and reversal of bone loss require a thorough understanding of the remodeling process in bone, the mechanism of bone formation, resorption, including the action of hormones such as estrogen and parathyroid hormone (PTH).

Albright et al. (1941), first called attention to estrogen deficiency as the cause of postmenopausal osteoporosis. It has now been widely accepted that estrogen deficiency plays an important role in the pathogenesis of osteoporosis and that estrogen therapy can prevent menopausal bone loss and reduces the risk of fracture. The mechanisms by which estrogen exerts its effects on bone remodeling process are not entirely understood, however, and several puzzling discoveries cannot be completely explained still. Recent studies (Albright et al., 1941; Prestwood et al., 1994) surprisingly indicated that short-term estrogen treatment of elderly women decreased values for biochemical markers of bone turnover significantly. Since estrogen therapy has some risks and side effects, the beneficial effect of prolonged estrogen treatment is put in question. Estrogen has important pharmacological side effects on skeletal tissues. Bone blood flow appears to be depressed by estrogen (Turner et al., 1994). A

change in blood flow might have profound effects on bone cell metabolism. High doses of estrogen result in weight loss in rats (Moon et al., 1991), and an increase in tumor formation was noted in aging rats following long-term treatment with estrogen.

The PTH has been proposed as an alternative agent that can replace lost bone and restore bone strength (Whitfield et al., 1998). Several researchers have investigated pulsatile PTH secretion in health and osteoporosis (Harms et al., 1989; Schmitt et al., 1996), concluding that pulsatile secretion of PTH in healthy young men is the physiological mode of secretion. Low pulsatile secretion of PTH might be related to low turnover osteoporosis. Paradoxically, however, PTH has been found (Kroll, 2000) to cause net bone loss (resorption) when administered in a continuous fashion, and net bone formation (deposition) when administered intermittently.

A sensible model of the process of bone formation and bone resorption should be capable of addressing and, to a certain extent, explain the puzzling discoveries mentioned before. We shall, therefore, develop a mathematical model for the differentiation of osteoblastic and osteoclastic populations in bone, based on the differential effects of PTH. The model is shown to admit pulsatile and chaotic secretory patterns in PTH levels conformal to clinical observations reported by Prank et al. (1995) recently. By expanding on the model, the question about the marked effect of short-term estrogen treatment, or the paradoxical effect of intermittent versus continuous PTH administrations mentioned before, can be explained as attributes of the highly diversified nonlinear dynamics which characterize this remodeling process.

#### 2. Model development

Bone, being a major reservoir of body calcium, is under the hormonal control of PTH (Kroll, 2000). Osteoclasts resorb bone and liberate calcium, but they lack receptors for PTH. The preosteoblastic precursors and preosteoblasts possess receptors for PTH, upon which the hormone induces differentiation from the precursors to preosteoblasts and from the preosteoblasts to osteoblasts. The osteoblasts, consequently generate IL-6, which induces preosteoclasts to differentiate into osteoclasts (Kroll, 2000).

Thus, bone remodeling is a continuous cycle of destruction and renewal of bone that is carried out by teams of osteoclasts and osteoblasts (Marcus, 1994). Osteoclasts and osteoblasts differentiate from less mature precursors, which line bone surfaces in an inactive state. In bone remodeling process, osteoclasts appear on a previously inactive surface of bone and then, they excavate a lacuna on the surface of cancellous bone or resorption tunnel in cortical bone. Osteoclasts are subsequently replaced by osteoblasts and finally, osteoblasts refill the resorption cavity. After osteoblasts have laid down their protein-based matrix, known as osteoid, they bury themselves in bony matrix, becoming osteocytes, or revert to an inactive cell form and line the bone surfaces as surface osteocytes or resting osteoblasts (Turner et al., 1994).

Therefore, the rate of bone deposition can be determined by the number of osteoblasts (B) while the rate of bone resorption can be determined by the number of osteoclasts (C), the balance between the number and activity of osteoblasts and osteoclasts determines whether net bone deposition or net bone resorption occurs. An excessively deep resorption space produced by osteoclasts, or an incomplete replenishment of the resorption space by the activation of osteoblasts can result in bone imbalance. If a remodeling imbalance exists after the completion of a remodeling cycle, the degree of bone loss will be exacerbated and that leads to osteoporosis (Turner et al., 1994).

We now proceed to construct our core model, the mathematical formulation of which is based biologically on clinical evidence observed in various reports such as that of Hock and Gera (1992), Dempster et al. (1993), Momsen and Schwarz (1997), Kong et al. (1999), Takahashi et al. (1999), Burgess et al. (1999), or Kroll (2000) amongst several others.

Firstly, since activated osteoclasts result from differentiation and activation of osteoclast precursors, we shall assume in what follows that a high level in osteoclast precursors is reflected in the high level of the resulting activated osteoclastic population C(t). Secondly, osteoclasts resorb bone and liberate calcium, in order to counter balance the high level of calcium in blood the rate of PTH secretion will decrease (Momsen and Schwarz, 1997). The equation for the rate of PTH secretion is then assumed to take the

form

$$\frac{\mathrm{d}P}{\mathrm{d}t} = \frac{c_1}{k_1 + C} - d_1 P \tag{1}$$

where P(t) denotes the level of PTH above the basal level. The first term on the right-hand side represents the secretion rate of PTH from the parathyroid grand which decreases with the increase in the number of active osteoclastic cells C(t),  $c_1$  and  $k_1$  being positive constants. This accounts for the above-mentioned observation that as active osteoclasts C resorb bone and liberate calcium, the rate of PTH secretion will decrease to counter balance the high level of calcium in blood. Therefore, a higher C should lead to lower PTH secretion rate. Finally, it is assumed that the hormone is removed from the system at the rate which is proportional to its current level with the removal rate constant  $d_1$ .

The dynamics of the osteoclastic population, on the other hand, can be described by the following equation

$$\frac{dC}{dt} = \frac{(c_2 + c_3 P)BC}{k_2 + P^2} - d_2 C \tag{2}$$

where the first term on the right-hand side represents the reproduction of active osteoclasts which requires the production of osteoclast differentiation factor (ODF) and its receptor on osteoclasts (Kroll, 2000). The more C means the more ODF receptors available for the reproduction of active osteoclasts, and hence the term is taken to depend on the number of osteoclasts C at that moment in time.

Moreover, osteoclasts precursors possess RANK, a receptor of tumor necrosis factor (TNF) family that recognizes ODF through a cell-to-cell interaction with osteoblasts (Kong et al., 1999; Takahashi et al., 1999; Burgess et al., 1999; Kroll, 2000), hence the rate of reproduction is taken to depend also on the number of active osteoblastic cells B(t) at any time t. Based on the well founded theory on mathematical modeling and population dynamics known as the law of mass action (Leah, 1988), when an event occurs through cell-to-cell interaction of the two populations involved, the rate may then be assumed to vary as their product, provided that the event occurs randomly. However, the rate of reproduction of C increases with the increase in the level of PTH (Dempster et al., 1993; Weryha and Leclere, 1995). On the other hand, it has been clinically observed (Kroll, 2000) that as PTH level

increases further, it begins to inhibit osteoclastic reproduction, and hence the saturation expression  $(c_2 + c_3 P)/(k_2 + P^2)$  is assumed for the stimulating effect of PTH, where  $c_2$ ,  $c_3$ , and  $k_2$  are positive constants.

Thus, without any active osteoclasts or osteoblasts (C=0, B=0), the reproductive rate of C should vanish. On the other hand, C will be produced at the rate which varies directly as the product BC, by the law of mass actions mentioned before, with the variation constant  $c_2/k_2$  at vanishing P. With PTH mediation, however, this variation parameter increases initially with increasing P but decreases when P becomes too high according to the saturation function utilized in Eq. (2), where  $c_3$  is a measure of how late the inhibition effect will set in.

Finally, the dynamics of the active osteoblastic population B(t) can be described by the following equation

$$\frac{\mathrm{d}B}{\mathrm{d}t} = c_4 P - \frac{c_5 PB}{k_3 + P} - d_3 B \tag{3}$$

where c4 is the specific rate at which PTH stimulates reproduction of active osteoblasts (Brown, 1991; Isogai et al., 1996), while the second term on the right-hand side of Eq. (3) accounts for the clinically observed inhibition of osteoblastic differentiation due to the PTH (Kroll, 2000). PTH stimulates osteoblast differentiation in immature osteoblasts but inhibits it in more mature cells (Isogai et al., 1996), through the process of down-regulation of the PTH receptors on osteoblasts. IL-6, a cytokine produced by osteoblasts, enhances the anti-proliferative effects of PTH by suppressing the PTH-induced Ca<sup>2+</sup> transients in addition to the down-regulation of the PTH receptor caused by chronic activation of the protein kinase A signal pathway. Therefore, PTH and IL-6 produced by osteoblasts exert a receptor-mediated negative feedback on the conversion of preosteoblasts to osteoblasts (Kroll, 2000). The inhibition effect is assumed here to take the form of the Holling type response function  $c_5P/(k_3 +$ P) which means that there should be no such inhibition if B or P vanishes. The inhibition term  $c_5PB/(k_3+P)$ then tends to  $c_5 B$  at high PTH level, so that the osteoblastic formation is predominantly stimulated positively by PTH according to the first term  $c_4P$  in Eq. (3) at higher levels of this hormone. This is consistent with observed clinical data reported by both Tam et al. (1982) and Hock and Gera (1992), some of which

is shown in Fig. 1. The parameters  $c_5$  and  $k_3$  may then be varied to accommodate different physiological data of different individuals. The higher  $k_3$  means the inhibition remains effective still at higher level of PTH. The last terms in the above three equations are the removal rates of the three components of the remodeling process with rate constants  $d_1$ ,  $d_2$ , and  $d_3$ , respectively.

Our reference core model, therefore, consists of Eqs. (1)–(3), possessing highly diversified nonlinear characteristics, upon which further analysis and investigation may be carried out in an attempt to explain the mystifying empirical observations previously mentioned.

#### 3. Theoretical analysis

Now, the argument for our assumption that the system is characterized by highly diversified dynamics goes as follows. According to Whitfield et al. (1998), the need to repair microdamage in a patch of cortical bone is sensed by an interconnected network of cells called osteocytes, each of which is locked in a tiny cubicle inside the dense cortical bone. The damage may only strain the osteocytes or it may be severe enough for them to suicidally trigger a process called apoptosis. When osteocytes are injured or die, they stop producing a major suppressor of osteoclastic biosynthesis. This removes a major restraint on the production of new osteoclasts, each of which will live and dig for the next 2 weeks (Whitfield et al., 1998).

When the osteoclasts dissolve the bone mineral, a lot of Ca<sup>2+</sup> is released. The Ca<sup>2+</sup> concentration serves as a 2-way switch: "off" for the osteoclasts and "on" for the bone-making osteoblasts (Whitfield et al., 1998). Osteoblasts take about five times longer to fill the tunnels and trenches than osteoclasts take to dig them. When the patch is finally repaired 6–9 months later, the distress signals have stopped, the approximately 3-month-old members of the last osteoblast crew are now out of work, so they "commit apoptotic suicide," as explained in great detail by Whitfield et al. (1998).

In view of the above discussion, therefore, it is reasonable to assume that PTH, being the stimulating agent in both bone resorption and formation, should possess very fast dynamics, responding quickly to

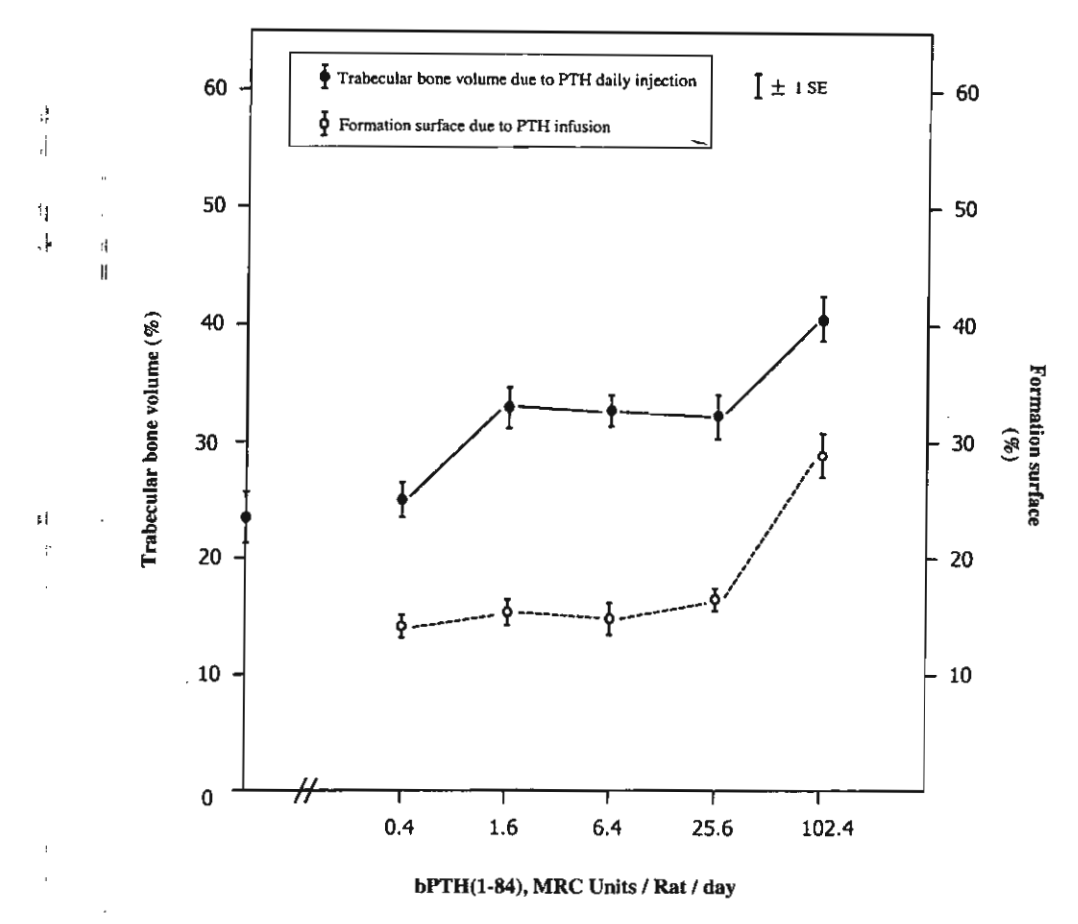


Fig. 1. Effects of PTH administration on bone surface formation and volume. (Adapted from Tam et al. (1982).)

changes in the cellular environment, specifically the Ca<sup>2+</sup>, concentration. The osteoclastic population is the component with intermediate dynamics and more stable than PTH, while the osteoblastic population possesses the slowest dynamics, lasting up to approximately 3 months, and therefore is the most stable of the three components in this system.

Supported by such well-documented clinical observation (Whitfield et al., 1998), we scale the components and parameters in terms of small parameters  $0 < \varepsilon \ll 1$  and  $0 < \delta \ll 1$  as follows. Letting x = P, y = C, z = B,  $a_1 = c_1$ ,  $a_2 = c_2/\varepsilon$ ,  $a_3 = c_3/\varepsilon$ ,  $a_4 = c_4/\varepsilon\delta$ ,  $a_5 = c_5/\varepsilon\delta$ ,  $b_1 = d_1$ ,  $b_2 = d_2/\varepsilon$ , and  $d_3 = d_3/\varepsilon\delta$ , we are led to the following system of differential equations.

$$\frac{dx}{dt} = \frac{a_1}{k_1 + y} - b_1 x \equiv F(x, y, z)$$
 (4)

$$\frac{\mathrm{d}y}{\mathrm{d}t} = \varepsilon \left[ \frac{(a_2 + a_3 x)yz}{k_2 + x^2} - b_2 y \right] \equiv \varepsilon G(x, y, z) \tag{5}$$

$$\frac{\mathrm{d}z}{\mathrm{d}t} = \varepsilon \delta \left[ a_4 x - \frac{a_5 x z}{k_3 + x} - b_3 z \right] \equiv \varepsilon \delta H(x, y, z) \quad (6)$$

which means that during transitions, when the right-hand sides of Eqs. (4)-(6) are finite and non-zero,  $|\dot{y}|$  is of the order  $\varepsilon$  and  $|\dot{z}|$  is of the order  $\varepsilon\delta$ . In the sequel, we will adopt the notation  $\dot{y} = O(\varepsilon)$  and  $\dot{z} = O(\varepsilon\delta)$ .

The system of Eqs. (4)–(6), with small  $\varepsilon$  and  $\delta$ , can be analyzed with geometric singular perturbation methods which, under suitable regularity conditions, allow approximation of solutions of the system by a sequence of simple dynamic transitions occurring at different speeds. A resulting singular curve, composed of these transitions, approximates an actual solution in

the sense that the real trajectory is contained in a tube around the curve, and that the radius of the tube tends to zero with  $\varepsilon$  and  $\delta$ . Examples where this technique has been applied to biological systems can be found in the work of Muratori and Rinaldi (1992) and that of Lenbury et al. (1997). A detailed description of singular perturbation theory can for instance be found in the work of O'Malley (1974) on this subject. The works by Jones (1994) and Kaper (1999) give good overviews of geometric singular perturbation methods. See also the classical text by Eckhaus (1979).

We call the system of Eqs. (4)–(6) the fast system. In the form of an intermediate system, where  $\varepsilon$  and  $\delta$  are positive, it can be written as follows

$$\varepsilon \frac{\mathrm{d}x}{\mathrm{d}\tau_1} = F(x, y, z) \tag{7}$$

$$\frac{\mathrm{d}y}{\mathrm{d}\tau_1} = G(x, y, z) \tag{8}$$

$$\frac{\mathrm{d}z}{\mathrm{d}\tau_1} = \delta H(x, y, z) \tag{9}$$

where  $\tau_1 = \varepsilon t$ , or in the form of the slow system

$$\varepsilon \delta \frac{\mathrm{d}x}{\mathrm{d}\tau_2} = F(x, y, z) \tag{10}$$

$$\delta \frac{\mathrm{d}y}{\mathrm{d}\tau_2} = G(x, y, z) \tag{11}$$

$$\frac{\mathrm{d}z}{\mathrm{d}\tau_2} = H(x, y, z) \tag{12}$$

with  $\tau_2 = \varepsilon \delta t$ . Evolution on the time-scale t is said to be fast, evolution on the time-scale  $\tau_1$  is intermediate, and evolution on the time-scale  $\tau_2$  is slow.

Geometric singular perturbation theory allows us to analyze the system of Eqs. (4)–(6) for small positive  $\varepsilon$  and  $\delta$  by suitably combining the dynamics of the fast, intermediate, and slow limits. Under certain regularity conditions and provided that the sets of critical points (critical manifolds) are normally hyperbolic for  $\varepsilon=0$ , and  $\delta=0$ , compact subsets of these critical manifolds persist as locally invariant slow or intermediate manifolds of the full problem Eqs. (4)–(6) for  $\varepsilon\neq0$ , and  $\delta\neq0$  but sufficiently small. These manifolds are  $O(\varepsilon)$  or  $O(\varepsilon\delta)$  close to  $\{F(x,y,z)=0\}$  and  $\{F(x,y,z)=0\}$ , respectively.

#### 4. Analysis of the manifolds

The shapes and relative positions of the manifolds  $\{F=0\}$ ,  $\{G=0\}$ , and  $\{H=0\}$  determine the directions, speeds, and shapes of the resulting solution trajectories. Therefore, we shall analyze each of the equilibrium manifolds in detail. The delineating conditions for the existence of limit cycle are arrived at from the close inspection of these manifolds.

#### 4.1. The manifold $\{F=0\}$

This manifold is given by the equation

$$x = \frac{a_1}{b_1(k_1 + y)} \equiv U(y) \tag{13}$$

We see that this manifold is independent of the slow variable z, thus this manifold is parallel to the z-axis and intersects the (x, z)-plane at the point where

$$x = \frac{a_1}{b_1 k_1} \equiv x_1 \tag{14}$$

Moreover, U(y) is a decreasing function of y, so that  $x \to 0$  as  $y \to \infty$  along this curve.

#### 4.2. The manifold $\{G=0\}$

This manifold consists of two submanifolds. One is the trivial manifold y = 0, while the other is the nontrivial manifold given by the equation

$$z = \frac{b_2(k_2 + x^2)}{a_2 + a_3 x} \equiv V(x) \tag{15}$$

We see that this nontrivial manifold, shown in Fig. 2, is independent of the intermediate variable y, and thus this manifold is parallel to the y-axis. It intersects the (x, z)-plane along a curve which is asymptotic to the line

$$x = -\frac{a_2}{a_3} \tag{16}$$

The curve intersects the z-axis at the point where x = 0, and

$$z = \frac{b_2 k_2}{a_2} \equiv z_0 \tag{17}$$

attaining its minimum at the point where

$$x = -\frac{a_2}{a_3} + \sqrt{\left(\frac{a_2}{a_3}\right)^2 + k_2} \equiv x_{\rm m} \tag{18}$$

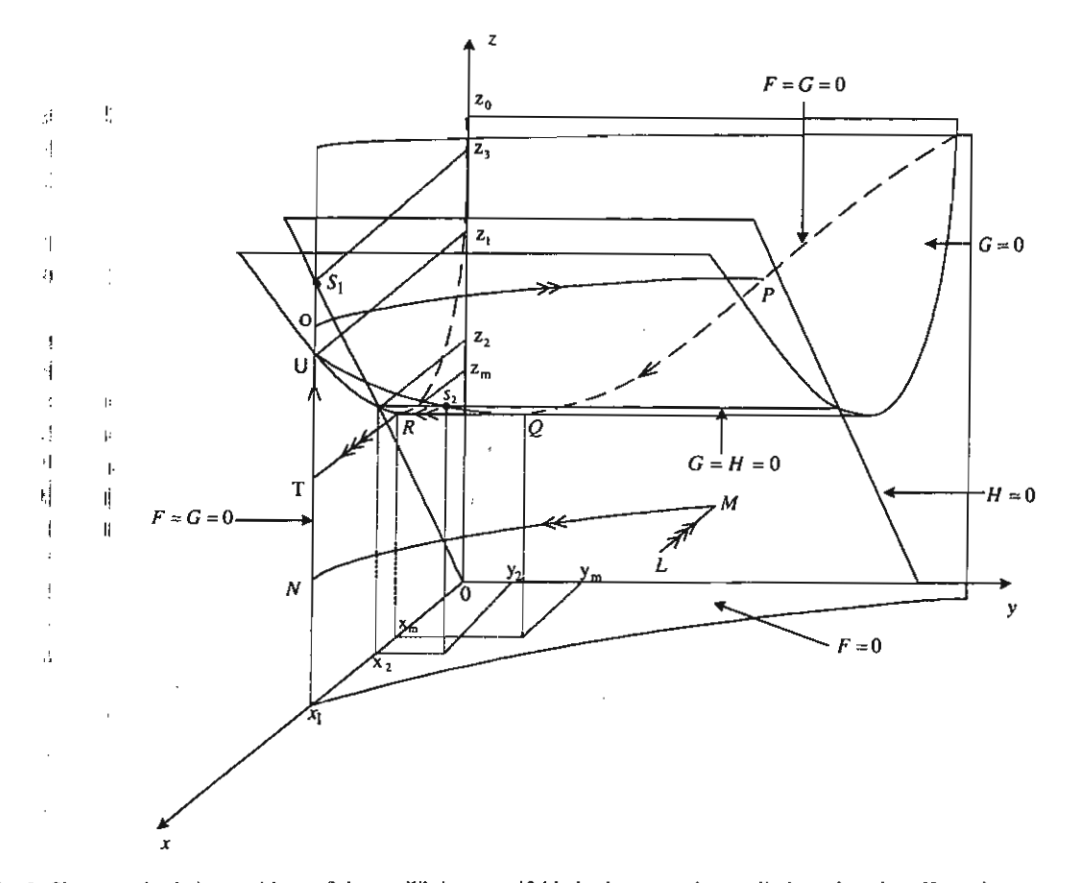


Fig. 2. Shapes and relative positions of the equilibrium manifolds in the case where a limit cycle exists. Here, three arrows indicate fast transitions, two arrows indicate transitions at intermediate speed, and a single arrow indicates slow transitions.

and 
$$z = V(x_m) \equiv z_m$$
 (19)

in the first octant.

Moreover, the manifold  $\{F=0\}$  intersects the trivial manifold y=0 along the line  $x=x_1$  on the (x,z)-plane. On the other hand, the manifold  $\{F=0\}$  intersects the nontrivial manifold given by (15) along the curve

$$z = \frac{b_2(k_2 + U^2(y))}{a_2 + a_3 U(y)}$$

which has a minimum point  $Q(x_m, y_m, z_m)$  where

$$y_{\rm m} \equiv \frac{a_{\rm 1-1}}{b_{\rm 1}x_{\rm m}} - k_{\rm 1} \tag{20}$$

utilizing (13). Also, the curve  $\{F = G = 0\}$  intersects the (x, z)-plane at the point U where y = 0,  $x = x_1$ ,

and

$$z = \frac{b_2}{b_1 k_1} \left( \frac{b_1^2 k_1^2 k_2 + a_1^2}{a_2 b_1 k_1 + a_1 a_3} \right) \equiv z_1$$
 (21)

Finally,  $z \to z_0$  as  $y \to \infty$  along this curve as shown in Fig. 2.

## 4.3. The manifold $\{H=0\}$

This manifold is given by the equation

$$z = \frac{a_4 x (k_3 + x)}{(a_5 + b_3) x + b_3 k_3} \equiv W(x)$$
 (22)

which is independent of y. Thus, this manifold is parallel to the y-axis, and intersects the (y, z)-plane along the y-axis. We also observe that W(x) is an increasing function of x in the first octant.

The manifold  $\{H = 0\}$  intersects the manifold  $\{G = 0\}$  along the straight line

$$\left\{ x = x_2, \quad z = \frac{b_2(k_2 + x_2^2)}{a_2 + a_3 x_2} \equiv z_2 \right\}$$
 (23)

which is parallel to the y-axis,  $x_2$  being the real solution of

$$(b_2a_5 + b_2b_3 - a_3a_4)x^3 + (b_2b_3k_3 - a_2a_4 - a_3a_4k_3)x^2 + (a_5b_2k_2 + b_2b_3k_2 - a_2a_4k_3)x + b_2b_3k_2k_3 = 0$$
(24)

which exists in the positive octant and is unique provided

$$b_2 a_5 + b_2 b_3 - a_3 a_4 < 0 (25)$$

$$b_2b_3k_3 - a_2a_4 - a_3a_4k_3 < 0 (26)$$

and

$$a_5b_2k_2 + b_2b_3k_2 - a_2a_4k_3 > 0 (27)$$

The manifold  $\{H = 0\}$  intersects the (x, z)-plane along the curve z = W(x) which intersects the line  $x = x_1$  at the point  $S_1 = (x_1, 0, z_3)$  where

$$z_3 = \frac{a_1 a_4 (b_1 k_1 k_3 + a_1)}{b_1 k_1 [a_1 (a_5 + b_3) + b_1 b_2 k_1 k_3]}$$
(28)

seen in Fig. 2.

Moreover, the curve  $\{F = G = 0\}$  intersects the curve  $\{G = H = 0\}$  at the point  $S_2 = (x_2, 0, z_2)$  located on the unstable portion QU of the curve  $\{F = G = 0\}$  as shown in Fig. 2, provided that

$$x_{\rm m} < x_2 < x_1$$

### 5. Existence of an attracting limit cycle

The relative positions of the manifolds  $\{F = 0\}$ ,  $\{G = 0\}$ ,  $\{H = 0\}$ , and in particular the existence and position of the point  $S_2$  are apparently important for the existence of a limit cycle. After the calculations of the previous section, we are ready to state the main result of this paper.

**Theorem 1.** Suppose inequalities (25)–(27) hold. If  $\varepsilon$  and  $\delta$  are sufficiently small, and

$$x_{\rm m} < x_2 < x_1$$
 (29)

$$z_1 < z_3 < z_0 \tag{30}$$

where all parametric values are defined as before, then the system of Eqs. (4)–(6) has a global attractor, in the positive octant of the phase-space. This attractor is a limit cycle that is singular in the limit  $\varepsilon \to 0$ ,  $\delta \to 0$ . In that limit it can formally be constructed by concatenating various transitions occurring at three different speeds.

The proof of the theorem is based on geometric singular perturbation methods, which are elaborated by Jones (1994) and Kaper (1999) and utilized successfully in many areas. These methods rely heavily on using the different types of flows that can be distinguished: the fast O(1) flow, the intermediate O( $\varepsilon$ ) flow, and the slow O( $\varepsilon$  $\delta$ ) flow. Orbits can consist of various parts; in Fig. 2 the fast parts are indicated by three arrows, the intermediate parts by two arrows, and the slow parts by a single arrow. Under the conditions identified in the theorem, the shapes and relative positions are as in Fig. 2.

Take an initial point  $L = (x_0, y_0, z_0)$ , with  $F(x_0, y_0, z_0) \neq 0$ . Under the conditions in Theorem 1, without loss of generality we assume that the position of L is as in Fig. 2. L lies in the fast field on an orbit governed by

$$\frac{\mathrm{d}x}{\mathrm{d}t} = F(x, y, z), \quad \frac{\mathrm{d}y}{\mathrm{d}t} = 0, \quad \frac{\mathrm{d}z}{\mathrm{d}t} = 0$$
 (31)

and the  $\varepsilon=0$  orbit through L tends to the point M on the fast stable manifold F=0 while y and z remain constant. Generically,  $G(x, y, z) \neq 0$  at this point M. Then, on this manifold the flow with respect to the intermediate time  $\tau_1$  is given by

$$0 = F(x, y, z), \quad \frac{\mathrm{d}y}{\mathrm{d}\tau_1} = G(x, y, z),$$
$$\frac{\mathrm{d}z}{\mathrm{d}\tau_1} = \delta H(x, y, z) \tag{32}$$

For sufficiently small  $\delta$ ,  $0 < \delta \ll 1$ , this is again a singularly perturbed system. Inspection of G yields that  $\{G=0\}$  is normally hyperbolic attracting for the  $\delta=0$  flow restricted to  $\{F=0\}$ , and that the full manifold  $\{F=0\}$  serves as a stable manifold of  $\{G=0\}$  for the restricted  $\delta=0$  flow. The flow on

 ${F = 0, G \neq 0}$  is given by

$$0 = F(x, y, z), \quad \frac{dy}{d\tau_1} = G(x, y, z), \quad \frac{dz}{d\tau_1} = 0$$
(33)

and is hence  $O(\varepsilon)$  or intermediate in the direction of decreasing y, since G < 0 here. As long as  $G \neq 0$  the orbits on  $\{F = 0\}$  have constant x and z coordinates. Then, the orbit reaches the point N on the stable part of  $\{F = 0, G = 0\}$ , where the flow is prescribed by

$$0 = F(x, y, z), \quad 0 = G(x, y, z),$$

$$\frac{dz}{d\tau_2} = H(x, y, z)$$
(34)

and is hence  $O(\varepsilon\delta)$  or slow in the direction of increasing z, since H > 0 here, until the point O is reached, where the stability of  $\{F = 0, G = 0\}$  is lost. (The existence and location of the point O has been discussed and proved by Schecter (1985) and Osipove'et al. (1986).) The  $O(\varepsilon)$  time-scale becomes dominant once again. Hence, the orbit follows an intermediate path to the point P on the other stable part of  $\{F = 0, G = 0\}$ . Then, it tends to the point Q during which the flow is  $O(\varepsilon\delta)$  in the direction of decreasing z, since H<0here. Once the point Q is reached, a saddle node bifurcation occurs and the stability of  $\{F = 0, G = 0\}$ will again be lost. The  $O(\varepsilon)$  time-scale becomes dominant again. This yields an intermediate trajectory to the point R followed by a fast transition to the point T on the stable part  $\{F = 0, G = 0\}$ . Consequently, a slow transition with increasing z, since H > 0here, will bring the system back to the point O, followed by flows along the same path described before repeatedly, resulting in the closed cycle OPQRTO.

Thus, the existence of a limit cycle in the system for  $\varepsilon$  and  $\delta$  sufficiently small is assured. Finally, since L was arbitrary, the limit cycle is a global attractor.

A computer simulation of Eqs. (4)–(6) is presented in Fig. 3, with parametric values chosen to satisfy the inequalities identified in Theorem 1. The solution trajectory, shown in Fig. 3a projected onto the (x, y)-plane, tends to a limit cycle as theoretically predicted. The corresponding time courses of PTH and active osteoclastic population level C are shown in Fig. 3b and c, respectively. Such oscillatory behavior in the level of PTH has often been observed in clinical data (Albright et al., 1941; Prank et al., 1995, 1994).

On comparing the spaces between PTH peaks in our numerical simulation to those in available clinical data, we are able to estimate that the scale of 1 day is equivalent to 917 time steps in our model simulations.

### 6. Nonlinear dynamics in PTH secretion

Several researchers (Albright et al., 1941; Prank et al., 1995, 1994) have reported evidence of non-linear dynamics in pulsatile secretion of PTH in normal human subjects. Prank et al. (1994) reported low-dimensional deterministic chaos in the pulsatile secretion of PTH in three young subjects. It appears that a phase-space analysis may allow the definition of health and disease by identifying the dynamic differences in the subjects' PTH secretory patterns.

In order to investigate the possibility of chaotic dynamics in the secretory pattern of PTH in our system, we carried out a numerical experiment on our model Eqs. (4)-(6). A bifurcation diagram was constructed by choosing parametric values that would lead to cycling in the x, y, and z components, guided by our work in the previous section, then letting the system run for  $10^5$  time steps. We retained only the last  $8 \times 10^4$  time steps to eliminate transient behavior, using the values of  $k_1$  between 0.08 and 0.1, and changing  $k_1$  in steps of  $10^{-5}$ . The relative maximum values  $x_{\text{max}}$  of x were collected during the last  $8 \times 10^4$  time steps and plotted against  $k_1$  as shown in Fig. 4. We discovered in this bifurcation diagram that periodic orbits of period 2 can be expected in the model system for values of  $k_1 > 0.097$ . Chaotic dynamics occur for  $k_1$  between 0.087 and 0.089, emerging through a period doubling route. In this chaotic range, the system is very sensitive to initial conditions. From experimenting numerically, we found that the time courses of solutions in this situation, which start at very slightly different initial values, will stay close for only a short time, before diverging and following drastically different paths as time passes.

A computer simulation of the model systems (4)–(6), with parametric values chosen under the above-mentioned guidelines and  $k_1 = 0.087$  in the chaotic range, is presented in Fig. 5. The strange attractor is shown projected onto the (x, y)-plane in Fig. 5a, and the corresponding chaotic time course of PTH is presented in Fig. 5b.

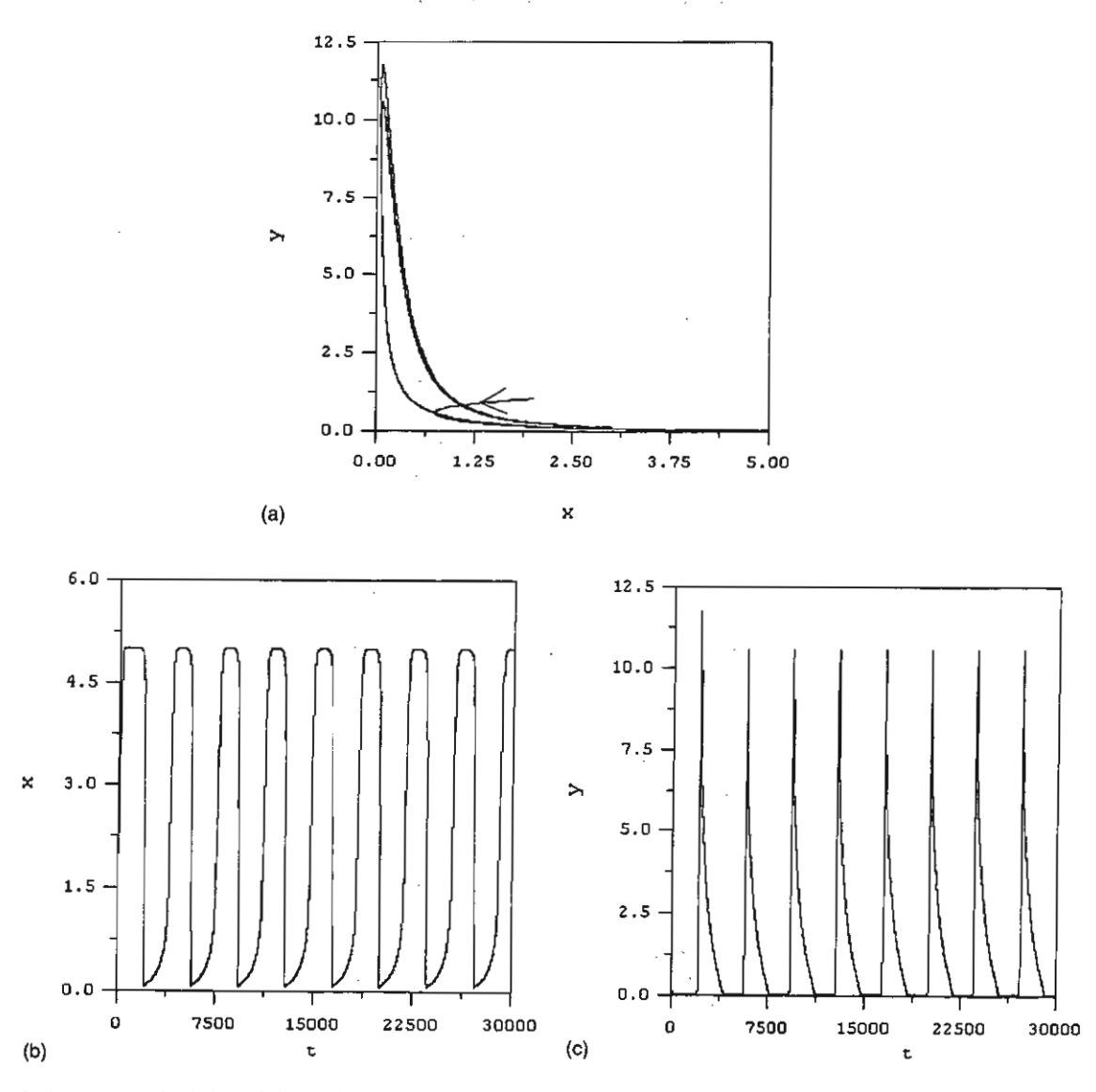


Fig. 3. A computer simulation of the model systems (4)–(6) with  $\varepsilon = 0.1$ ,  $\delta = 0.9$ ,  $a_1 = 0.05$ ,  $a_2 = 0.009$ ,  $a_3 = 0.675$ ,  $a_4 = 0.01$ ,  $a_5 = 0.005$ ,  $b_1 = 0.1$ ,  $b_2 = 0.3$ ,  $b_3 = 0.01$ ,  $k_1 = 0.1$ ,  $k_2 = 0.5$ ,  $k_3 = 0.025$ ,  $k_3 = 0.025$ ,  $k_4 = 0.025$ ,  $k_5 = 0.025$ ,  $k_6 = 0.025$ ,  $k_8 = 0.025$ ,  $k_8$ 

Thus, our model admits chaotic dynamics of PTH secretion, conforming to the clinical evidence in the above-mentioned reports which suggests a new interpretation of osteoporosis and hyperparathyroidism as dynamic diseases (Prank et al., 1994), associated with the loss of an adaptive hormonal rhythm.

# 7. Responses to PTH/estrogen therapy

We further illustrate how the characteristics of nonlinear diversified time responses inherent to the system modeled by Eqs. (4)–(6) can give rise to different surprising dynamic behavior which might seem puzzling when observed in clinical data.

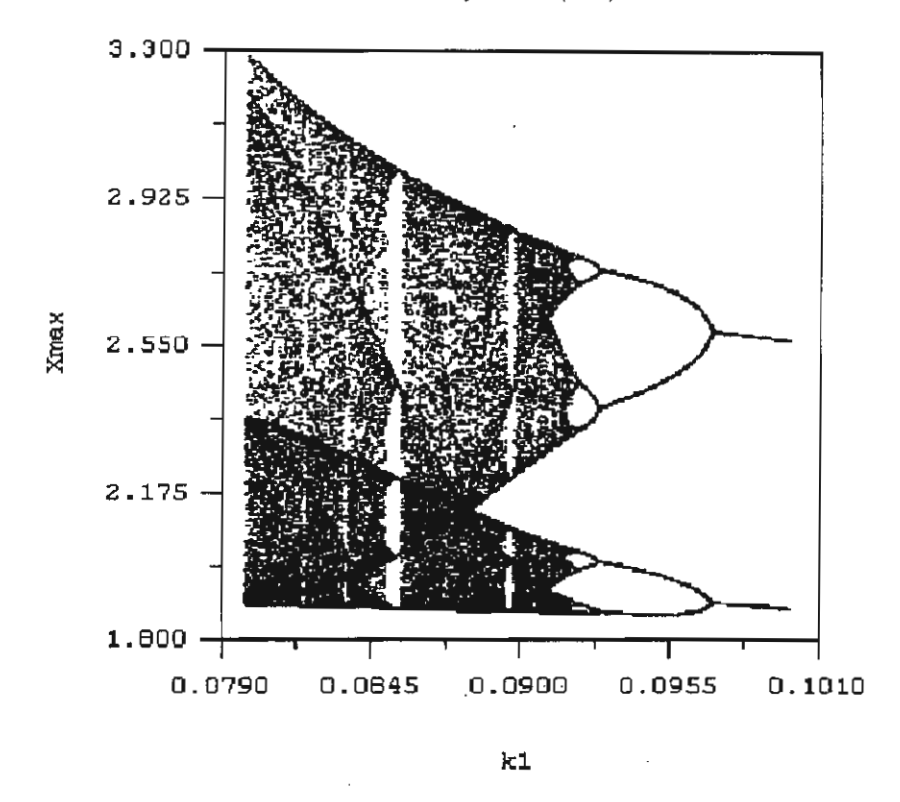


Fig. 4. Bifurcation diagram for the model systems (4)-(6) with  $\varepsilon = 0.8$ ,  $\delta = 0.1$ ,  $a_1 = 0.0900$ ,  $a_2 = 0.01125$ ,  $a_3 = 1.3750$ ,  $a_4 = 0.1125$ ,  $a_5 = 0.0625$ ,  $b_1 = 0.1500$ ,  $b_2 = 0.4375$ ,  $b_3 = 0.1250$ ,  $k_2 = 1.5000$ ,  $k_3 = 0.0250$ , and  $0.08 < k_1 < 0.1$ . Plots are of  $x_{\text{max}}$  against  $k_1$ .

### 7.1. Responses to PTH administration

We investigate the action of PTH, administered continuously and intermittently, by first incorporating a term  $k_p > 0$  into the rate Eq. (4) to represent continuous administration of the PTH. The result of a computer simulation of the modified model system:

$$\frac{\mathrm{d}x}{\mathrm{d}t} = \frac{c_1}{k_1 + y} - b_1 x + k_p \tag{35}$$

$$\frac{\mathrm{d}y}{\mathrm{d}t} = \varepsilon \left[ \frac{(a_2 + a_3 x)yz}{k_2 + x^2} - b_2 y \right]$$
 (36)

$$\frac{\mathrm{d}z}{\mathrm{d}t} = \varepsilon \delta \left( a_4 x - \frac{a_5 x z}{k_3 + x} - b_3 z \right) \tag{37}$$

is shown in Fig. 6a. Here,  $k_p = 0.5$  and administration starts at  $t = t_0 = 10,000$ . We observe that oscillatory behavior in the active osteoblastic population ceases and the level tends toward a steady level higher than the peak levels attainable prior to the administration.

However, the active osteoclastic population shows an exponential increase, and hence a net bone loss can, therefore, be expected. Looking closely at the positions of the three equilibrium manifolds in Fig. 2, we can see that the addition of  $k_p > 0$  means a re-location of the manifold  $\{F = 0\}$  which results in the violation of the necessary condition for limit cycle behavior and the solution trajectory is forced to follow the curve on the manifold  $\{F = 0\}$  while  $x \to 0$ , and y increases without bound.

However, if we add the term  $k_p > 0$  only in pulses or intermittently, a different dynamic behavior is obtained, although the same value of  $k_p = 0.5$  is used. Fig. 6b shows the simulation result of daily administration of PTH which lasts for 6h at a time (using the time scale estimate mentioned at the end of Section 5). Although the active osteoblastic population still oscillates about a mean which is close to that prior to the start of the protocol, the active osteoclastic population now oscillates around a lower mean value

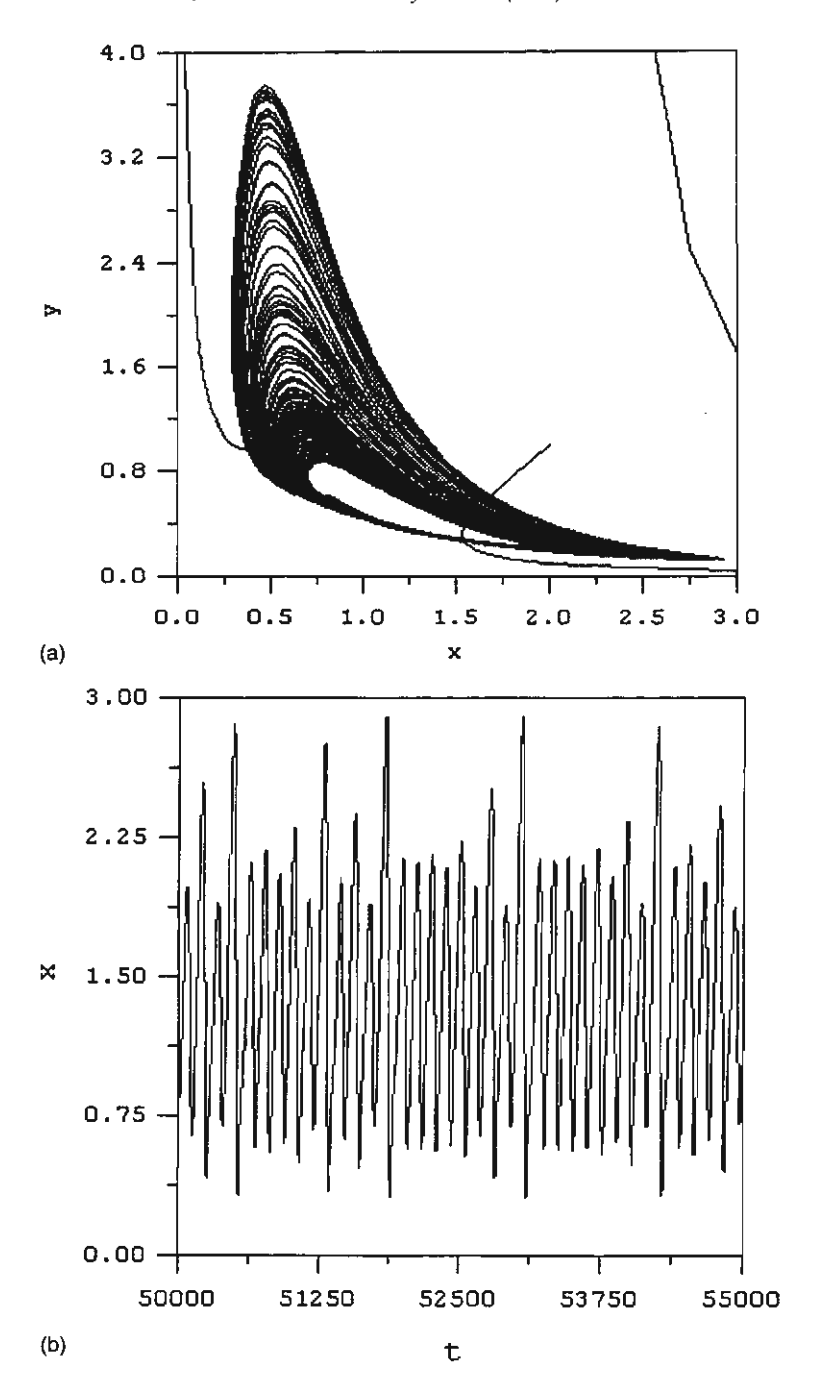


Fig. 5. A computer simulation of the model systems (4)–(6) with  $\varepsilon = 0.8$ ,  $\delta = 0.1$ ,  $a_1 = 0.0900$ ,  $a_2 = 0.01125$ ,  $a_3 = 1.3750$ ,  $a_4 = 0.1125$ ,  $a_5 = 0.0625$ ,  $b_1 = 0.1500$ ,  $b_2 = 0.4375$ ,  $b_3 = 0.1250$ ,  $b_2 = 1.5000$ ,  $b_3 = 0.0250$ , and  $b_4 = 0.087$  in the chaotic range, showing a strange attractor projected onto the (x, y)-plane in (a). The corresponding time series of PTH (x) is shown in (b).

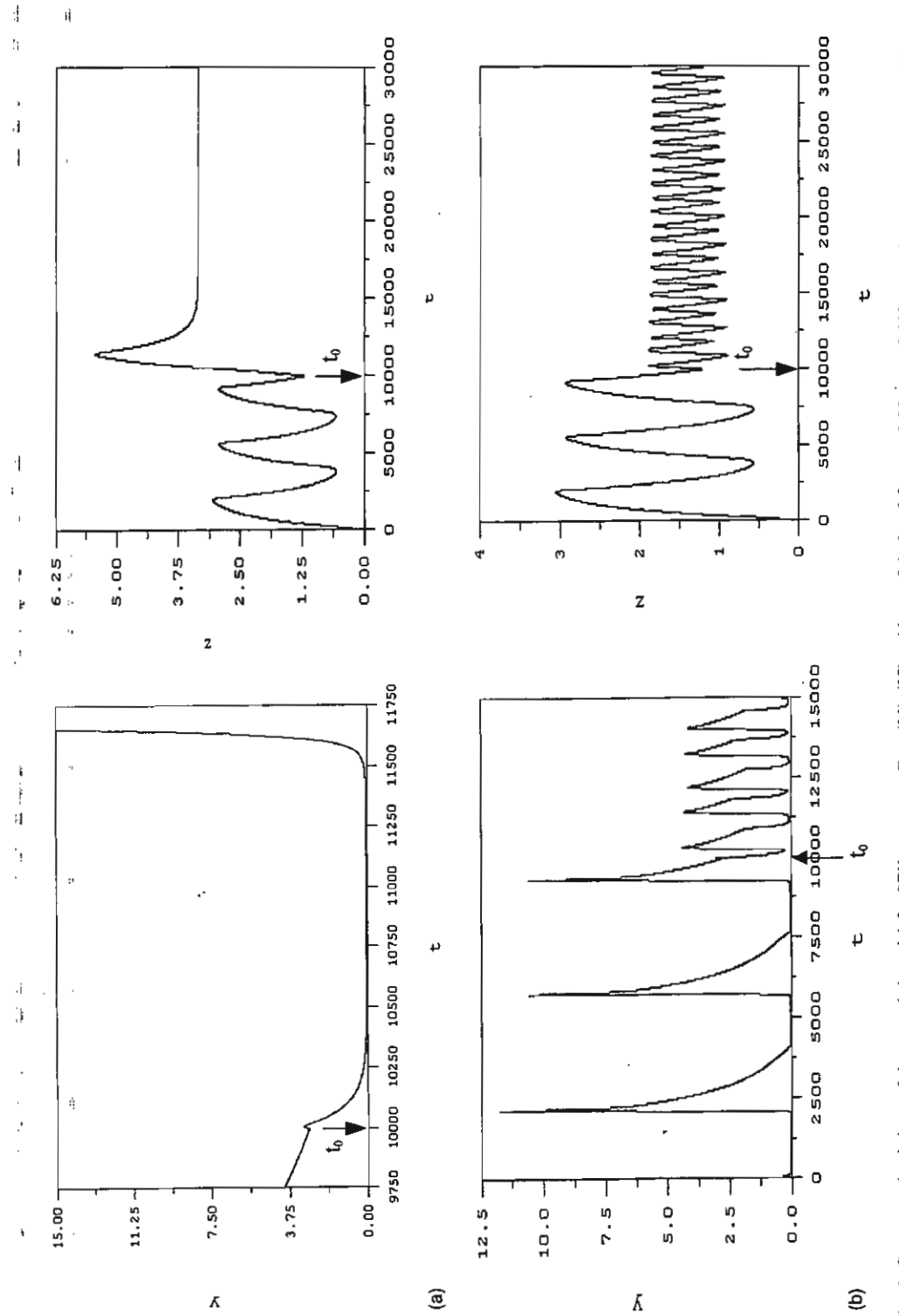


Fig. 6. Computer simulations of the extended model for PTH treatment, Eqs. (35)–(37), with e = 0.1,  $\delta = 0.9$ ,  $a_1 = 0.05$ ,  $a_2 = 0.009$ ,  $a_3 = 0.675$ ,  $a_4 = 0.01$ ,  $a_5 = 0.005$ ,  $b_1 = 0.1$ ,  $b_2 = 0.3$ ,  $b_3 = 0.01$ ,  $b_1 = 0.1$ ,  $b_2 = 0.3$ , and  $b_3 = 0.01$ ,  $b_3 = 0.025$ . PTH treatment, initiated at the time  $b_0 = 10,000$ , is continuous in (a) and for 6h daily in (b), with  $b_1 = 0.5$ .

and peaks at a much lower level. This results in apparent net bone formation, which is in agreement with the reports from several researchers (Kroll, 2000; Tam et al., 1982; Hock and Gera, 1992) that daily injection of the hormone caused an increase in the bone apposition rate, accompanied by an increase in the formation surface without an increase in the resorption surface. Continuous infusion, on the other hand, resulted in an increased apposition, increases in both formation and resorption surfaces, and a net decrease in bone volume.

Studying the three equilibrium manifolds more closely, we understand that the addition of  $k_p$  increases the rate of change of PTH in an episodic manner. The x-component (PTH) now has even faster dynamics and changes very quickly with time. Thus, C does not have time to reach a high peak, because it is pulled back down as the PTH level starts to rise very early and quickly, and similarly for the osteoblastic population. But since the effect only lasts 6 h at a time, the system returns to its oscillatory patterns in a short space of time. Thus, it appears that the behavior clinically observed is one of the manifestations of the nonlinearity property of the system together with the fact that the process is characterized by highly diversified dynamics. If PTH therapy is to develop into a viable alternative to estrogen treatment against osteoporosis, possibilities of such nonlinear or dissipative effects admitted by the system must be more closely scrutinized.

## 7.2. Responses to estrogen administration

On the other hand, realizing that long-term treatment of estrogen poses risks of side effects, we also attempted to better understand the action of estrogen on bone remodeling by again incorporating an extra term into the second rate Eq. (5) for the active osteoclastic population. According to Whitfield et al. (1998), in a young woman, a normal premenopausal estrogen concentration may limit the size of the preosteoclast population by stimulating apoptosis. But as her estrogen level declines with menopause, so does the estrogen receptor-mediated signaling; osteoclast precursors may thus live longer. Thus, to simulate the effect of daily intake to supplementary estrogen, we increase the removal rate of C by subtracting the term  $k_C y$ ,  $k_C > 0$ , from the rate Eq. (5) for a duration  $\Delta T$ of every interval of p days.

In so doing, we are assuming that estrogen is more stable than PTH and remains effective in the human body accumulatively over a long enough period so that daily intake of estrogen can be taken as equivalent to continuous application of the steroid, all through the time period  $\Delta T$ , during which time the model equations then become

$$\frac{\mathrm{d}x}{\mathrm{d}t} = \frac{a_1}{k_1 + y} - b_1 x \tag{38}$$

$$\frac{\mathrm{d}y}{\mathrm{d}t} = \varepsilon \left[ \frac{(a_2 + a_3 x)yz}{k_2 + x^2} - b_2 y - k_C y \right] \tag{39}$$

$$\frac{\mathrm{d}z}{\mathrm{d}t} = \varepsilon \delta \left( a_4 x - \frac{a_5 x z}{k_3 + x} - b_3 z \right) \tag{40}$$

Fig. 7 shows the results of computer simulations in two different cases. In Fig. 7a, the term  $-k_C y$  is kept in Eq. (39) for a duration of  $\Delta T = 12$  days, every interval of p = 28 days. We observe that when the administration period  $\Delta T$  is over, the effect still lasts for quite some time before the system recovers itself and there is a resetting of oscillatory behavior in the active osteoblastic population. The "plateau" is much wider than  $\Delta T$ . This is again a result of the diversified time responses of the three components in this nonlinear system. Since B is the very slow variable, it takes a long time to respond to the change in the proliferation rate of C. In particular, the plateau width is inversely proportional to  $\varepsilon$  and  $\delta$ . We also found, upon experimenting with different values, that different dosage (or  $k_C$ ) will yield different plateau width.

In Fig. 7b,  $\Delta T=21$  days, and p=28 days. We see that there is no longer any resetting of oscillatory behavior. Even though estrogen has already been cut off, the dissipative effect still lasts long enough to overlap with the next application of estrogen. This seems to suggest that with appropriate choices of  $\Delta T$ , p, and the prescribed dosage, administration may not necessarily be kept on for the entire time, while a net bone surface formation can still be expected.

### 7.3. Investigating estrogen action in monthly bursts

In several clinical data, such as those mentioned in Muse et al.'s report (1986), estrogen level was

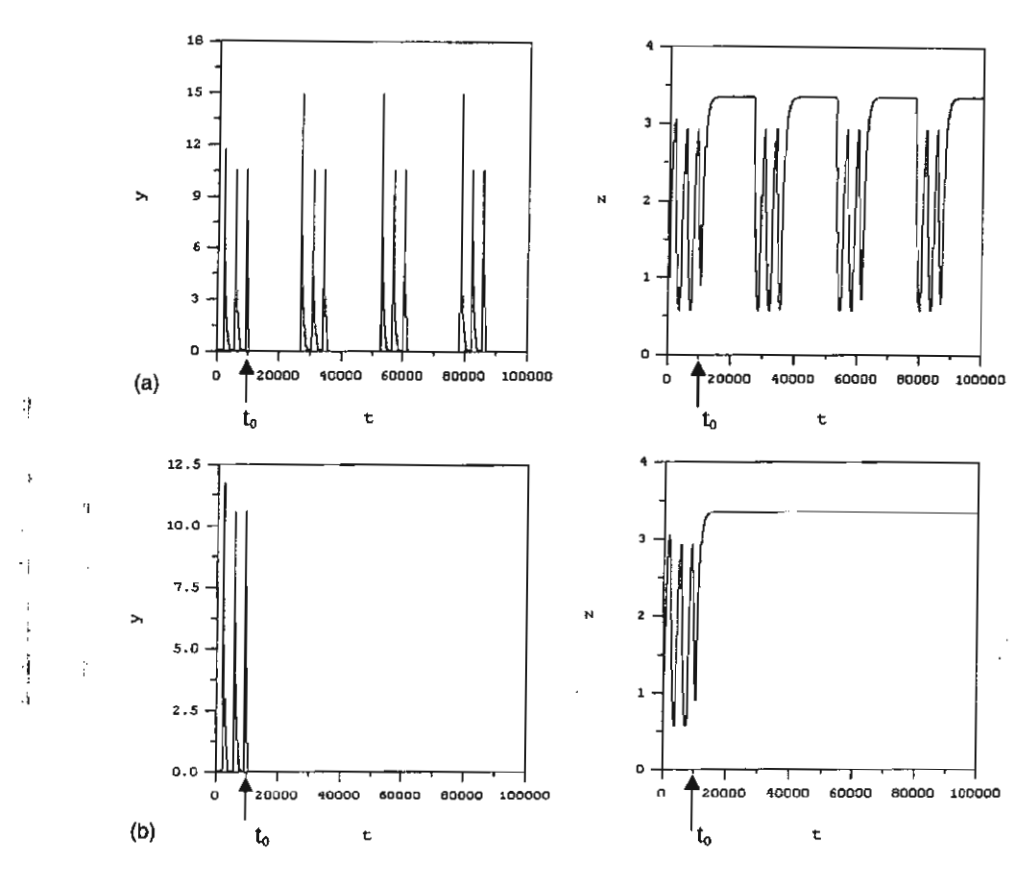


Fig. 7. Computer simulations of the extended model for estrogen treatment, Eqs. (38)–(40), with  $\varepsilon = 0.1$ ,  $\delta = 0.9$ ,  $a_1 = 0.05$ ,  $a_2 = 0.009$ ,  $a_3 = 0.675$ ,  $a_4 = 0.01$ ,  $a_5 = 0.005$ ,  $b_1 = 0.1$ ,  $b_2 = 0.3$ ,  $b_3 = 0.01$ ,  $k_1 = 0.1$ ,  $k_2 = 0.5$ , and  $k_3 = 0.025$ . The duration of estrogen treatment, initiated at the time  $t_0 = 10,000$ , is (a) 12 days, (b) 21 days, with  $k_C = 0.2$ .

observed to peak for a short period just a couple of days prior to menstruation across a woman's menstrual cycle. This may lead us to wonder whether such monthly bursts in estrogen secretion could play an important role in the controlling mechanism by which estrogen takes part in the regulation of bone mass balance in the premenopausal women. We investigate theoretically whether administration of estrogen in monthly (equivalently every 28 days) bursts to a postmenopausal subject could effect some observable change in the dynamics of the bone remodeling process which may compensate for the functional role of estrogen secretion in the premenopausal period. This is done by taking the system of Eqs. (38)-(40) to the limit as  $\Delta T \rightarrow 0$ , while p = 28 days, such that the single-bursts of estrogen across the menstrual cycle can be modeled by the original system Eqs. (4)-(6)

with the additional resetting conditions:

$$x(m+) = x(m-) \tag{41}$$

$$y(m+) = (1 - k_C)y(m-)$$
 (42)

$$z(m+) = z(m-) \tag{43}$$

where m = pn, n = 0, 1, 2, ... and  $k_C$  represents the amplitude of the estrogen bursts. We can carry out an analysis of the dynamics of solutions to the system of Eqs. (4)-(6) with resetting conditions (41)-(43) by following the technique described by Robert and Kao (1998) in their work on the dynamics of infectious diseases with birth pulses.

If (x(t), y(t), z(t)) is a solution of (4)–(6) for  $t \in (0, p)$ , and boundary conditions

$$x(0) = x(p) \tag{44}$$

$$y(0) = (1 - k_C)y(p)$$
 (45)

$$z(0) = z(p) \tag{46}$$

then Eqs. (4)-(6) with (41)-(43) have a periodic solution defined by

$$(x_p(t), y_p(t), z_p(t)) = (x(t), y(t), z(t))$$
  
for  $t \in (0, p)$ 

and

$$(x_p(t+p), y_p(t+p), z_p(t+p))$$
  
=  $(x_p(t), y_p(t), z_p(t))$ 

for all non-integer t (Robert and Kao, 1998; Heesterbeek and Robert, 1995).

The local stability of the period 1 solution  $(x_p(t),$  $y_p(t)$ ,  $z_p(t)$ ) of (4)–(6) with (41)–(43) may be determined by considering the behavior of small-amplitude perturbations of the solution. Defining

$$(x(t), y(t), z(t)) = (x_p(t) + \chi(t), y_p(t) + \eta(t), z_p(t) + \xi(t))$$

these may be written as

$$\begin{pmatrix} \chi(t) \\ \eta(t) \\ \xi(t) \end{pmatrix} = \Phi(t) \begin{pmatrix} \chi(0) \\ \eta(0) \\ \xi(0) \end{pmatrix}$$

where  $\Phi(t)$  satisfies

$$\frac{\mathrm{d}\Phi(t)}{\mathrm{d}t} = J_1 \bigg|_{(x_n, y_n, z_n)} \Phi(t)$$

while 
$$J_{1} = \begin{pmatrix} -b_{1} & -\frac{a_{1}}{(k_{1}+y)^{2}} & 0\\ \varepsilon \left[ \frac{a_{3}k_{2} - 2a_{2}x - a_{3}x^{2}}{(k_{2}+x^{2})^{2}} \right] yz & \varepsilon \left[ \frac{(a_{2}+a_{3}x)z}{k_{2}+x^{2}} - b_{2} \right] & \varepsilon \left[ \frac{(a_{2}+a_{3}x)y}{k_{2}+x^{2}} \right]\\ \varepsilon \delta \left[ a_{4} - a_{5}z \left( \frac{k_{3}}{(k_{3}+x)^{2}} \right) \right] & 0 & \varepsilon \delta \left( -\frac{a_{5}x}{k_{3}+x} - b_{3} \right) \end{pmatrix}$$

with  $\Phi(0) = I$ , the identity matrix. The resetting conditions (41)-(43) become

$$\begin{pmatrix} \chi(m+) \\ \eta(m+) \\ \xi(m+) \end{pmatrix} = J_2 \begin{pmatrix} \chi(m-) \\ \eta(m-) \\ \xi(m-) \end{pmatrix}$$

where

$$J_2 = \begin{pmatrix} 1 & 0 & 0 \\ 0 & 1 - k_C & 0 \\ 0 & 0 & 1 \end{pmatrix}$$

Hence, if all three eigenvalues of

$$M = \begin{pmatrix} 1 & 0 & 0 \\ 0 & 1 - k_C & 0 \\ 0 & 0 & 1 \end{pmatrix} \Phi(1)$$

have absolute values less than one, then the period 1 solution is locally stable (Heesterbeek and Robert, 1995).

Now, through some straightforward manipulations, it can be found, for small-amplitude solutions about the steady state  $(x_1, 0, z_3)$ , that the conditions for the absolute values of the three eigenvalues of M to be less than one will be assured if those conditions for the eigenvalues of  $J_1(x_1, 0, z_3)$  to have negative real parts are satisfied. To be precise, the stability conditions for the eigenvalues of M to have absolute values less than one are that

$$\frac{(a_2 + a_3 x_1) z_3}{k_2 + x_1^2} < b_2 \tag{47}$$

$$1 - k_C < \exp\left[\varepsilon \left(b_2 - \frac{(a_2 + a_3 x_1) z_3}{k_2 + x_1^2}\right)\right]$$
 (48)

if all parametric values are assumed positive. However, if (47) holds then (48) is automatically satisfied. But, (47) is the required condition for the eigenvalues of  $J_1(x_1, 0, z_3)$  to have negative real parts.

$$\begin{bmatrix}
\varepsilon \left[ \frac{(a_2 + a_3 x)y}{k_2 + x^2} \right] \\
\varepsilon \delta \left( -\frac{a_5 x}{k_3 + x} - b_3 \right)
\end{bmatrix}$$

This means that if the steady state  $(x_1, 0, z_3)$  is stable before the application of estrogen in monthly bursts, it will remain stable afterwards, apart from the spikes appearing every period of 28 days in the osteoclasts time series due to external estrogen administration.

The analysis of small perturbations about a different solution, other than  $(x_1, 0, z_3)$ , is not so straightforward, however, and we resorted to carrying out numerical experiments instead. As a result, we found not so surprisingly that estrogen applications in monthly bursts do not appear to effect any change in the dynamic behavior of the solution to the system model in all the cases that we attempted, irrespective of the magnitude of  $k_C$ , discounting the appearance of spikes due to external estrogen each menstrual cycle. Noticeable affect is only observed if the hormone application lasts for a significant duration  $\Delta T$ , as has been noted in Section 7.2. This is, in fact, in agreement with the conclusion made by Muse et al. (1986), from their investigation, that the alterations in calcium-regulating hormones and bone mass that occur during menopause, and several amenorrhea states, appear to occur when perturbations of gonadal steroids are of greater magnitude and duration than those in the normal menstrual cycle. We note, however, that clinical reports are still contradictory and the mechanisms behind this steroid's action remain unclear. Further careful study and investigation need to be carried out before any definite conclusions can be made.

## 8. Conclusion

We have demonstrated, through the construction and analysis of a core model for the bone formation and resorption process mediated by PTH, that several nonlinear dynamic behavior can be deduced which closely simulates clinical data. Even though the model is kept relatively simple, it incorporates the nonlinearity property of the system as well as the way the state variables possess highly diversified time responses. The model can then elucidate certain aspects of the underlying mechanisms. Apart from yielding valuable insights, such investigation, taken with great care, can suggest new possibilities, new interpretations, or a different approach in dealing with this complexed remodeling process.

Moreover, it has been proposed (Prank et al., 1995; Prank et al., 1994) that in simple organisms, the detection of nonlinear behavior in information transfer is in fact associated with differentiation and proliferation. Modulation of the amplitude and/or the frequency of the hormone pulses in higher organisms can modify

intracellular signaling pathways, gene expression, cell proliferation, and cellular function (Goldbeter and Li, 1989). Further studies on the effects of pulsatile hormone secretion on the regulation of cell and organ function and structure can be found in the work of Veldhuis (2000) and that of Brabant et al. (1992). More recently, Hock et al. (2002) also gave a very clear outline of the actions of PTH, focusing on the physiological and cellular effects of PTH on the skeleton but also considering the kidney and the cardiovascular system, the latter being a recently recognized target of PTH action. This line to investigation, therefore, deserves closer attention and further study, since it could help explain the physiological linkage between functional and genetic programs of the living organisms.

### Acknowledgements

This work is supported by the Thailand Research Fund with a senior researcher grant (contract number RTA/02/2542) and a scholarship of the Royal Golden Jubilee Ph.D. Program (contract number PHD/0016/2543, 3 M.MU/43/A.1).

#### References

Albright, F., Smith, P.H., Richardson, A.M., 1941. Postmenopausal osteoporosis. JAMA 116, 2465-2474.

Albright, J.A., Sauders, M., 1990. The Scientific Basis of Orthopaedics. Appleton & Lange, Norwalk, CT.

Brabant, G., Prank, K., Schofl, C., 1992. Pulsatile patterns in hormone secretion. Trends Endocrinol. Metab. 3, 183-190.

Brown, E.M., 1991. Extracellular Ca<sup>2+</sup> sensing, regulation of parathyroid cell function, and role of Ca<sup>2+</sup> and other ions as extracellular (first) messengers. Physiol. Rev. 71, 371-411.

Burgess, T.L., Qian, Y., Kaufman, S., Ring, B.D., Van, G., Capparelli, C., Kelly, M., Hsu, H., Boyle, W.J., Dunstan, C.R., Hu, S., Lacey, D.L., 1999. The ligand for osteoprotegerin (OPGL) directly activates mature osteoclasts. J. Cell Biol. 145, 527-538.

DeCherney, A., 1993. Physiologic and pharmacologic effects of estrogen and progestins on bone. J. Reprod. Med. 38 (Suppl. 12), 1007-1014.

Dempster, D.W., Cosman, F., Parisisen, M., Shen, V., Linsay, R., 1993. Anabolic actions of parathyroid hormone on bone. Endocr. Rev. 14, 690-709.

Eckhaus, W., 1979. Asymptotic analysis of singular perturbation. North-Holland, Amsterdam.

Goldbeter, A., Li, Y.X., 1989. In: Goldbeter, A. (Ed.), Cell to Cell Signalling: From Experiments to Theoretical Models. Academic Press, London.

- Harms, H.M., Kaptaina, U., Kulpmann, W.R., Brabant, G., Hesch, R.D., 1989. Pulse amplitude and frequency modulation of parathyroid hormone in plasma. J. Clin. Endocrinol. Metab. 69 (4), 843-851.
- Heersche, J.N.M., Cherk, S., 1989. Metabolic Bone Disease: Cellular and Tissue Mechanisms. CRC Press, Boca Raton.
- Heesterbeek, J.A.P., Robert, M.G., 1995. Threshold quantities for helminth infections. J. Math. Biol. 33 (4), 415-434.
- Hock, J.M., Gera, I., 1992. Effects of continuous and intermittent administration and inhibition of resorption on the anabolic response of bone to parathyroid hormone. J. Bone Miner. Res. 7 (1), 65-72.
- Hock, J.M., Fitzpatrick, L.A., Bilezikian, J.P., 2002. Principle of Bone Biology, vol. 1, 2nd ed. Academic Press, London.
- Isogai, Y.T., Akatsu, T., Ishizuya, T., Yamaguchi, A., Hori, M., Tokahashi, N., Suda, T., 1996. Parathyroid hormone regulates osteoblast differentiation positively or negatively depending on differentiation stages. J. Bone Miner. Res. 11, 1384-1393.
- Jones, C.K.R.T., 1994. Geometric singular perturbation theory. Dyn. Syst. Montecatibi Terme Lect. Notes Math. 1609, 44-118.
- Kaper, T.J., 1999. An introduction to geometric methods and dynamical systems theory for singular perturbation problems. Analyzing multiscale phenomena using singular perturbation methods. In: Cronin, J., O'Malley Jr., R.E. (Eds.), Proceedings of the Symposia on Applied Mathematics, vol. 56. American Mathematical Society.
- Kong, Y.Y., Yoshida, H., Sarosi, I., Tan, H.L., Timms, E., Capparelli, C., Morony, S., Santos, A., Van, G., Itie, A., Khoo, W., Wakeham, A., Dunstan, C., Lacey, D., Mak, T., Boyle, W., Penninger, J., 1999. OPGL is a key regulator of osteoclastogenesis, lymphocyte development and lymph-node organogenesis. Nature 397, 315-323.
- Kroll, M.H., 2000. Parathyroid hormone temporal effects on bone formation and resorption. Bull. Math. Bio. 62, 163-188.
- Leah, E.K., 1988. Mathematical Models in Biology. Random House, New York.
- Lenbury, Y., Kumnungkit, K., Novaprateep, B., 1997. Detection of slow-fast limit cycles in a model for electrical activity in the pancreatic β-cell. IMA. J. Maths. Appl. Med. Biol. 133 (1), 49-97.
- Marcus, R., 1994. Osteoporosis. Blackwell Scientific Publication, Oxford.
- Momsen, G., Schwarz, P., 1997. A mathematical/physiological model of parathyroid hormone secretion in response to blood-ionized calcium lowering in vivo. Scand. J. Clin. Lab. Invest. 57, 381-394.
- Moon, L.Y., Wakley, G.K., Turner, R.T., 1991. Dose-dependent effects of tamoxifen on long bones in growing rats: influence of ovarain status. Endocrinology 129, 1568-1574.
- Muratori, S., Rinaldi, S., 1992. Low- and high-frequency oscillations in three-dimensional food chain systems. Siam. J. Appl. Math. 52, 1688–1706.

- Muse, K.N., Manolagas, S.C., Deftos, L.J., Alexander, N., Yen, S.S.C., 1986. Calcium-regulating hormones across the menstrual cycle. J. Clin. Endocrinol. Metab. 62 (2), 1313– 1315.
- O'Malley Jr., R.E., 1974. Introduction to Singular Perturbations. Academic Press, London.
- Osipove, A.V., Soderbacka, G., Eirold, T., 1986. On the existence of positive periodic solutions in a dynamical system of two predator-one prey type. Viniti Deponent No. 4305-B4386 (in Russian).
- Prank, K., Harms, H., Dammig, M., Brabant, G., Mitschke, F., Hesch, R.D., 1994. Is there is low-dimensional chaos in pulsatile secretion of parathyroid hormone in normal human subjects? Am. J. Physiol. 266, E653–E658.
- Prank, K., Harms, H., Brabant, G., Hesch, R.D., 1995. Nonlinear dynamics in pulsatile secretion of parathyroid hormone in normal human subjects. Chaos 5, 76-81.
- Prestwood, K.M., Pilbeam, C.C., Burleson, J.A., Woodiel, F.N., Delmas, P.D., Deftos, L.J., Raisz, L.G., 1994. The short-term effects of conjugated estrogen on bone turnover in older women. J. Clin. Endocrinol. Metab. 79, 366-371.
- Robert, M.G., Kao, R.R., 1998. The dynamics of an infectious disease in a population with birth pulses. Math. Biosci. 149, 23-36.
- Schecter, S., 1985. Persistence unstable equilibria and closed orbits of a singularly perturbed equation. J. Diff. Equas. 60, 131– 141.
- Schmitt, C.P., Schaefer, F., Bruch, A., Veldhuis, J.D., Gayk, H.S., Stein, G., Ritz, E., Mehls, O., 1996. Control of pulsatile and tonic parathyroid hormone secretion by ionized calcium. J. Clin. Endocrinol. Metab. 81, 4236–4243.
- Takahashi, N., Udagawa, N., Suda, T., 1999. A new member of tumor necrosis factor ligand family, ODF/OPGL/TRANCE/ RANKL, regulates osteoclast differentiation and function. Biochem. Biophys. Res. Commun. 256, 449-455.
- Tam, C.S., Heersche, J.N.M., Murray, T.M., Parsons, J.A., 1982. Parathyroid hormone stimulates the bone apposition rate independently of its resorptive action: differential effects of intermittent and continuous administration. Endocrinology 110 (2), 506-512.
- Turner, R.T., Lawrence, B.R., Thomas, C.S., 1994. Skeletal effects of estrogen. Endocr. Rev. 15 (3), 275-300.
- Veldhuis, J.D., 2000. Nature of altered pulsatile hormone release and neuroendocrine network signaling in human ageing: clinical studies of the somatotropic, gonadotropic, corticotropic and insulin axes. Novartis Found. Symp. 227, 163– 189.
- Weryha, G., Leclere, J., 1995. Paracrine regulation of bone remodeling. Horm. Res. 43, 69-75.
- Whitfield, J.F., Morley, P., Willick, G.E., 1998. The parathyroid hormone: an unexpected bone builder for treating osteoporosis. Landes Bioscience Company, Austin, Tex.

# A delay-differential equation model of the feedback-controlled hypothalamus-pituitary-adrenal cortex hormone secretion system in humans

YONGWIMON LENBURY\*and PORNSARP PORNSAWAD

Department of Mathematics, Faculty of Science, Mahidol University,

Rama 6 Road, Bangkok 10400, Thailand

September 30, 2004

The present work develops and analyzes a model system of delay-differential equations which describes the core dynamics of the stress-responsive hypothalamus-pituitary-adrenal axis. This neuroendocrine ensemble exhibits prominent pulsatile secretory patterns governed by nonlinear and time-delayed feedforward and feedback signal interchanges. Formulation and subsequent bifurcation analysis of the model provide qualitative and mathematical frame work for better understanding of the delayed responsive mechanisms as well as the dynamic variations in different pathological situations.

Keywords: cortisol secretion; delay-feedback controlled system; Hopf bifurcation; nonlinear model.

### 1 Introduction

The hypothalamus-pituitary-adrenal axis is a critical stress-responsive component which initiates life sustaining adaptive reactions to internal stresses, such as disease, and external stresses, such as hard work or lack of sleep. Signals may originate from either outside or inside the body and are mediated by the central nervous system. Thus, many changes in the environment ultimately can stimulate the secretion of releasing hormones, which produce effects in the body in order to adapt to the change.

<sup>\*</sup>Corresponding author

Neurons synthesize and package releasing hormone precursors in their cell bodies, and these products are transported down the length of their axons to the nerve endings, where a signal is awaited for secretion (Norman & Litwack, 1997). Since most of the cell bodies of these neurons are found in different areas of the hypothalamus, signals for secretion come from higher levels, usually from aminergic or cholinergic neurons in various parts of the brain. The hippocampus of the limbic system may signal the neurons to release the hormone by changing the firing rate of electric signals or by chemical interneuronal contacts (Norman & Litwack, 1997). The response of the hypothalamus to signals from the limbic system is the secretion of the corticotropin-releasing hormone, CRH. CRH is released from specific cells in the hypothalamus into a closed portal circulation intimately connected with the anterior pituitary. Releasing hormones act at cognate plasma membrane receptor levels either to cause an increase in cyclic AMP or to stimulate the phosphatidylinositol cycle, leading to the stimulation of protein kinase C and an increase in cytoplasmic calcium ion concentration. The increased level of cyclic AMP stimulates protein kinase A leading to ACTH release from the corticotroph of the anterior pituitary. Vasopressin also increases the secretion of ACTH, although the main role of vasopressin appears to be one of helping CRH in this activity. Also, according to Engler et al. (1999) the nanopeptide vasopressin is a weak ACTH secretagog in rat and in man, although it appears to be potent in the bovine species. Therefore, we shall not consider its direct stimulatory effect in this work.

Following the secretion of ACTH into the blood circulation after stimulation by CRH from the hypothalamus, ACTH molecules bind to a specific receptor on the outer cell membranes of all three layers of cells of the adrenal cortex, the zona glomerulosa, the zona fasciculata, and the zona reticularis. Cortisol is the main product of ACTH stimulation of the zona fasciculate and reticularis cells of the human adrenal cortex. A glucocorticoid essential to life, cortisol acts on different cells in different ways. Without the secretion of cortisol during stress, a human could not survive. When cortisol is overproduced, often by a pituitary tumor causing high level of circulating ACTH, the resulting disease is known as Cushing's disease. When cortisol is underproduced, the resulting disease is known as Addison's disease, which is most frequently the result of adrenal destruction.

When cortisol is produced in response to ACTH, it has negative feedback effects on various elements of the hormonal cascade system, schematically described in Fig 1. Malfunctions in this negative feedback mechanisms can lead to several complications. Lowered cortisol levels or enlarged output of ACTH by the anterior pituitary, due to reduced negative feedback, results in adrenal hyperplasia and hypersecretion, which, together with adrenal testosterone, can lead to masculinization of female babies. Precocious puberty in males can also result from this condition (Norman & Litwack, 1997).

It is therefore crucial that a better biomathematical description of such a process be attempted to provide more solid framework for the study and assessment of dynamic interfaces in health and disease. Such studies are necessary especially since a recent report by Ilias et al. (2002) on the complexity of cortisol seems to

A delay-differential equation model of the feedback-controlled hypothalamus-pituitary-adrenal cortex3

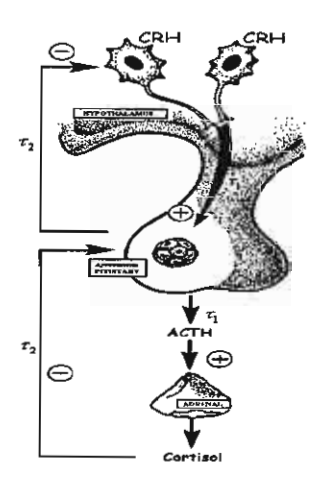


Figure 1: A schematic representation of feedforward-feedback model of plasma CRH, ACTH, and cortisol.

confirm that cortisol secretion operates under non-regular dynamics. Its fractal dimension after sleep deprivation (a weakened state) is lower than that measured before sleep deprivation (healthier state). In the past, basal cortisol secretion has been proposed to arise via linear mechanisms. Then, in 1991 Lenbury and Pacheenburawana presented a mathematical model in which cortisol secretion was described by nonlinear differential equations with exponential feedback terms. However, Ilias et al. (2002) were the first, to our knowledge, to utilize nonlinear/fractal analysis in the experimental study of the complex mechanisms underlying the circadian secretion of cortisol.

Complexity and nonlinear methods have become one of the most versatile and promising new research tools for the study and characterization of circadian rhythmicity in humans. Episodic secretion of cortisol has been clinically observed and reported in several research works (Carnes et al., 1991; Carnes et al., 1989; Krieger et al., 1971; Weitzman et al., 1971) as early as that of Weitzman et al. (1971) which reported on twenty-four hour patterns of episodic cortisol secretion in normal subjects. Their data seriously challenged the concept that a "steady state" or "basal level" of cortisol is present during any extended time compartment of the 24-hour cycle. In a different report in the same year, Krieger et al. (1971) attempted to delineate more precisely the time course of adrenal secretory activity in the normal human and patients with Cushing's syndrome. Later, Moore-Ede et al. (1983) pointed out several advances in characterization of the properties of hypothalamic circadian pacemakers and the implications of such rhythmicity for medical diagnosis. It was not until very recently, however, that an attempt was made by Ilias et

al. (2002) to use mathematical methods based on nonlinear/fractal analysis in the experimental study of the underlying complex mechanisms. Their conclusion, that post-sleep deprivation changes the fractal dimensions of cortisol, supports Lenbury and Pacheenburawana's (1991) suggestion that nonlinear dynamics analysis may be a viable tool in our attempts to delineate pulsatile secretory patterns in health and disease.

Lenbury and Pacheenburawana's (1991) nonlinear model did not, however, account for the delays associated with the time interval needed before an action in response to the stimulating signal can be taken by the release of the appropriate hormones. Several studies have presented clinical evidence of such delayed responses in the hypothalamus-pituitary-adrenal cortex (Norman, 1997; Posener et al., 1997; Won et al., 1986). Specifically, Posener et al. reported in 1997 that cortisol exerted a feedback effect by significantly decreasing plasma ACTH levels with a time delay of approximately 60 min. An earlier study by Hermus et al. (1984) reported a 30 min. delay in the positive feedforward effects of CRH on plasma ACTH levels, the increase of which was followed by a rise in the cortisol level with time delay of an extra 30 minutes.

To our knowledge, mathematical modelling and analysis of hormonal secretion systems with delays have up to date been the subject of few published reports in humans. In 2001, Keenan et al. presented a biostatistical model which incorporated expected within axis physiological linkages via time-delayed, nonlinear, dose-responsive, rate-sensitive, and integral feedforward and feedback controls. Although the model appeared to generate realistic pulsatile secretory patterns, it contributed little towards the illumination of the underlying mechanism of the secretion network or the crucial role which the delayed responses might play in this important feedback controlled system. Because of its nonlinear structure, the introduction of a time delay in feedback loops can alter the stability and dynamic properties of the hormonal cascade yielding insightful clinical implications.

We propose, therefore, to incorporate such time delays into the earlier model by Lenbury and Pacheenburawana (1991) and subsequently analyze the model by Hopf bifurcation in order to find the critical time delay, beyond which the model system may exhibit periodic dynamics. With the set of parameters appropriately chosen through such analysis, we shall construct a bifurcation diagram in order to identify the ranges of the system's parametric values for which chaotic secretory patterns are permitted by our time-delay differential equation model. The simulated solution in such a case appears to compare well with clinical data which consistently showed multifactorical frequency structure (Carnes et al., 1991).

# 2 A Feedforward-Feedback Delay Model

In formulating our mathematical model of the negative feedback regulation of cortisol secretion, the following events are considered. CRH (R) is secreted from the hypothalamus and stimulates the secretion of ACTH (A) from the anterior pitu-

itary with a delay of  $\tau_1$  in time. ACTH then stimulates the cortisol (C) secretion from the adrenal gland with the same time delay  $\tau_1$  as that in the short loop feedforward effect of CRH on ACTH secretion. Thus, we assume equal delays in both short feedforward loops in the cascade, following the clinical evidence reported by Hermus et al. (1984) mentioned above. We also take into account the negative feedback effects of cortisol on ACTH, incorporating a time delay of  $\tau_2$ , supported by the clinical evidence already mentioned above (Moore-Ede et al., 1983). The investigation by Posener et al. (1998) also utilized a covariance analysis which suggested that the inhibition effects of ACTH on CRH were not due to the rise in cortisol caused by the rise in ACTH itself. Thus, we shall ignore the long-loop negative feedback effect of cortisol on CRH and only consider the short-loop feedback effect of ACTH on CRH not mediated by cortisol, which is then assumed to occur with a delay time of  $\tau_2$  as well.

These assumptions on delay are made here in order to carry out a theoretical analysis to investigate the stability and the possibility of periodic solutions of the system comparable to clinically observed behavior. In the later section, the time lags in the feedforward or feedback loops are allowed to be different in our numerical experiment to investigate the possibility of chaotic dynamics

In 1986, Won et al. investigated the mechanisms responsible for glucocorticoid feedback on nonstress induced ACTH secretion in normal subjects and reported a linear relationship between the degree of inhibition of ACTH ( $\Delta$ ACTH) levels after cortisol administration. The degree of inhibition was measured as the reduction in ACTH as percentages of the mean baseline level. They found that "A linear correlation between the degree of inhibition of ACTH level and the corresponding cortisol concentrations does exist at 60 min. after administration (r=0.95, P<0.05)". From such clinical evidence, we see that the specific rate of change of ACTH at time t,  $A_t$ , due to the negative feedback effect of high cortisol concentration at time  $t-\tau_2$ ,  $C(t-\tau_2)$ , may be described by the following equation

$$\frac{1}{A_t} \frac{d}{dC(t - \tau_2)} A_t = -kC(t - \tau_2)$$
 (2.1)

where k is some positive constant of variation. Integrating (2.1) yields  $k_2e^{\gamma(C_0^2-C^2(t-\tau_2))}$  for the rate  $A_t$ , where  $\gamma=\frac{k}{2}$  and  $k_2$  corresponds to the rate  $A_t$  when  $C=C_0$ . Thus,  $C_0$  is the critical value of A, which means that if C falls below  $C_0$  then the secretion rate of A should rise above  $k_2$ . If C rises above  $C_0$ , on the other hand, the secretion rate of A should be reduced in magnitude below  $k_2$ , with a time delay of  $\tau_2$ . Similar arguments can be applied to the rate of change  $R_t$ . However, the rate of change of ACTH should also vary in direct proportion to plasma CRH concentration at time  $t-\tau_1$ ,  $R(t-\tau_1)$ . This concentration-dependent effects of CRH on ACTH was investigated by Engler et al. (1999), who reported clinical data showing ACTH release (not its level) increasing exponentially as the log of CRH. This means, in fact, that ACTH secretion rate may be assumed to depend in a linear fashion on CRH level, at least to the first order. It is reasonable to

also assume the same linear dependence between the secretion rate of cortisol and ACTH level. Therefore, the three component hormonal cascade can be described by the following system of nonlinear differential equations:

$$\frac{dR(t)}{dt} = -\delta_1 R(t) + k_1 e^{\alpha (A_0^2 - A^2(t - \tau_2))}$$
(2.2)

$$\frac{dA(t)}{dt} = -\delta_2 A(t) + k_2 R(t - \tau_1) e^{\gamma (C_0^2 - C_0^2 (t - \tau_2))}$$
(2.3)

$$\frac{dC(t)}{dt} = -\delta_3 C(t) + k_3 A(t - \tau_1) \tag{2.4}$$

where R(t) is the concentration of CRH at any time t; A(t) and C(t) are the concentrations of ACTH and cortisol, respectively, above their respective residual levels, while  $k_1, k_2$ , and  $k_3$  the respective secretion rate constants of R, A, and C, while  $\alpha$  and  $\gamma$  are the feedback potency constants.  $\delta_1, \delta_2$ , and  $\delta_3$  are the removal rates of R, A, and C, respectively. It is assumed that each of these hormones is cleared from the blood stream according to the first-order kinetics. In order to arrive at the above mathematically tractable model, we have assumed that the stimulating/inhibitory effects of other known factors are relatively weak and thus negligible. More detail of the derivation of the model can been seen in the paper by Lenbury and Pacheenburawana (1991).

We associate the initial values of the form:

$$R(t) = \phi_1(t)$$
 for  $-\tau_1 \le t \le 0$ ,  
 $C(t) = \phi_2(t)$  for  $-\tau_2 \le t \le 0$ ,  
 $A(t) = \phi_3(t)$  for  $-\tau_3 \le t \le 0$ , (2.5)

where  $\tau_3 = max(\tau_1, \tau_2), \ \phi_i \in C([-\tau_i, 0], \Re^+) \ \text{and} \ \phi_i(0) > 0, \ i = 1, 2, 3.$ 

We now introduce dimensionless variables by letting  $x=\frac{R}{R_0},\ y=\frac{A}{A_0},\ z=\frac{C}{C_0},\ K_1=\frac{k_1}{R_0},\ K_2=\frac{k_2}{A_0}R_0,\ \beta_1=\alpha A_0^2,\ \beta_2=\gamma C_0^2,\ \text{and}\ K_3=\frac{k_3}{C_0}A_0,\ \text{where}\ R_0,A_0,\ \text{and}\ C_0$  are the critical values of R,A, and C, respectively. We are then led to

$$\dot{x}(t) = -\delta_1 x(t) + K_1 e^{\beta_1 (1 - y^2 (t - \tau_2))}$$
(2.6)

$$\dot{y}(t) = -\delta_2 y(t) + K_2 x(t - \tau_1) e^{\beta_2 (1 - z^2(t - \tau_2))}$$
(2.7)

$$\dot{z}(t) = -\delta_3 z(t) + K_3 y(t - \tau_1). \tag{2.8}$$

So that the steady state values of R, A, and C are  $R_0$ ,  $A_0$ , and  $C_0$ , respectively, at which point the 3 state variables should be stationary, we see that we need to put  $K_1 = \delta_1$ ,  $K_2 = \delta_2$ , and  $K_3 = \delta_3$  in (2.6)-(2.8). We also note further that  $\alpha$  and  $\gamma$  represent the strength of the negative feedback effect of ACTH on CRH and that of cortisol on ACTH, respectively. Since ACTH and cortisol are secreted at noticeably different orders of magnitude  $\alpha$  and  $\gamma$  may be different. However, after

A delay-differential equation model of the feedback-controlled hypothalamus-pituitary-adrenal cortex?

rescaling by  $A_0$  and  $C_0$ , the corresponding feedback potency constant  $\beta_1$  should be comparable to  $\beta_2$ . Therefore to carry out our bifurcation analysis, we first put  $\beta = \beta_1 = \beta_2$ , but will allow them to be different in our later investigation. We now arrive at the following core model equations:

$$\dot{x}(t) = -\delta_1 x(t) + \delta_1 e^{\beta(1 - y^2(t - \tau_2))}$$
(2.9)

$$\dot{y}(t) = -\delta_2 y(t) + \delta_2 x(t - \tau_1) e^{\beta(1 - z^2(t - \tau_2))}$$
(2.10)

$$\dot{z}(t) = -\delta_3 z(t) + \delta_3 y(t - \tau_1). \tag{2.11}$$

# 3 Bifurcation Analysis

The model system (2.9)-(2.11) has one positive steady state  $(x_0, y_0, z_0)$ , that is,  $(x_0, y_0, z_0) = (1, 1, 1)$ .

Letting  $X = x - x_0$ ,  $Y = y - y_0$ , and  $Z = z - z_0$ , we are led to the following linearized system of (2.9)-(2.11) at  $(x_0, y_0, z_0)$ .

$$\begin{pmatrix} \dot{X} \\ \dot{Y} \\ \dot{Z} \end{pmatrix} = \begin{pmatrix} -\delta_1 & -2\beta\delta_1 e^{-\lambda\tau_2} & 0 \\ \delta_2 e^{-\lambda\tau_1} & -\delta_2 & -2\beta\delta_2 e^{-\lambda\tau_2} \\ 0 & \delta_3 e^{-\lambda\tau_1} & -\delta_3 \end{pmatrix} \begin{pmatrix} X \\ Y \\ Z \end{pmatrix}$$
(3.21)

The associated characteristic equation of the model system (2.9)-(2.11) is then

$$F(\lambda) \equiv \lambda^3 + a\lambda^2 + b\lambda + c + (d_1\lambda + d_2)e^{-\lambda(\tau_1 + \tau_2)} = 0$$
(3.13)

where

$$a = \delta_1 + \delta_2 + \delta_3 \tag{3.14}$$

$$b = \delta_1 \delta_2 + \delta_1 \delta_3 + \delta_2 \delta_3 \tag{3.15}$$

$$c = \delta_1 \delta_2 \delta_3 \tag{3.16}$$

$$d_1 = 2\beta \delta_2 [\delta_1 + \delta_3] \tag{3.17}$$

$$d_2 = 4\beta \delta_1 \delta_2 \delta_3 \tag{3.18}$$

using the steady state relations that  $\dot{x} = \dot{y} = \dot{z} = 0$  at the point (x, y, z) = (1, 1, 1). We let  $\tau = \tau_1 + \tau_2$  be the composite lag-time and first consider equation (3.13) when  $\tau = 0$ . That is,

$$\lambda^{3} + a\lambda^{2} + (b + d_{1})\lambda + (c + d_{2}) = 0.$$
(3.19)

Using (3.14)-(3.18), it is easily shown that a > 0,  $c + d_2 > 0$ , and  $a(b + d_1) - c - d_2 > 0$ , for all positive parametric values. Thus, by the Routh-Hurwitz condition, all roots of equation (3.19) have negative real parts. Therefore, the steady state (1,1,1) is stable when  $\tau = 0$ .

If we let  $\lambda(\tau) = \alpha(\tau) + i\omega(\tau)$ , where  $\alpha$  and  $\omega$  are real, then we have  $\alpha(0) < 0$ , by the above reason. By continuity, we know that  $\alpha(\tau) < 0$  for positive value of  $\tau$  which is sufficiently small. Thus, the steady state shall remain stable for values of  $\tau$  such that  $0 \le \tau < \tau_0$  for some  $\tau_0 > 0$ .

Suppose  $\alpha(\tau_0) = 0$  for some  $\tau_0 > 0$ , and  $\alpha(\tau) < 0$  for  $0 \le \tau < \tau_0$ , then the stability of (1, 1, 1) is lost at  $\tau = \tau_0$ , at which point  $\lambda = i\omega(\tau_0)$ .

Now,  $i\omega$  is a root of (3.13) iff

$$-i\omega^3 - a\omega^2 + ib\omega + c + (id_1\omega + d_2)(\cos\omega\tau - i\sin\omega\tau) = 0.$$
 (3.20)

Equating real and imaginary parts of both sides of (3.20), we obtain

$$-\omega^3 + b\omega + d_1\omega\cos\omega\tau - d_2\sin\omega\tau = 0 \tag{3.21}$$

$$-a\omega^2 + c + d_1\omega\sin\omega\tau + d_2\cos\omega\tau = 0. \tag{3.22}$$

Adding up the squares of (3.21) and (3.22), one obtains

$$f(\omega) \equiv \omega^6 + (a^2 - 2b)\omega^4 + (b^2 - 2ac - d_1^2)\omega^2 + c^2 - d_2^2 = 0.$$
 (3.23)

If we let  $s = \omega^2$ ,  $p = a^2 - 2b$ ,  $q = b^2 - 2ac - d_1^2$ , and  $r = c^2 - d_2^2$ , then equation (3.23) becomes

$$h(s) \equiv s^3 + ps^2 + qs + r = 0. (2.24)$$

We can consequently write down the following result.

**Lemma 1.** Suppose  $s_1 = \frac{-p + \sqrt{p^2 - 3q}}{3}$ .

(i) Equation (3.24) has a positive root if either

$$(a) r < 0 (3.25)$$

or

(b) 
$$r \ge 0,$$
 (3.26)

$$p^2 - 3q > 0, (3.27)$$

$$s_1 > 0, \tag{3.28}$$

and 
$$h(s_1) < 0.$$
 (3.29)

(ii) Equation (3.24) has no positive real roots if

$$r \ge 0$$
 and 
$$p^2 - 3q < 0.$$

A delay-differential equation model of the feedback-controlled hypothalamus-pituitary-adrenal cortex9

### Proof.

- (i) Suppose r < 0, then h(0) < 0. Since  $\lim_{s \to \infty} h(s) = \infty$ , equation (3.24) must have a positive root where h = 0, by the intermediate value theorem. Suppose  $r \ge 0$ , on the other hand, and  $p^2 3q > 0$ , then  $s_1 = \frac{-p + \sqrt{p^2 3q}}{3}$  is the stationary point of h(s) located on the positive x-axis if  $s_1 > 0$ . Thus, if  $h(s_1) < 0$  while  $h(0) = r \ge 0$ , by the intermediate value theorem, h must vanish somewhere between 0 and  $s_1$ .
- (ii) If  $r \ge 0$  while h'(s) > 0, h is then an increasing function and does not vanish anywhere along the positive x-axis  $\square$ .

If conditions in Lemma 1(ii) hold, then all roots of the characteristic equation (3.13) have negative real parts for all  $\tau \geq 0$ . Thus, the steady state (1,1,1) is always stable in this case.

If, on the other hand, conditions in Lemma 1(i) hold, then equation (3.24) has a positive root. Without loss of generality, we may denote the three positive roots of (3.24) by  $s_1$ ,  $s_2$ , and  $s_3$ . Then, equation (3.23) has three positive roots

$$\omega_k = \sqrt{s_k}, \quad k = 1, 2, 3.$$

Now, let  $\tau_0 > 0$  be the smallest of such  $\tau$  for which  $\alpha(\tau_0) = 0$ . Substituting  $\omega_k$  into equations (3.21)-(3.22) and solving for  $\tau$ , one obtains

$$\tau_k^{(j)} = \frac{1}{w_k} \arcsin\left[\frac{(ad_1 - d_2)\omega_k^3 + (bd_2 - cd_1)\omega_k}{d_2^2 + d_1^2\omega_k^2}\right] + \frac{2\pi(j-1)}{\omega_k}$$
(3.30)

where k = 1, 2, 3, and j = 1, 2, ...

Thus,

$$\tau_0 = \tau_{k_0}^{(j_0)} = \min_{1 < k < 3, j > 1} \left\{ \tau_k^{(j)} \right\} \tag{3.31}$$

and

$$\omega_0 = \omega_{k_0} \tag{3.32}$$

Now, for our model system (2.9)-(2.11), the following result can be shown.

**Lemma 2.**  $s_1 < 0$  if

$$\beta < \beta_0 \equiv \sqrt{\frac{\delta_1^2 \delta_2^2 + \delta_1^2 \delta_3^2 + \delta_2^2 \delta_3^2}{4\delta_2^2 (\delta_1 + \delta_3)^2}}$$
 (3.33)

10

**Proof.** From (3.14)-(3.17), we find that

$$q = \delta_1^2 \delta_2^2 + \delta_1^2 \delta_3^2 + \delta_2^2 \delta_3^2 - 4\beta^2 \delta_2^2 (\delta_1 + \delta_3)^2$$

which is positive if (3.33) holds. We will then have

$$p^2 - 3q < p^2$$

and

$$p = \delta_1^2 + \delta_2^2 + \delta_3^2 > 0.$$

Hence,

$$s_1 = \frac{-p + \sqrt{p^2 - 3q}}{3} < 0.$$

We now make the claim that  $i\omega_0$  is a simple root of equation (3.13), provided (3.33) holds.

Lemma 3. If (3.33) holds, then

$$\frac{dF}{d\lambda}(i\omega_0) \neq 0$$

**Proof.** Suppose, by contradiction, that  $\frac{dF}{d\lambda}(i\omega_0) = 0$ , while  $F(i\omega_0) = 0$ , then after some lengthy manipulations, it can be shown that

$$\frac{d}{d\omega}f(\omega_0) = 0$$

However,

$$\frac{df}{d\omega}(\omega_0) = 2\omega_0 \frac{dh}{ds}(s_0)$$

where  $s_0 = \omega_0^2$ . Since  $\omega_0 > 0$ , we would have  $\frac{dh}{ds}(s_0) = 0$  also. However, the solution of  $h'(s_0) = 0$  would be

$$s_0 = \frac{1}{3} \left[ -p \pm \sqrt{p^2 - 3q} \, \right] = s_1.$$

But,  $s_1<0$  when (3.33) is satisfied, by Lemma 2. This would mean that  $s_0<0$  which contradicts its definition. Therefore,  $h'(s_0)\neq 0$  and so  $\frac{dF}{d\lambda}(i\omega_0)\neq 0$  as claimed

This then leads us to conclude that  $i\omega_0$  is a simple root of equation (3.13) which implies that

 $A\ delay-differential\ equation\ model\ of\ the\ feedback-controlled\ hypothalamus-pituitary-adrenal\ cortex 11$ 

$$\frac{d}{d\tau} \operatorname{Re} \lambda(\tau) \bigg|_{\tau = \tau_0} \neq 0. \tag{3.34}$$

Thus, the steady state (1,1,1,) shall lose its stability and Hopf bifurcation will occur as  $\tau$  increases past the critical value  $\tau_0$ , provided the conditions in Lemma 1(ia) and (3.33) are satisfied.

Summarizing the above analysis, we have the following theorem.

**Theorem 1.** For the composite lag-time  $\tau = \tau_1 + \tau_2$ , let the critical composite lag-time  $\tau_0$  be defined as in (3.31), then the system of delay differential equations (2.9)-(2.11) exhibits the Hopf bifurcation at  $(x_0, y_0, z_0) = (1, 1, 1)$  if  $\frac{1}{4} < \beta < \beta_0$ , when  $\beta_0$  is as defined in (3.33). That is, there exists  $\epsilon > 0$  such that the system (2.9)-(2.11) will have periodic solutions for  $\tau \in (\tau_0, \tau_0 + \epsilon)$ .

**Proof.** It remains only to note that if  $\beta > \frac{1}{4}$  then, considering equations (3.16) and (3.18), we would have r < 0 which is condition (ia) in Lemma 1. Thus, the condition  $\beta > \frac{1}{4}$  ensures that there is a  $\tau_0 > 0$  such that the steady-state (1,1,1) loses its stability at the point  $\tau = \tau_0$ . The condition  $\beta < \beta_0$ , by Lemma 2, ensures that (3.34), which is a necessary condition for Hopf bifurcation, is satisfied  $\square$ .

# 4 Numerical Results

Fig. 2 shows a computer simulation of equations (2.9)-(2.11) with parametric values chosen to satisfy the requirements for Hopf bifurcation set out in the previous section (Theorem 1). The solution trajectory, projected onto the (y,z) plane, tends to a limit cycle as theoretically predicted. The corresponding time courses of CRH and ACTH are shown respectively in Fig. 2b) and 2c) where they become periodic as time passes.

Since there has been evidence (Carnes et al., 1991; Carnes et al., 1989; Ilias et al., 2002; Krieger et al., 1971) of low-dimensional chaos in pulsatile secretion of plasma adrenocorticotropin mentioned in the introduction, we carried out a numerical investigation to discover whether chaotic behavior may occur in our delay feedback controlled model of the hormonal secretion cascade. To this end, a bifurcation diagram was constructed by using parametric values that would lead to cycling in the three state variables, guided by our work in the previous section. Then the system of equations (2.6)-(2.8) was allowed to run for  $10^5$  time steps. We retained only the last  $2\times10^4$  time steps to eliminate transient behavior, using values of  $\beta_2$  between 3.75245 and 3.7538 and changing  $\beta_2$  in steps of  $10^{-5}$ . The relative maximum values of x (CRH) were collected during the last  $2\times10^4$  time steps and plotted as a function of  $\beta_2$  as shown in Fig. 3.

We discover in this bifurcation diagram a period doubling route to chaotic dynamics which can be expected for values of  $\beta_2$  beyond 3.7532. We observe that

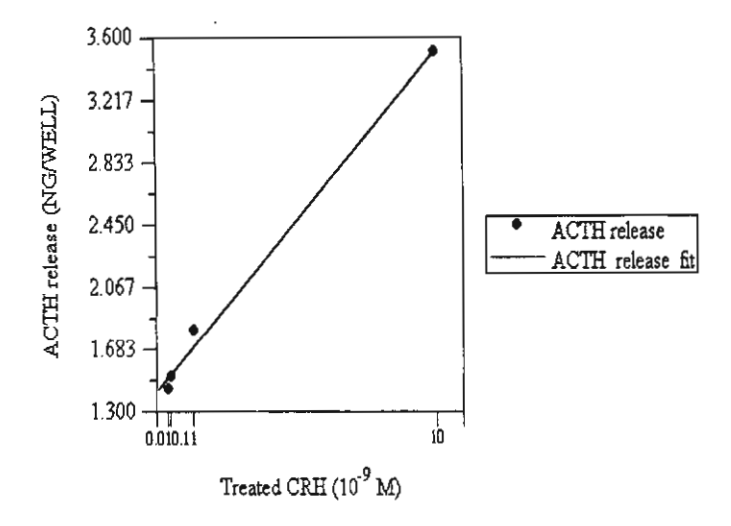


Figure 2: Computer simulation of equation (2.9)-(2.11) with  $\delta_1 = 0.5, \delta_2 = 0.38, \delta_3 = 0.6, \beta = 1.091, \tau_0 = 1.22, \tau_1 = 0.5$  and  $\tau_2 = 0.77$ .

periodic orbits can be found for values of  $\beta_2$  in the range  $0.25 < \beta_2 < 3.7528$  suggesting that chaotic mode of secretion is adopted when the negative feedback effects are relatively strong. When the feedback signals are weak, a more regular episodic secretory patterns are exhibited.

Fig. 4 shows a computer simulation of the model system (2.6)-(2.8) using the parametric values in the chaotic range, with  $\beta_2 = 3.75346$ . The strange attractor is seen in Fig. 4a) projected onto the (y,z)-plane, while the corresponding time series of CRH (x), ACTH (y), and cortisol (z) are shown in Fig. 4b)-4d), respectively.

Characteristic of such chaotic dynamics is the sensitivity to initial conditions. We illustrate this sensitivity by simulating our model system, using the parametric values in the chaotic range employed in Fig. 4, starting from two initial conditions which are different only by  $10^{-9}$  in x(0), while y(0) and z(0) are the same in the two simulations. The two time courses follow the same path only for a short time initially, but diverge to drastically different paths as time progresses as seen in Fig. 5. This clearly demonstrates the sensitivity to initial conditions of the system under nonlinear dynamics which, for this reason, makes any attempts at system control an extremely difficult task to tackle.

A delay-differential equation model of the feedback-controlled hypothalamus-pituitary-adrenal cortex13

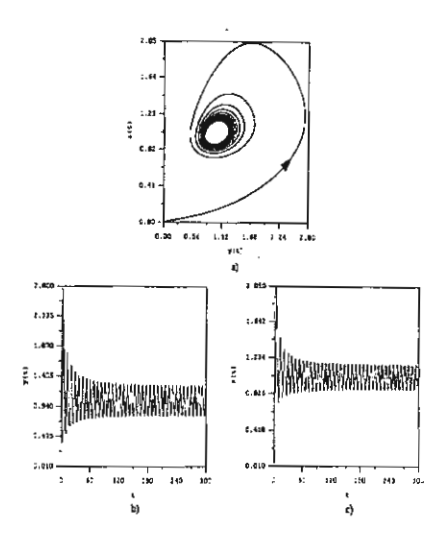


Figure 3: Bifurcation diagram of equations (2.6)-(2.8) with  $\delta_1=0.47, \delta_2=0.401, \delta_3=0.422, K_1=0.477, K_2=0.422, K_3=0.411, \beta_1=0.001, \tau_0=0.522,$  and  $\tau=10$ .

# 5 Discussion and Conclusion

We present in Fig. 6a) some clinical data partly adapted from the report by Engler  $et\ al.$  (1999) on the review of the evidence for the existence of inhibitory as well as stimulatory hypophysiotropic regulation of adrenocorticotropin secretion and biosynthesis. The figure shows pituitary venous concentrations of CRH in two mares given naloxone at a low dose rate at the arrow. In Fig. 6b), actual data of plasma ACTH concentration in a rat sampled every 2 min. is shown, taken from Carnes  $et\ al.$ 's (1989) earlier work. The time series exhibits irregular characteristics in agreement with those simulated from our model, an example of which is shown in Fig. 4, where we need to recall that the state variables x,y, and z plotted in Fig. 4 are ratios of the three hormones over their respective critical levels.

However, there are at least three factors that complicate the interpretation, if not the measurement, of CRH concentration, as cautioned by David N. Orths (1992) in his work on CRH in humans. First, like other hypothalamic releasing factors, the concentration of CRH, presumed to be present in the hypothalamic hypophysial portal venous blood, is hugely diluted by the time it reaches the peripheral veins. Secondly, CRH is produced and presumably secreted by many extrahypothalamic tissues, even though we have assumed this to be of relatively small and thus negligible amount in our model. Finally, there are specific high-affinity, high-capacity CRH-binding proteins present in human plasma. Thus, even

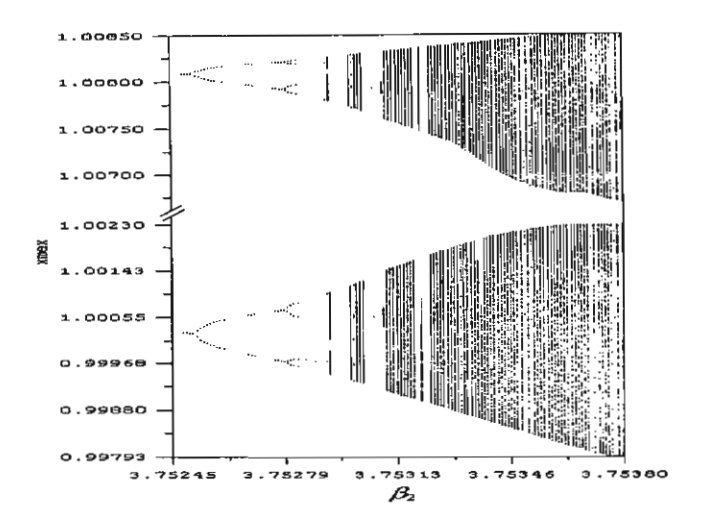


Figure 4: Computer simulation of equations (2.6)-(2.8) with  $\delta_1 = 0.47, \delta_2 = 0.401, \delta_3 = 0.422, K_1 = 0.477, K_2 = 0.422, K_3 = 0.411, \beta_1 = 0.001, \beta_2 = 3.75346, \tau_0 = 0.522, \text{ and } \tau = 10.$ 

though it is possible to measure immunoreactive CRH in peripheral plasma, the absolute peripheral plasma CRH concentration at any moment may not accurately reflect hypothalamic CRH secretion, and thus should be considered with caution.

ACTH measurement also poses problems associated with its bioassays at low plasma concentration. Detection of primary abnormal functioning at the pituitary level is made easier only by the availability of the releasing hormones that make evocater tests possible. In cases of inadequate availability of a pituitary hormone, such as ACTH supply, the target gland hormone (cortisol) is supplied instead (Norman & Litwack, 1997).

In spite of such cautionary notes, our model still provides a viable means by which the complexity and non-linear dynamics of diurnal hormone secretory patterns can be analyzed and qualitative description can be made of this complex delay feedback controlled systems. Our analysis yielded, for each set of physical parameters, a critical composite time delay  $\tau_0$  beyond which value the system exhibits episodic secretory pattern if  $\beta > \frac{1}{4}$ . As the feedback response factor  $\beta$  increases further, more irregular secretory patterns may be expected. Low dimensional chaotic dynamics would appear if  $\beta_2$  increased beyond a certain critical value  $\beta_c$  identified in the bifurcation diagram. This seems to suggest, considering Ilias *et al.*'s (2002) result from their nonlinear analysis of cortisol secretory patterns before and after sleep deprivation, that if the negative feedback effects are too weak, a diseased state is the reasonable diagnosis which then corresponds to the more regular secretory

 $A\ delay-differential\ equation\ model\ of\ the\ feedback-controlled\ hypothalamus-pituitary-adrenal\ cortex 15$ 

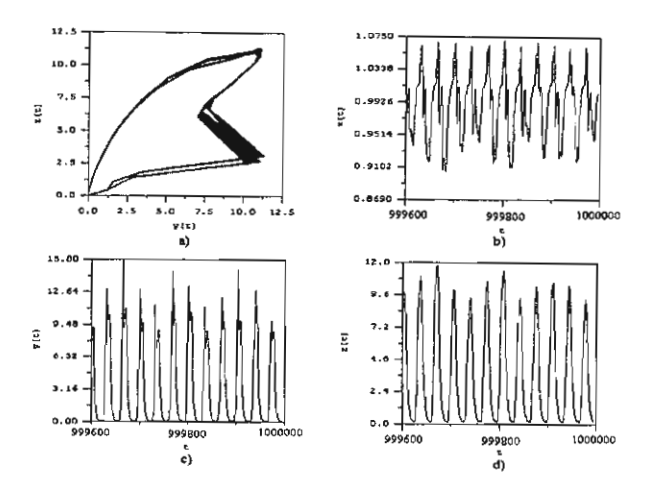


Figure 5: Divergence of time courses, when  $\beta_2 = 3.75346$  in the chaotic range, initiating from two different initial conditions only by  $10^{-9}$  in the initial value of x.

patterns. A relatively strong negative feedback mechanism for larger  $\beta$  leads to a more irregular pattern characteristic of a higher dimensional chaotic dynamics associated then with health. When  $\beta_2$  increases further, becoming greater than approximately 3.87549, the feedback mechanism is now faulty and the system returns to more regular periodic behavior which appears to be the mode of secretion in a diseased state.

Also, there is a critical composite time-delay  $\tau_0$  below which all state variables tend asymptotically to the respective steady-state levels as  $t \to \infty$ . We observe that it is the value of the composite time-delay  $\tau$  which delineates different dynamic behavior in the Hopf bifurcation analysis, not each of the feedforward delay  $\tau_1$  or the feedback delay  $\tau_2$  in our model. We may deduce from this that, in the human body, the feedforward and feedback response processes may be operating in a complimentary fashion. In health, an over zealous response in the feedforward loop can be compensated for by a late response in the feedback loop, and vise versa, resulting in an optimal turn-around time for all components in the whole cascade. When this complimentary mechanism is not functioning properly, a diseased state may be expected. In Fig. 4, where the apparently irregular secretion pattern is shown, comparable to the data presented in Fig. 6, the critical composite time-delay is  $\tau_0 = 0.522$  in the unit in which t is measured. We also observe that in Fig. 6b) ACTH peaks approximately 3 times during a 4 hour period in a rat. Comparing this with the corresponding simulated ACTH level in Fig. 4 where 3

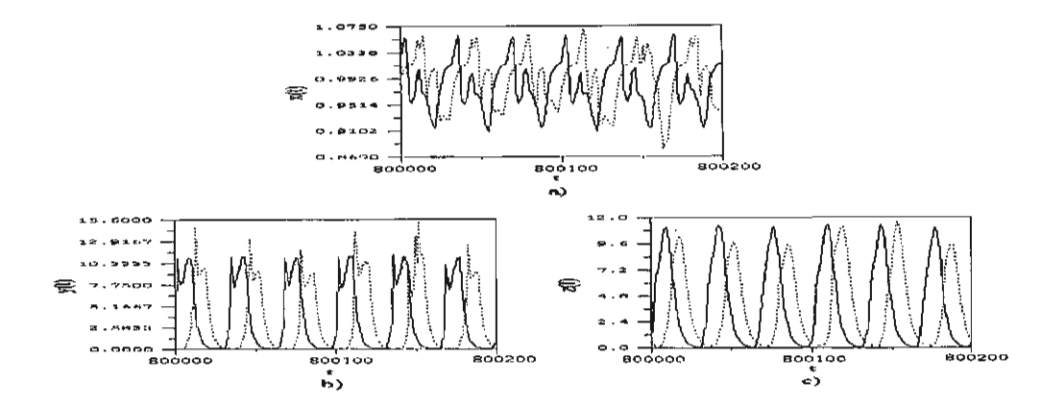


Figure 6: a) Pituitary venous concentrations of CRH in two mares ( $\blacksquare$ , marel;  $\bullet$ , mare2) given naloxone (adapted from the work of Engler *et al.*'s (1999)). b) Plasma ACTH concentration in a rat (taken from the work of Carnes *et al.*'s (1989)).

peaks are observed in 100 units of time t, we may then scale accordingly by taking t to be measured in the unit of 24 min., so that t=100 is equivalent to 4 hours. Then, the critical composite time-delay may be estimated as

$$\tau_0 \approx 0.522 \times \frac{240}{100} \approx 1.25 \text{ min.}$$

in a rat, and the composite time-delay may be estimated as

$$au pprox 10 imes rac{240}{100} = 24 ext{ min.}$$

based on the parametric values used in the simulation shown in Fig. 4. Unfortunately, similar estimates cannot be arrived at for humans, since frequent enough hormone measurements cannot be made and less peaks may then appear in the time series than there actually are. However, from the reports by Posener et al. (1997) and Hermus et al. (1984) mentioned earlier, in humans the delay in the short feedforward loop was observed to be around 30 min., while that in the short feedback loop was around 60 min.

From the above observation, we are also led to conclude that the role of individual time lag  $(\tau_1 \text{ or } \tau_2)$  in each of the responsive mechanisms is apparently not as significant to the well being of the cascade as the potency  $\beta$  of each feedback responsive signal. As seen in the bifurcation diagram shown in Fig. 3,  $\beta_2$  was found to be the bifurcation parameter which delineates different dynamical behavior and identifies the interfaces between sickness and health.

Although more intensive experimental/theoretical studies are necessary before definite conclusions can be made, such nonlinear approaches promise to offer sig-

 $A\ delay-differential\ equation\ model\ of\ the\ feedback-controlled\ hypothalamus-pituitary-adrenal\ cortex 17$ 

nificant contributions in our attempts to give a more qualitative description of the diurnal variations of hormone secretion in order to better understand the dynamic interfaces among different pathological situations.

### Acknowledgment

Y.L. and P.P. would like to extend their deepest appreciation to the Thailand Research Fund for the financial support.

### REFERENCES

- Berson, S. A., and Yalow, R. S. 1968 Radioimmunoassay of ACTH in plasma. J. Clin Invest. 47, 2725–2750.
- Carnes, M., Goodman, B. M., and Lent, S. J. 1991 High resolution spectral analysis of plasma adrenocorticotropin reveals a multifactorial frequency structure. Endocrinology 128, 902–910.
- Carnes, M., Lent, S., Feyzi, J., and Hazel, D. 1989 Plasma adrenocorticotropic hormone in the rat demonstrates three different rhythms within 24 h. Neuroendocrinology 50, 17-25.
- Engler, D., Redei, E., and Kola, I. 1999 The corticotropin-release inhibitory factor hypothesis: A review of the evidence for the existence of inhibitory as well as stimulatory hypophysiotropic regulation of adrenocorticotropin secretion and biosynthesis. *Endocr. Rev.* 20(4), 460–500.
- Hermus, A.R.M.M., Pieters, G.F.F.M, Smals, A.G.H., Benraad, T.J., Kloppenborg, P.W.C. 1984 Plasma adrenocorticotropin, cortisol, and aldosterone responses to corticotropin-releasing factor: modulatory effect of basal cortisol levels. J. Clin. Endocr. and Metab. 58 (1), 187-191.
- Ilias, I., Vgontzas, A. N., Provata, A., and Mastorakos, G. 2000 Complexity and non-linear description of diurnal cortisol and growth hormone secretory patterns before and after deprivation. *Endocrine Regulations* **36**, 63–72.
- Keenan, D. M., Licinio, J., and Veldhuis, J. D. 2001 A feedback-controlled ensemble model of the stress-responsive hypothalamo-pituitary-adrenal axis. *Proc Natl Acad Sci*, 98 (7), 4028–4033.
- Krieger, D. T., Allen, W., Rizzo, F., and Khieger, H. P. 1971 Characterization of the normal temporal pattern of plasma corticosteroid levels. J Clin Endocrinol Metab 32, 266-284.
- Lenbury, Y. and Pacheenburawana, P. 1991 Modelling fluctuation phenomena in the plasma cortisol secretion system in normal man. *Biosystems* 26, 117–125.